Linköping Studies in Science and Technology
Dissertation No. 2234

Hybrid Materials for Wearable Electronics and Electrochemical Systems

Mehmet Girayhan Say

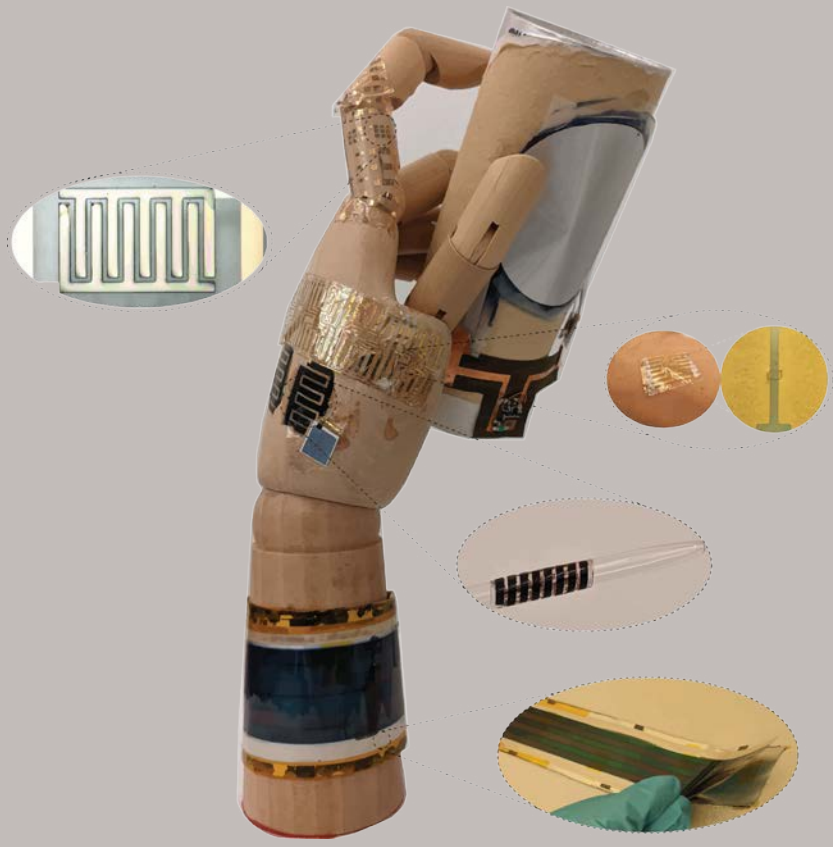

LINKÖPING UNIVERSITY

Linköping Studies in Science and Technology, Dissertation No. 2234

Hybrid Materials for Wearable Electronics and Electrochemical Systems

Mehmet Girayhan Say

Department of Science and Technology
Linköping University, Sweden
Laboratory of Organic Electronics (LOE)
Norrköping, 2022

Description of the cover image:

The cover image shows a picture of a model hand with attached wearable devices that are developed during the thesis. Photo by Mehmet Girayhan Say

Hybrid Materials for Wearable Electronics and Electrochemical Systems

During the course of research underlying this thesis, Mehmet Girayhan Say was enrolled in Agora Materiae, a multidisciplinary graduate school at Linköping University, Sweden.

Printed by LiU-Tryck, Linköping, Sweden, 2022
Electronic Publication: www.ep.liu.se
ISBN 978-91-7929-353-6 (print)
ISBN 978-91-7929-354-3 (PDF)
ISSN 0345-7524

To my big-hearted supporters…

Abstract

Flexible electronic systems such as wearable devices, sensors and electronic skin require power sources and sensing units that are mechanically robust, operational at low bending radius, and environmentally friendly. Recently, there has been an enormous interest in active materials such as thin film semiconductors, conductive polymers, and ion-electron conductors. These materials can be deposited with both printing and microfabrication techniques onto the flexible substrates such as plastics and paper. In addition, paper-based composites with nanofibrillated cellulose are favorable due to their mechanical strength, porosity, and solution-processability. Printing of such systems enables mass-production of large area electrochemical devices i.e., batteries, supercapacitors and fuel cells. Moreover, designing ultrathin devices for such concepts are promising for implantable and skin-like conformable electronics.

The aim of this thesis is the development of flexible electronic devices where, both organic and inorganic materials are explored, and examples of smart packaging and wearable electronics are demonstrated. Within the thesis, two different fabrication approaches are presented to achieve flexible electronics: (1) fabrication of porous paper electrodes for printable, wearable supercapacitor applications, where our efforts towards sustainable solutions for energy storage and (2) development of ultraflexible devices for electronic skin and implantable electronics to attain miniaturized, ultrathin device concepts. Overall, high performance electronic devices and demonstrators shown here have a significant impact on portable hybrid systems and flexible electronics applications.

Sammanfattning

Flexibla elektroniska system såsom kroppsburna enheter, sensorer och elektronisk hud kräver strömkällor och sensorenheter som är mekaniskt robusta, fungerar i böjt tillstånd och är miljövänliga. På senare tid har detta lett till ett enormt intresse för aktiva material som tunnfilmshalvledare, ledande polymerer och kombinerade jon- och elektronledare. Dessa material kan deponeras med både tryck- och mikrotillverkningstekniker på flexibla substrat som plast och papper. Vidare är pappersbaserade kompositer med nanofibrillerad cellulosa intressanta på grund av deras mekaniska styrka, porositet och möjlighet att processa i lösning. Tryckning av sådana system möjliggör massproduktion av elektrokemiska enheter med stor yta, dvs batterier, superkondensatorer och bränsleceller. För att ge hudliknande formbarhet och biokompatibilitet för implanterbara enheter är ultratunna enheter ett lovande koncept.

Syftet med denna avhandling är att utveckla flexibla elektroniska enheter där både organiska och oorganiska material utforskas, och att demonstrera exempel på smarta förpackningar och kroppsburen elektronik. I avhandlingen presenteras två olika tillverkningsmetoder för flexibel elektronik: (1) tillverkning av porösa papperselektroder för tryckbara, kroppsburna superkondensatorer, syftande till hållbara lösningar för energilagring och (2) utveckling av ultraflexibla enheter för elektronisk hud och implanterbar elektronik för att uppnå miniatyriserade, ultratunna enhetskoncept. Sammantaget kan de högpresterande elektroniska enheter och demonstratorer som visas här ha stor betydelse för utvecklingen av bärbara hybridsystem och flexibel elektronik.

Acknowledgments

I would like to sincerely thank all inspirational people who guided, helped and motivated me on this path and lifestyle.

First and foremost, I would like to thank my supervisors **Isak Engquist** and **Magnus Berggren** for giving me this amazing opportunity to work at Laboratory of Organic Electronics. With their guidance and encouragements to find my own research path, I feel confident and not scared about jumping into a new research field. Big thanks for your support, optimism, patience, and letting me for bouncing around. Thank you **Isak** for showing me good tips regarding parenting and **Magnus** for motivating me to stay in science. Of course, I should thank my cool supervisors to motivate me to join the activities, where I've found a chance to meet Kungafamiljen and rich people. I will always feel your unlimited support.

My sincere gratitude goes to LOE bosses (**Xavier**, **Simone**, **Mats**, **Klas**, **Renee**, **Eleni** and **Daniel**) for all the courses, short discussions and nice fika times. My mentors at LOE and RISE, your contribution to this guy and his thesis is enormous: **Andrea**, **Dagmawi**, **Rob**, **Jesper** and **Mary**. I will always remember your support, help and guidance for all experimental procedures, how everything works and my integration to this scientific society.

I would like to express my greatest appreciation to **Mary Donahue**, and **Eric Glowacki** for answering my dumb questions, and teaching me their way of conducting science and discussions about all the scientific and philosophical questions about 21st century crap. **Mary**! Thanks a lot for suffering with me instead of spending time with your kids, dogs, cats. Additionally, I would like to thank **Ihor Sahalianov** and **Igor Zozoulenko** to teach me how to deliver a clear scientific message and their guidance to conduct science.

I would like to acknowledge all the people of RISE Norrkoping and Stockholm scientists for providing a pedagogical research environment and collaboration opportunities. I've learned a lot from **Göran Gustafsson**, **David**, **Valerio**, **Astrid**, **Roman, Mats, Yusuf** and **Xin.** I am thankful to KTH, WWSC, Treesearch and RISE scientists (**Lars Wågberg**, **Stephan Roth**, **Daniel Söderberg**, **Hjalmar** and **Karl**) for cellulose discussions, tutorials and update meetings. Special thanks to **Stephan** and **Daniel** for their encouragement regarding synchrotron science and collaboration projects.

I would like to thank TPE members (**Marzieh**, **Robert**, **Hongli**, **Patrik**, **Makara**, **Neha**, **Kristin**, **Desalegn**) for all the scientific work, gatherings, and Friday morning meetings. Thank you **Patrik** for all Swedish speaking club and lunchmöte sessions.

Many thanks to Electrochemistry team (**Mikhail**, **Viktor**, **Zia**, **Zia 2.0**, **Ujwala**, **Fareed, Kosala, Valerio** and **Xavier**) for always reminding me that I know nothing about the things going on at the electrode processes.

Big thanks to my close colleagues. **Ludovico** for all the fun and full of music loaded time in cleanroom and dinners. **Igor** for all the boring physics related discussions and cooking sessions. Enjoyed your company while discussing history and politics. **Marie** for recipes, fun time in lab and motivation boosters. **Maciej** for finding all the smartest but cheapest solutions. **Andrea** for all the electrical engineering know-how share, lab hacks and his years long friendship. **Zia** for all the quick scientific discussions, sharing goodwill activities and grant writing tips. **Donghak** for answering my shocking questions during our lithography meetings. **Rob** for all the sarcasm during the PEA experiments. **Gabor** for Japanese lifestyle lessons, life hacks in Japan and crazy ideas (experimental). **Calvin** for all the fun/lab time in Hamburg and also in KTH. It was a great experience to learn with you, really hoping to see you in science business.

I would like to give special thanks to:
Lars Gustavsson, **Thomas Karlsson**, **Slawomir Braun, Meysam, Peter** and **Anna Malmström, Jenny** for keeping the lab running and solving the issues immediately. **Marie** and **Ek** for all the engineering tips to find the smartest solutions. Administrative team members **Katarina**, **Lesley**, **Ami**, **Ulrika, Jennie** and **Kristin** for always making my life easier. Without their support this work cannot be completed.

Special thanks to the **Greek** team for all the joy and fun time. Specially, a big hug to my sister (kardeş) **Maria** for all the support and true friendship. Without you, Norrkoping would be a prison. I will always remember your kindness and friendship, also your family's cuteness. Ela re **Yianni**! Thanks for all the crazy activities, gossips and always being here for me. **Elina** to ease my transition to Swedish lifestyle. **Xeno** for career planning discussions and football. **Thobias**, awesome human being. Thanks, my dear friend for showing a giant hospitality. I would like to thank you guys for keeping this immigrant (me) busy and happy.

I would like to thank party people: **Sami** for all the social activities, and fun stuff. **Dennis** for all the drinking activities, **Eva** for conferences, outdoor activities and nice fika times. **Chiara** for being an awesome flat mate and outdoor enthusiast. **Mina** for always being positive and all the laughs, **Nadia** for taking action in forcing nerds to go out and do something for a healthy life. **Angela**, **Manos**, **Malvina** and **Olga** for Mediterranean picnics and laughs.

I would also like to thank dear collaborators and friends, **Johannes**, **Nara**, **Vasilis**, **Marios**, **Gabor**, **Bernard**, **Kristin**, **Najmeh**, **Alex**, **Suhao**, **Iwona**, **Pawel**, **Erik G.**, **Ulrika**, **Pelle**, **Changbai**, **Benjamin**, **Anna**, **Johanna**, **Hanne**, **Arman**, **Alexandra**, **Hamid**, **Cyril**, **Jennifer**, **Arghya**, **Gwen**, **Aiman**, **Ilaria**, **Mohsen**, **Donghyun**, **Evan**, **Jee-Woong**, **Tero**, **Daniela**, **Shangzhi**, **Theresia**, **Simone** & **Chiara**, **Dan**, **Magnus J.**, **Negar**, **Felipe**, **Sergi**, **Glib**, **Vedran**, **Malin**, my fencing mates (**Mats** and **Ludwig**), all my Swedish teachers.

The past and present members of the research school Agora Materia, and especially **Carro**, for organizing seminars, study visits, and pushing me to take some responsibilities.

A huge thanks goes to **Zia**, **Igor, Mary** and **Isak** for helping me with reviewing my thesis.

It is pleasure to show my gratitude to Turkish crew; **Şenol** and **Melih** for all the support for 5 years long journey. Our friendship will be lifelong, and you guys are a huge piece of my Sweden journey, and this brotherhood will last forever. Lastly, I would like to thank **Güle** for bringing joy to my life with her noble charm and kind soul. This thesis acknowledges you for keeping the writer mentally stable.

I would like to express my gratitude to my family. My first mentors, my parents, this work is dedicated to you. Thank you, baba, for always pushing me to learn chemistry, write my own story and also showing by living, especially advising me to 'do the right thing, not the popular one and no matter what the cost is'. Anne! A big thanks to you to keep this weird family standing. Special thanks to my patron Arzu and Bionkit researchers for being mentors and role models for me, also to my sister, Dilbeste for all the rehabilitation sessions during my masters, PhD studies and fun time during summer vacations. Finally, I would like to thank my big family and friends for their love and support.

List of included papers

Paper 1:

Volumetric double-layer charge storage in composites based on conducting polymer PEDOT and cellulose

Ihor Sahalianov*, Mehmet Girayhan Say*, Oliya S. Abdullaeva, Fareed Ahmed, Eric Glowacki, Isak Engquist, Magnus Berggren

ACS Applied Energy Materials, 2021, 4, 8629 (*equal contribution)

Contribution: Most of the experimental work and some of the writing of the manuscript.

Paper 2:

Spray coated paper supercapacitors

Mehmet Girayhan Say, Robert Brooke, Jesper Edberg, Andrea Grimoldi, Dagmawi Belaineh, Isak Engquist, Magnus Berggren

npj Flexible Electronics, 2020, 4, 14

Contribution: All experimental work and most of the writing of the manuscript.

Paper 3:

Scalable paper supercapacitors for printed wearable electronics

Mehmet Girayhan Say, Calvin J. Brett, Jesper Edberg, Stephan V. Roth, Daniel Soderberg, Isak Engquist, Magnus Berggren

Submitted manuscript

Contribution: Most of the experimental work and most of the writing of the manuscript.

Paper 4:

Ultrathin paper micro-supercapacitors for electronic skin applications

Mehmet Girayhan Say, Ihor Sahalianov, Robert Brooke, Ludovico Migliaccio, Eric Glowacki, Mary Donahue, Magnus Berggren, Isak Engquist

*Advanced Materials Technol*ogies, 2022, 2101420

Contribution: Most of the experimental work and most of the writing of the manuscript.

Paper 5:

Ultrathin indium tin oxide accumulation mode electrolyte-gated transistors for bioelectronics

Ludovico Migliaccio*, Mehmet Girayhan Say*, Gaurav Pathak, Ihor Sahalianov, Imrich Gablech, Magnus Berggren, Mary Donahue, Eric Glowacki

Manuscript in preparation (*equal contribution)

Contribution: Some of the experimental work and some of the writing of the manuscript.

Paper 6:

Ultrathin polymer microcapacitors for on-chip and flexible electronics

Mehmet Girayhan Say, Mary Donahue, Renee Kroon, Isak Engquist, Magnus Berggren

Manuscript in preparation

Contribution: Conceptualization, most of the experimental work and writing.

Additional publications not included in the thesis

Supercapacitors on Demand: Printed energy storage devices with adaptable design
Robert Brooke, Jesper Edberg, Mehmet Girayhan Say, Anurak Sawatdee, Andrea Grimoldi, Jessica Åhlin, Göran Gustafsson, Magnus Berggren, Isak Engquist
Flexible and Printed Electronics, 2019, 4, 15006

The effect of crosslinking on ion transport properties of nanocellulose based membranes
Hongli Yang, Jesper Edberg, Viktor Gueskine, Mikhail Vagin, Mehmet Girayhan Say, Johan Erlandsson, Lars Wågberg, Isak Engquist, Magnus Berggren
Carbonhydrate Polymers, 2022, 278, 118938

Printable carbon-based supercapacitors reinforced with cellulose and conductive polymers
Dagmawi Belaineh, Robert Brooke, Negar Sani, Mehmet Girayhan Say, Karl M.O. Håkansson, Isak Engquist, Magnus Berggren, Jesper Edberg
Journal of Energy Storage, 2022, 50, 104224

Upscalable ultrathick rayon carbon felt based hybrid organic-inorganic electrodes for high energy density supercapacitors
Xin Wang, Mehmet Girayhan Say, Robert Brooke, Valerio Beni, David Nilsson, Roman Lassnig, Magnus Berggren, Jesper Edberg, Isak Engquist
Accepted Manuscript (Energy Storage)

3D printed and patterned electronic paper from nanocellulose and PEDOT: PSS
Makara Lay, Mehmet Girayhan Say, Magnus Berggren, Isak Engquist
Manuscript in preparation

Nanocellulose and PEDOT: PSS composites and their applications
Robert Brooke, Makara Lay, Karishma Jain, Hugo Francon, Mehmet Girayhan Say, Dagmawi Belaineh, Xin Wang, Karl M.O. Håkansson, Lars Wågberg, Isak Engquist, Jesper Edberg, Magnus Berggren
Submitted (review)

Contents

PART I
BACKGROUND

CHAPTER I

1. Introduction

1.1. Research Background

Our society's growing demand for smart and miniaturized systems stimulates the development of new functional materials and wearable devices. The commercial market for wearable technologies has projected to expand to $30 billion by 2020 [1]. Efficient energy supply is one of the biggest challenges supporting such systems. It requires a balance between maintaining high life quality, accessibility, and low cost. With the Nobel Prize in chemistry in 2000, organic electronics provides an essential set of technologies for flexible electronics applications such as energy harvesting and storage, biosensing, and bioelectronics[2]. These technologies allowed the development of complete systems in wearable, implantable and even ingestible electronics[3]. Softness and flexibility, solution processability and environmentally friendly synthesis make organic electronic materials (including conducting polymers) excellent candidates for green flexible devices and systems[4].

Up to now, organic electronics have provided applications in the field of organic light emitting diodes (OLED), photovoltaics, and thin film transistor (TFT) technologies and introduced mixed ion-electron conductors, where coupling ions and electrons expand new applications based on capacitive or redox effects at the electrode/electrolyte interfaces[2][5]. Mixing of electronic properties of conducting polymers with other forest-based scaffolds and water based materials leads to porous, mechanically robust organic composites for sustainable paper electronics systems[6]. As a nanoscale unit of paper and the most abundant polymer in the world, cellulose attracts great attention in composite science, especially in combination with functional electronic materials[7]. Using printing technologies, such paper composites can accomplish high capacitance devices with controlled thickness, large area and roll to roll production capability. Specifically, possible energy storage devices are supercapacitors and batteries that can supply energy to conformable wearable devices with low cost to maintain the needs of conventional electronics[8]. High power density supercapacitors are in high demand in wearable electronics, healthcare, medical technologies, smart packaging, and Internet of Things (IoT). In addition, supercapacitors take part in self-sufficient wearable power packages where another application of the wearable organic electronics is ready to be demonstrated in prototypes.

Another branch of flexible electronics is new concepts of implantable devices. Skin attached and implantable electronics utilizing organic, inorganic or hybrid materials can find applications in sensing, signal transduction, and advanced healthcare technologies[9]. The first and the most significant consideration is power management for the implantable device or electronic skin[10]. The pacemaker developed in 1958 is the first example of an implanted system with Ni-Cd battery[11]. Since then, the need for environmentally friendly, thin, planar and miniaturized energy storage systems inspired material scientists and engineers [12]. Anatomically compliant designs, ultrathin substrates with conformal mechanics and robust packaging materials are necessary for such systems. Besides developing ultrathin, micro-energy storage devices is quite crucial to deliver energy to low power, chip scale, miniaturized transistors that can amplify weak electrophysiological signals when interfaced with body fluids.

Along with the robust encapsulation, such systems are ideal candidates for both in vivo and in vitro applications as well as skin interfaced, lightweight and wearable electronics.

1.2. The aim of the Thesis

The thesis aims to explore both organic and inorganic materials in terms of flexible device fabrication and shows use cases in wearable electronics for possible daily life applications. The focus of the thesis can be divided into two parts: (1) printing/coating of porous paper electrodes for wearable supercapacitor applications and (2) development of ultrathin capacitance driven devices for electronic skin and implantable electronics. One way of realizing flexible devices demonstrated in the thesis is using the concept of paper electronics, which employs sustainable and green materials and approaches. Investigations of functional paper-based (cellulose) composites and formulating inks into scalable printing techniques are highly required for wearable electronics and electronic skin applications. We have contributed to the field by introducing and processing our mixed ion-electron conductor composite system into the printable energy storage technologies. We have shown applications in the field of smart packaging, solar cell/supercapacitor integration for wearables and electronic skin applications. Besides, implantable, transparent oxide-based transistors to amplify weak electrophysiological signals and miniaturization of on chip energy storage devices are also an object of interest within the thesis. It should be noted that all the devices developed here were designed to be all solid-state, flexible and mechanically stable after thousands of deformation cycle tests. With that motivation, we have aimed to develop and introduce concepts and device architectures for wearable, skin compatible and implantable electronics.

1.3. Thesis Outline

The thesis consists of two parts, the first part describes the fundamentals and gives background information to grasp the thesis's concept. Chapter 2 summarizes the needs of next generation flexible electronics, and mechanical considerations to achieve the goal of wearable and implantable electronics. This chapter is also planned as a commentary for current technologies and presents a viewpoint on existing material and device concepts for the reader. Chapter 3 introduces the materials and Chapter 4 gives a theoretical background of the devices, which were developed. Chapter 5 describes the basics of printed electronics and the implementation the spray coating method for large area organic electronics. A short review of the major laboratory scale manufacturing, electrochemical methods and material characterization techniques is given in Chapter 6. Lastly, a summary of each paper included in the thesis with a comparison of current state of the art is presented in Chapter 7.

Part II focuses on the scientific papers that were developed during the research projects conducted throughout the entire PhD thesis. Paper I-IV present the investigation of an organic composite, which is an amalgamation of nanocellulose and conductive polymer PEDOT: PSS. Understanding of this composite's capacitance both theoretically and experimentally was summarized in Paper I. Paper II uses this material as an electrode in all printed, flexible supercapacitor. We have used sequential printing and coating methods to achieve flexible supercapacitors for smart packaging. Paper III is a study for the expansion of the manufacturing

method in Paper II, where spray coating is investigated as a scalable manufacturing of large area, paper-based electrode-making strategy. Collaborations with specialists in synchrotron X-ray scattering analysis bear fruit as a deep understanding of nanoscale formation of paper electrode and attaining an exciting platform to combine a fully printed and organic supercapacitor and a solar cell. This work demonstrates a route to fabricate flexible and large area supercapacitors to function within the self-powered wearable power packages. Paper IV, we discuss the ultrathin microsupercapacitors for electronic skin applications. This paper combines the methods for achieving ultrathin (~10 μm) supercapacitor fabrication both using printing/coating methods and ultrathin substrate and packaging material Parylene-C. Although organic electronic materials are the main interest of the thesis, with the Paper V, the focus of the thesis moves more on implantable electronics. Paper V reports an ultrathin (~2.5 μm), transparent n-type electrolyte gated field effect transistor (EGFET) based on amorphous indium tin oxide (ITO) channel material capped with oxides to provide long-term operation capability. Paper VI demonstrates a method of fabricating micro-energy storage devices (~4.0 μm), where on-chip, polymer interdigitated cathodes or symmetric supercapacitors can be manufactured to supply short-term power to implanted MEMS or sensors.

CHAPTER II

2. Concept of Wearable Electronics

Since the first demonstration of polymer transistors on flexible sheets in 1994, flexible electronics has become prominent for the technologies where flexibility and mechanical robustness is needed during the device operation[13]. For the last two decades, necessity for flexible device components come forward to realize applications for wearables, energy storage/harvesting, and implants. Great number of techniques, materials and systems were investigated in the fields of sensors, microfluidics[14]–[16], 3D bioprinting[17]–[19], bioelectronics[20], energy harvesting and storage[21], [22]. To be specific, roll up displays[23], flexible solar cells[24], epidermal electronics[25], hydrogel electronics[26] and stretchable[27] devices were created/invented throughout the years of development. The performance of such devices under mechanical deformation, their tolerance towards harsh mechanical tests and the performance retention are objects of study to achieve fully integrated, robust systems. Therefore, mechanical considerations became essential to design both wearable and implantable electronics[28], [29].

2.1. Mechanical Considerations and Bending Mechanics

The mechanical concepts should be discussed to further understand the stress and strain, build up on the device layers. One key parameter to be explained is the bending mechanics. The simplest case (assume homogenous sheet) is the thin film on a flexible substrate structure. As Figure 2.1a shows, the strain is zero at the neutral plane, and critical strain is a main parameter to be considered since values below ε_{crit} do not cause cracks or failure. The outer surface endures tensile strain and inner experiences compressive strain. This is an important parameter to be considered for flexible electronics. Let's assume a homogeneous sheet with the same Young modules of film and substrate, the bending strain is the distance from the neutral plane (thickness of the film, t_f and substrate, t_s) divided by radius of curvature, R[30], [31].

$$\varepsilon_{crit} = \frac{(t_s + t_f)}{2R_{crit}} \tag{2.1}$$

Using the formula, it can be concluded that the strain linearly decreases with the film and substrate thickness. Controlling thickness can achieve lower radius of curvature and designing devices that can operate at millimeter range bending radius (R) can overcome the mechanical limits in the field of implantable and wearable electronics.

The bending strain ε for a random position from the surface of the layered structure can be given with the formula[28],

$$\varepsilon = \frac{r - b}{R + b} \tag{2.2}$$

Where R is bending radius, r and b denote the arbitrary position from the bottom layer and neutral mechanical plane, respectively.

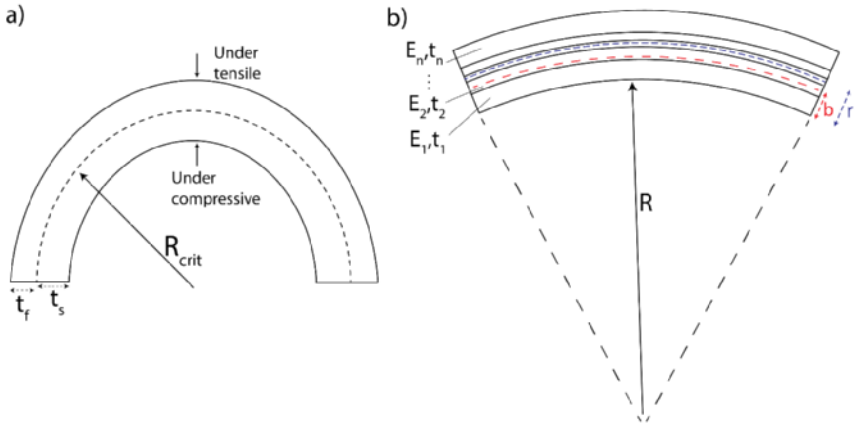

Figure 2.1. a) Schematic illustration of bent structure with substrate and thin film (in a homogenous sheet, dashed line demonstrates the neutral plane), b) Schematic of multi-layer system, showing mechanical neutral plane (black dashed line) and device layers.

As can be seen from Figure 2.1b and using eqn. 2.2, degradation (cracking, delamination etc.) can be minimized with a functional layer, which yields the weakest strain response at the zero-strain position (neutral mechanical plane). Utilizing ultrathin substrates and encapsulation succeeds superior bending stability due to the neutral strain-position strategy. Therefore, even using brittle inorganic materials or stiff organic materials can achieve successful applications for the conformable electronics.

Flexural rigidity (D) is another parameter, that is needed to be considered to understand conformable devices[32].

$$D = \frac{Et^3}{12\,(1-v^2)} \tag{2.3}$$

where E, t, and v refer to the Young's modulus, thickness, and Poisson's ratio of the film, respectively. The analysis of this equation simply gives that reducing the thickness is the most crucial approach to decreasing the flexural rigidity, which provides better conformability for wearable and implantable electronics.

With this theoretical background, we should note that the mechanical properties are being investigated with computational solid mechanics by combining experimental methods. Finite element analysis (FEA) explores and analyzes the strain and stress distribution for the films and structures under deformation. Bending strain, minimum bending radius and failure point of the designed device can be predicted with FEA[33]. The combination of FEA with bending tests gives a complete understanding of the robustness of the flexible device and predicts the robustness of the system for the application. Together with the numerous of investigations and demonstrators, the flexible electronics field has evolved and the need for extreme applications

make the field to shift towards skin attachable, ultrathin body integrated concepts to fulfill the needs for 21st century gadgets, advanced healthcare and robotics.

2.2. Device Concepts

Although there are many electronic devices within the branch of flexible electronics[34], this thesis circles around the printed paper energy storage devices, ultrathin electrolyte gated transistors and polymer microsupercapacitors. Therefore, the concepts related with these devices will be explained and perspective regarding the device performance will be given. Operation mechanisms of supercapacitors, microsupercapacitors and electrolyte gated transistors depend on the capacitance of the active material, which plays a crucial role in the device architecture. Figure 2.2. shows the areal capacitance range of the materials that are used in the preparation of flexible electronic devices within the thesis.

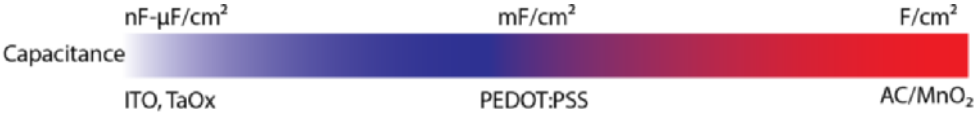

Figure 2.2. Areal capacitance range of the flexible (thin film or bulk) materials proposed in the thesis.

The growth of unconventional microelectronic devices in wearables and implantable electronics has demanded high-performance energy storage devices or modules that combine storage and harvesting units [10], [35]–[37]. Among these, skin-interfaced and skin-like devices are receiving considerable interest to achieve batteries and supercapacitors that are extremely flexible and endure extreme mechanical scenarios when operated onto skin or bio-surfaces [28], [29], [38], [39]. Structural requirements, including substrate, layer thickness within the device sub-sections, encapsulation or preservation of mechanical neutral plane are design considerations for a successful application[28]. Since these points decide the mechanical integrity, one field comes forward. Paper electronics finds itself in this highly competitive area with providing paper as a substrate, cellulose nanofibrils as porous networks, scaffolds, building blocks or membranes[40]. The use of forest-based materials dates back to centuries ago. Today, paper-based materials can provide flexibility and solution processability for the fabrication of next generation electronic devices. Although unique materials (silk, albumin) and well-known materials (plastics) over the decades were used to construct the flexible electronic devices, paper-based materials are lower in cost[41], [42]. Paper substrates, cellulose-based binders, hydrogels and electroactive materials from the wood provide sufficient flexibility and functionality to achieve wearable electronics[7]. Using such forest-based materials can flourish the field to achieve sustainable, conformable electronic devices with low cost, scalable manufacturing.

To introduce printed paper electronics as an manufacturing approach, importance of cellulose in printing technologies and the question of why we use cellulose is worth to answer to explain the concepts[6], [43]. Using cellulose in energy storage stems from being low-cost, porous, light weight and enabling high active mass loadings to achieve high energy and power density devices. Since cellulose can be manufactured at large quantities, dispersed in water or solvents,

large area device manufacturing is possible, i.e., paper making or roll to roll printing. By incorporating cellulose fibrils as a scaffold into the device layers (electrode, electrolyte, separator membranes) mechanical strength and functionality can be provided[6], [44]. A combination of electroactive materials with cellulosic networks (cellulose fibrils, pulp, and paper substrates) creates ample opportunities to achieve mechanically robust, lightweight, and low-cost electrodes for energy systems[6]. Such composite electrodes provide high surface area electrodes with multiple ionic pathways, all of which are needed for supercapacitors, which offer millions of cycles, high peak power, exhibit high tolerance towards fluctuating charging currents and safe operation. With the low equivalent series resistance (ESR), and capability to provide high power, supercapacitors are being regarded as excellent candidates to sustain the long-term operation of self-powered systems[45].

Paper supercapacitors are favorable because of

1. Capacitance can be tuned by active material deposition, highly porous electrodes
2. High Power (low ESR)
3. Safe, printable, and scalable
4. All solid state but mechanically flexible due to the paper properties
5. Size control and on-chip integration possibility with printing methods

With these advantages as an energy storage device, we have aimed to design printable paper supercapacitors. The motivation here is to manifest a fabrication route for conformable, large area supercapacitors with large area manufacturing capability and with desired mechanical properties for wearables. We have investigated the spray coating technology throughout the thesis, to fabricate supercapacitors due to providing good adhesion, thickness control and large area coating properties. Such issues especially thickness control and continuous deposition of the layers to prevent delamination are the prominent concerns needed to be solved and spray coating provided good contact with current collectors and low roughness paper electrodes (Paper II and III).

With the 1D scaffold, the electroactive materials can be hosted in the electrode with high active material mass. With the motivation of organic electronics, PEDOT: PSS has been selected to fabricate paper electrodes for large area supercapacitor fabrication. The last decade has been focused to manufacture PEDOT-based materials, deposited through different techniques such as vapor-phase (VP), electro-polymerization and or solution processed based methods, for the fabrication of micro-supercapacitors[46]–[50]. Although electro- or VP-polymerization methods can provide high capacitance PEDOT, the fabrication processes are limited with thickness and area control, and therefore scalability is an issue to achieve large areas[46], [47]. Printing of functional inks from water-dispersible PEDOT:PSS inks overcomes these drawbacks and provide control over the thickness, and extended area coverage, meanwhile maintain high energy and power density without expensive infrastructure[51]–[53]. Using CNF as a nanoscale binder and PEDOT as active material, the nanoporous electrode ink becomes available to investigate using spray-coating for a highly controlled electrode manufacturing[51], [54].

For energy storage device fabrication, spray coating enables to deposit several hundreds of nanometers of electroactive films, using carbon-based, inorganic materials and conductive

polymers[55]–[57]. In view of the thickness limitation, spray coating has mostly involved fabrication of electrodes on thick and solid substrates with nanometer-scale coating, which is not preferable for high energy density devices with desirable mechanics[56], [58]. These films were fabricated with gas-driven systems, either using a simple airbrush (Paper II) or an atomizer[59] (Paper III). One note here is that in case of organic materials for enabling adhesion and maintaining mechanical integrity, interface engineering is a requirement using processes such as silanization[60], [61]. With the help of spray coating this issue is quickly solved. Due to the layer-by-layer approach, thin films of paper electrodes are produced with spray coating. The good contact motivated us for investigating possibilities for wearable, skin compatible supercapacitors. This approach may lead to coat active materials for symmetric or asymmetric supercapacitors, battery cathodes and anodes using functional inks onto readily available PET substrates. The possibility to roll to roll approach, large area coating with good adhesion properties steps forward for the fabrication, where screen printing cannot deliver the needs. The supercapacitors delivered up to 9.1 mF cm^{-2} areal capacitance, a very low ESR (~0.3 Ω) due to the good electrical contact and outstanding mechanical stability (bending radii 6 mm, 5000 cycles, 95 % retention). Flexible paper supercapacitors are combined to power printed organic electronic devices, such as electrochromic displays, operate during the bending state showing mechanical robustness and as well as connected with power management circuits to supply 3V for commercial electronic applications. Additionally, as demonstrated in paper III, paper supercapacitors can deliver enough energy and be used for solar cell integration to demonstrate self-sustained power packages.

Besides printing and manufacturing wearable devices with well-known plastic substrates, ultrathin substrates are performing well under physical deformations and opening up new avenues for flexible electronics. With that said, the history of flexible energy storage devices starts with the batteries. Batteries manufactured on bulky substrates with vacuum deposition methods have recently been investigated; however, the use of complex cathodic materials, physical vapor deposition-based electrodes and electrolytes, and area-limited fabrication causes the device structure expensive and complicated [62]–[64]. Thick substrates cause limited flexibility (high bending radius) and bending cyclability, and require high processing expenses, which contradict the requirements of the skin-compatible electronics[29], [65]. Thin substrates such as polyimide[66], parylene C[67], or PET (1.4 or 4.5 µm) foil with a carrier support[68] were used for ultrathin electrochemical energy storage devices.

Among them, parylene C is an excellent material to prepare substrates around 1.0 µm thickness. Due to the good adhesion, low roughness and compatibility with photolithography, it is the right material for wearable and implantable electronics. In addition, it is a good encapsulation material (low roughness, low permeability to moisture and chemical barrier) to achieve mechanically robust devices. Ultrathin devices on parylene C substrates are fabricated throughout the thesis to provide new concepts to wearable and implantable electronics. Consecutively, microsupercapacitors fabricated with spray coating, miniaturized, interdigitated symmetric capacitors with parylene peel-off method and electrolyte gated transistors fabricated with photolithography are demonstrated for the electronic skin and implantable electronics. The energy storage devices (printed and on-chip microsupercapacitors) show the example of ultrathin device architecture to maintain overall thickness of 10 µm and 4.0 µm. Such fully encapsulated implantable devices showed mechanical robustness (1000 cycles, capacitance

retention of 98%) under extreme bending (rolling) and kept operational at bending radius down to 2 mm. Finite element method (FEM) simulations were carried out to analyze the mechanical properties of the device, resulting a volumetric strain and stress lower than 0.05%. Together with these properties the method of fabrication clears the way for on chip energy storage modules.

The last flexible device that is capacitance driven and in the configuration of ultrathin is the flexible electrolyte gated transistors (EGFET). EGFET operation depends on ions forming an electrical double layer at the electrolyte-electrode interface, $\mu F/cm^2$ value of capacitance leading to high switching speed; additionally, the high transconductance of EGFETs originates from the high charge carrier mobility. The materials that can provide such properties are highly interesting and motivating the implantable electronics. One oxide is deep routed in the solid-state electronics for display technology and motivated us to provide flexible designs for implantable devices.

Display technologies are crucial and most interesting market in the consumer electronics area, transparent and flexible displays are expected to bring revenues of $87.2 billion by 2025[69]. Since Indium Tin Oxide (ITO) is the most well-known and ready to use material, it deserves to be investigated in depth. Transparent conducting oxide family exhibits high transparency in the visible part of the electromagnetic spectrum and high electrical conductivity. These properties are crucial for applications such as active matrices for displays, thin film transistor technology and field effect biosensor technologies. ITO is widely used in these applications for high performance transparent conductive layer.

Oxides are typically regarded delicate materials as they are considered due to the brittle nature. Although this observation may be true for thick films, this concern can be avoided with engineering layers of thin film amorphous oxides, where deposition takes place onto ultrathin substrates in which the mechanical neutral plane is preserved. Recent decade showed the examples of using Indium Oxide, Indium gallium zinc oxide (IGZO) and ITO as a ion sensitive channel material of FETs in the field of pH sensing and biosensing [70]–[72]. Another use of these binary and ternary oxides finds application within the neuromorphic devices to achieve low power electronics[73]–[75].

Last motivating point is optical transparency, which is another need in the field of imaging, local signal amplification as well as optogenetics, where transparent conductive materials (Graphene and ITO) find itself in such applications as a transparent electrode[76], [77]. The efforts towards achieving transparent cathodes or a top contact with ITO shows good transparency at the current collector component of the devices however, all ITO configuration is not investigated in depth to achieve transparent devices[78], [79]. The features such as ion sensitivity, EDL switching, and providing transparency inevitably attracted our attention to study fully encapsulated, ultrathin (overall ~3 μm) ITO EGFETs. The stack of thin film oxide layers such as tantalum oxide and aluminum nitride (Ta_2O_5 /AlN) on top of 35 nm thick ITO semiconducting layer protected the semiconductive ITO from electrochemical side reactions. Our ultrathin ITO EGFETs constructed on parylene C substrates, are demonstrating good flexibility, high transconductance values, fast switching speed, and high on/off current ratios, shows stable operation at 6.5 mm bending radius. Together with these properties another application within the ultrathin device technology has been accomplished to supply a device technology for implantable and body integrated electronics.

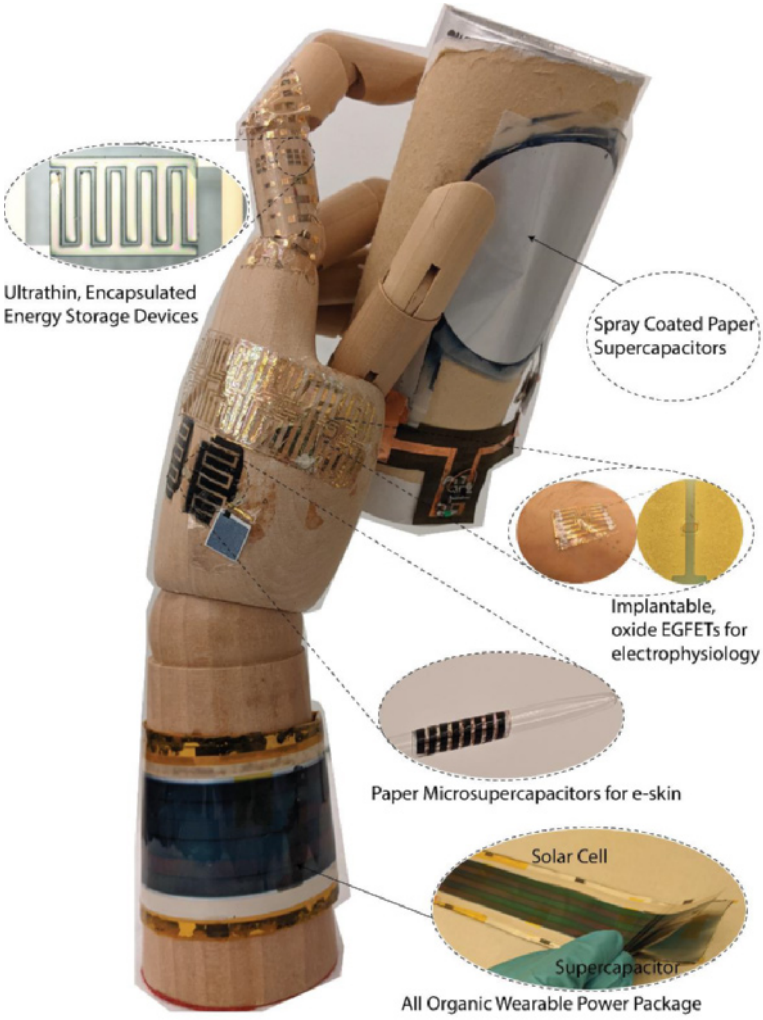

Figure 2.3. Wearable electronic devices, developed in this thesis. Model hand highlights the skin-attachable devices.

In summary, this thesis shows prototypes, use cases and demonstrators for skin attachable, wearable devices as shown in Figure 2.3. The devices and concepts were constructed to use electrical double layers (EDL) that are formed at the electrode electrolyte interfaces. Paper II shows sequential coating/printing methods to achieve flexible pouch-cell type supercapacitors. The devices were connected with flexible circuitry to demonstrate smart packaging application, where the supercapacitors can conformably cover the packaging material. With Paper III, upscaling of energy storage devices was achieved with coating/printing methods. Large area, paper supercapacitors were fabricated to combine with solar cells for the application of self-sufficient wearable system. All organic power package was demonstrated to be used in wearable electronics applications. Paper IV investigates the fabrication of ultrathin micro-

supercapacitors using spray coating for electronic skin applications. We have aimed to keep the entire device thickness around 10 μm to show low bending radius operation capability, skin-like devices. The method enables to design power supply systems for printed electrochromic displays and electronic skin. Paper V investigates fully encapsulated electrolyte gated oxide FETs for implantable electronics. We have implemented well-known EDL system ITO, as a channel material and designed EGFETs to be used in signal amplification of bio-signals and as a perfect candidate for flexible complementary logic circuits. Lastly, Paper VI demonstrates a fabrication route to achieve fully encapsulated, ultrathin energy storage devices. The hybrid fabrication method (microfabrication & lithography) was shown to control the thickness and interdigitated electrode structure. Overall, we have achieved energy storage and sensor devices for wearable electronics, which will open ways for the next generation commercial electronics and healthcare applications. Performance retention more than 90% after thousands of mechanical bending cycles and operation capability under bending radius of minimum 2 mm and long-term operation stability were achieved and proven to be highly robust for wearable and skin compatible flexible electronics applications.

CHAPTER III

3. Materials

This chapter explains and gives the details of the materials (substrates, active materials) used in the fabrication of flexible devices.

3.1. Substrates

Depending on scalability and the type of application, several substrate types and encapsulation materials were used in the thesis. Polyethylene terephthalate (PET), Parylene-C, and paper-based substrates were used along with typical encapsulation materials such as polydimethylsiloxane (PDMS), Polyimide (Kapton) and Parylene-C.

3.1.1. PET

PET is one of the most stable (mechanically and thermally) thermoplastic substrates used in flexible electronics[80]. It is commercially available in a wide thickness range from 4.5 µm to 200 µm, allows roll to roll printing and coating processes. 18 µm PET laminated with Aluminum coating and carbon adhesion layer has also been used in Paper **II** and **III** as the main flexible component of the current collectors (Figure 3.1). The combination allows high processing conditions up to 150 °C, where in the spray coating of paper electrodes, it performed well without buckling or cracking at the processing temperature of 90 °C.

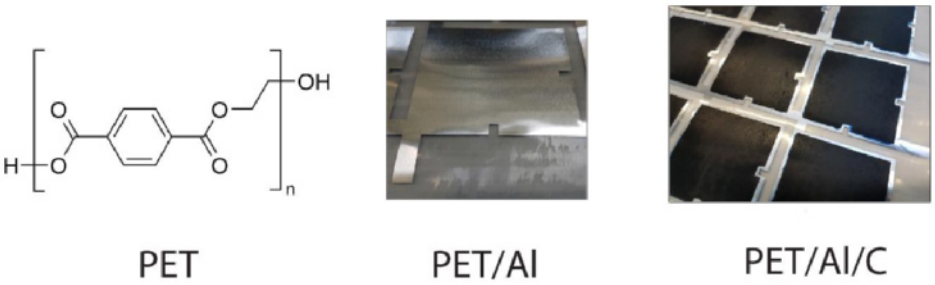

Figure 3.1 Substrate material used for printed energy storage devices.

3.1.2. Parylene-C

Parylene C is an excellent substrate for ultrathin, conformable devices for bioelectronics, skin electronics and wearable technologies [77], [81]. Parylene C can be produced by polymerization of para-xylylene using a Chemical Vapor Deposition (CVD) system. The chlorinated version of Parylene has chlorine in the aryl ring (Figure 3.2). This semicrystalline polymer can be grown by polymerization of monomer, where polymerization depends on dimer weight and CVD system properties such as pressure and deposition rate. Parylene C can provide a pin hole free, low roughness, excellent humidity barrier and chemically stable substrate and encapsulation material[82]. It is biocompatible, transparent, and electrochemically stable. For paper **IV**, **V** and **VI**, Parylene C was implemented as ultrathin (~ 2 µm) substrate and encapsulation material (1.4 µm).

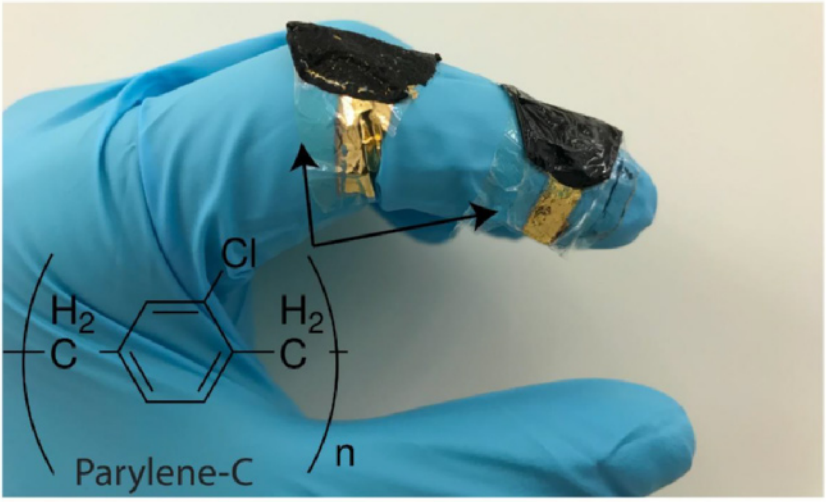

Figure 3.2. Parylene-C as a substrate material for ultrathin electronic devices.

3.1.3. Paper & Cellulose

Cellulose is the most abundant polymer and can be found in cell walls of the plants, some bacteria and even animals such as tunicates[7]. It is an important product for forestry industry since cellulose is the main component of paper. The main source of the cellulose and its derivatives is wood; therefore paper and pulp industries are interested with wood processing (mechanical and chemical) to separate and process wood fibrils. The cell walls consist of these fibrils with a diameter of 10-100 µm, which can be classified as pulp and with chemical treatment it can be used as microfibrillated cellulose (MFC). The pulp can further be used in different types of paper production. For the 'nano' cellulose term, there are several classifications: Cellulose Nanofibrils (CNF), Cellulose Nanocrystals (CNC), and bacterial Nanocellulose (BCC). Figure 3.3 shows the structure of MFC and CNF. There are important tools such as spectroscopy and diffraction methods to extract structural details and information regarding size, shape, crystallinity, and organization[83]. Several chemical modification routes can be used to modify CNFs, that offer additional functionalities. Typical chemical functionalization includes TEMPO ((2,2,6,6-tetrame-thylpiperidine-1-oxyl radical) oxidation and carboxymethylation [84], [85]. The chemical treatment on the nanofibrils (i.e. carboxymethylated) provides repulsion between the fibrils so that dispersion has stable colloidal suspension. CNF are nanostructures with 5-10 nm in diameter and up to 10 µm in length, which is the chosen cellulose material to produce paper electrodes in this thesis. We have implemented water dispersed CNF in our composite electrode to provide paper-like characteristics of porosity, water dispersibility and mechanical strength.

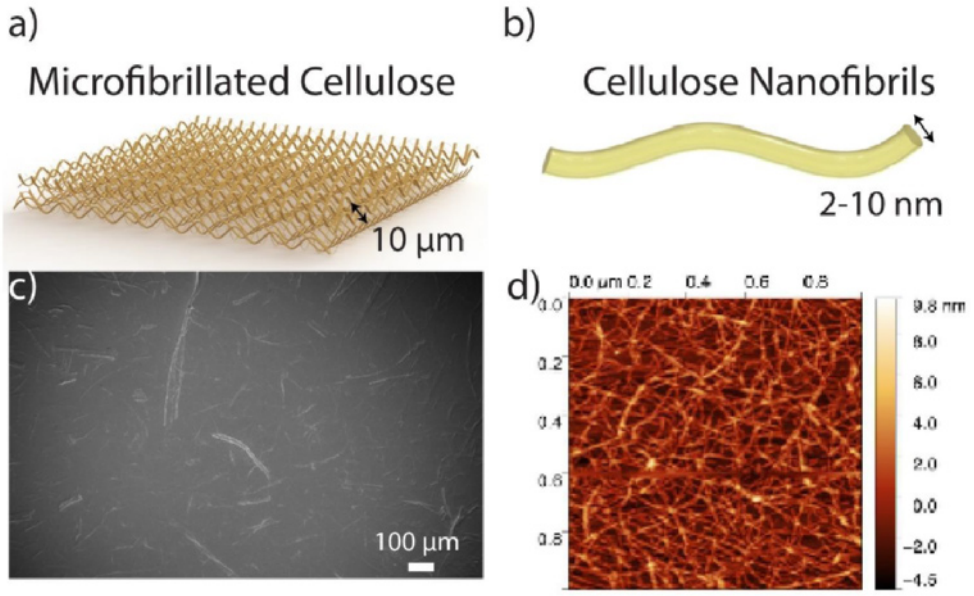

Figure 3.3. a) Schematic representation of MFC and b) CNF. c) SEM image of MFC, d) AFM image of cellulose nanofibrils.

3.2. Active Materials

Organic and inorganic active materials have been used in the fabricated devices. For upscaling printing and coating methods, solution-processable PEDOT:PSS is used to develop flexible paper based organic supercapacitors. For the EGFET device, ITO (Indium tin oxide) is sputtered as semiconducting channel material and transparent source/drain electrodes. Several other active materials such as MnO_2 and active carbon have also been tested to fabricate energy storage devices.

3.2.1. PEDOT:PSS

Poly(3,4-ethylenedioxythiophene), abbreviated to PEDOT, is one of the well-known conductive polymers that belongs to the group of π-conjugated systems. This polymer was developed in 1988 and has found applications in antistatic coatings and stable packaging material mainly in Bayer AG and capacitor manufacturers in Japan[52]. Some years later, the introduction of a polyelectrolyte, Polystyrenesulfonic acid (PSS), in the polymerization process opened enormous opportunities. Using the PSS polyanion as counterion created a water dispersible and ionically conductive material, and the mixed ion-electron conductor was achieved[5].

Figure 3.4a shows the optical image and molecular structure of PEDOT:PSS. In its neutral form, PEDOT coating (depending on thickness) exhibit light to dark blue color. Polymer films that are produced from PEDOT: PSS inks have low conductivity (< 1 S/cm), which is attributed to the excess insulating PSS agglomerations around the PEDOT grains. To overcome this limitation secondary doping or morphology enhancers were introduced[86], [87]. The process

includes adding high boiling point solvent such as dimethyl sulfoxide, sorbitol and ethylene glycol or ionic liquids to the PEDOT: PSS mixture and depositing the ink followed by an annealing process. After adding secondary dopant material, phase difference leads a morphology change where, PEDOT rich grains become larger and interconnected. Excess PSS is reduced, leading to more pathways for electron conduction[88], [89].

PEDOT-based materials have attracted interest in many fields due to high conductivity (~1000 S/cm), high capacitance (from 1 μF/cm^2 to 2.24 F/cm^2), and low impedance; prominent examples are found in biomedical and energy storage applications [90]–[93].

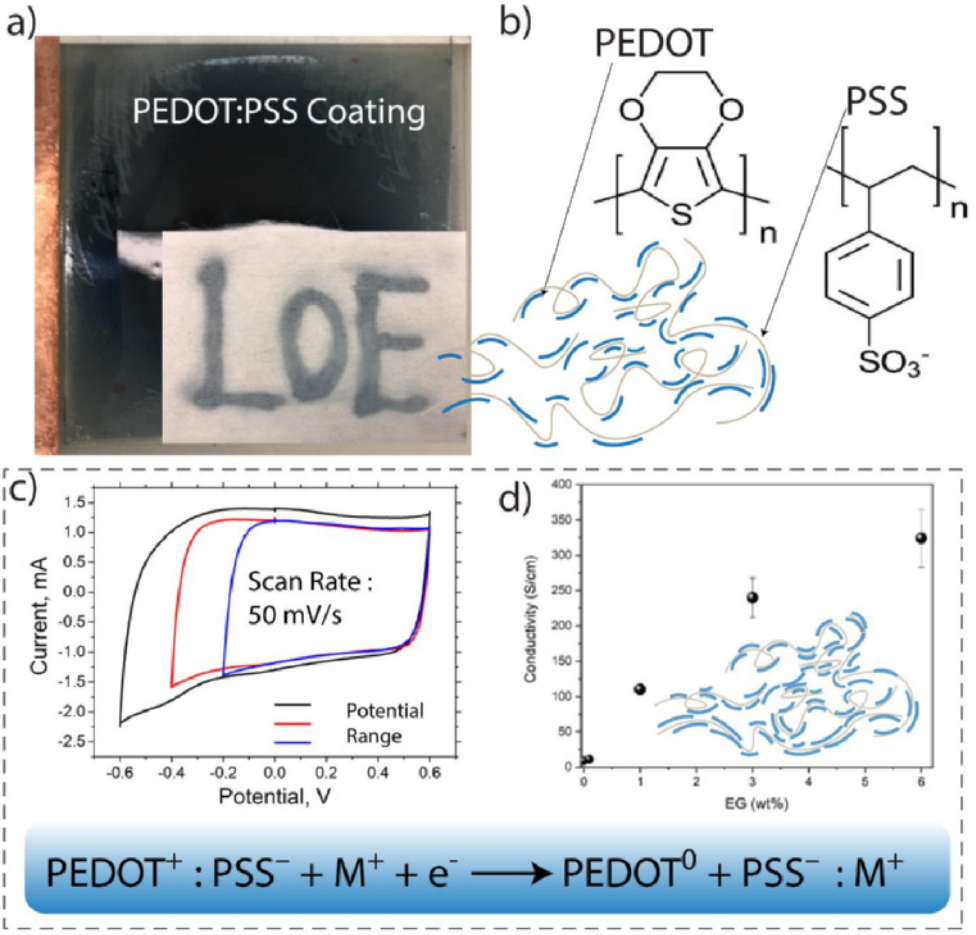

e)

Application	Function	Technology Readiness
Capacitors (ECS)	Cathode	Established
Solar Cell	HTL/ Transparent electrode	R & D
Packaging	Antistatic Layer	Established
Smart Window	Electrochromic layer	R & D

Figure 3.4. PEDOT: PSS properties. a) Optical image of PEDOT: PSS film for transparent cathode, inset shows the patterned PEDOT: PSS coating with spray coating on a paper substrate.

b) Schematics of polymer structure. c) and d) Electrochemical and electrical footprints of PEDOT: PSS as an active material in a composite system. e) Applications related the commercialization of PEDOT: PSS.

Besides conductivity, capacitance and redox activity are two important parameters (Figure 3.4c and Figure 3d) that define the performance of many electrochemical devices based on PEDOT: PSS and its composites, such as supercapacitors, electrochromic displays, electrochemical transistors, and sensors. Electronic and ionic charge transport in PEDOT provides fundamentals for device physics, and enable functional operation governed by volumetric PEDOT:counterion double layers. Although numerous data has been reported on the charge-storage mechanism, there is a debate on the nature of the capacitance in these systems[94], [95].
Conductive polymers, including PEDOT, are often considered as pseudo-capacitors (Chapter 4) in literature [96], [97]. Recent studies explain the charge storage mechanism using microscopic electrical double layers formed between the counterions and charged polymeric chains organized at nanoscale.[95], [98]–[100]. Experimentally extracted capacitance values vary significantly depending on the fabrication, characterization method and ion movements. In such methods the morphology of films, such as porosity, thickness, specific surface area, and type of counterions play important role [94], [101].
Another essential property of PEDOT is electrocatalytic activity, where possible oxygen reduction reactions (ORR) involve oxidation of the polymer through two- or four-electron reaction pathways [102]–[104] and mass production of peroxide[105], [106] can be selected as examples of the direct ORR influence.
Upon oxidation and reduction of PEDOT, a phenomenon known as electrochromism is also observed in PEDOT, which finds application in printed electrochromic displays and smart windows. Upon electrochemical reduction, PEDOT switches from a light blue (depending on the thickness) state to dark blue color.

3.2.2. ITO

Transparent electronics has gained a great deal of attention during the last decades and has played a pivotal role in the development of flat panel displays, active matrix for organic light emitting diodes (AMOLED), thin film transistors (TFTs), and solar cells[107]–[110]. Transparent conductive oxides (TCO) and Transparent semiconductive oxides (TSO) are the main investigated materials to attain such devices[69]. Indium tin oxide (ITO), or tin doped indium oxide, is one of the most well-known transparent, conductive materials, where the conduction mechanism is scientifically interesting and this oxide has been widely used for a variety of applications (photovoltaics, biomedical devices) over other transparent conductors [111], [112].
The prominent aim of TCOs is to bridge sufficient transparency with a moderate conductivity. Several other materials such as Indium (III) oxide (In_2O_3), Tin (IV) oxide (SnO_2), and Zinc oxide (ZnO) can fulfil these needs but in their undoped stoichiometric state, these oxides are insulators. Substitutional doping (n-type) and oxygen vacancies play important roles in the conductivity of such oxides[111]. In an n-type TCO, lattice defects in the crystal, substitutional defects, and oxygen vacancies can create excess of electrons.

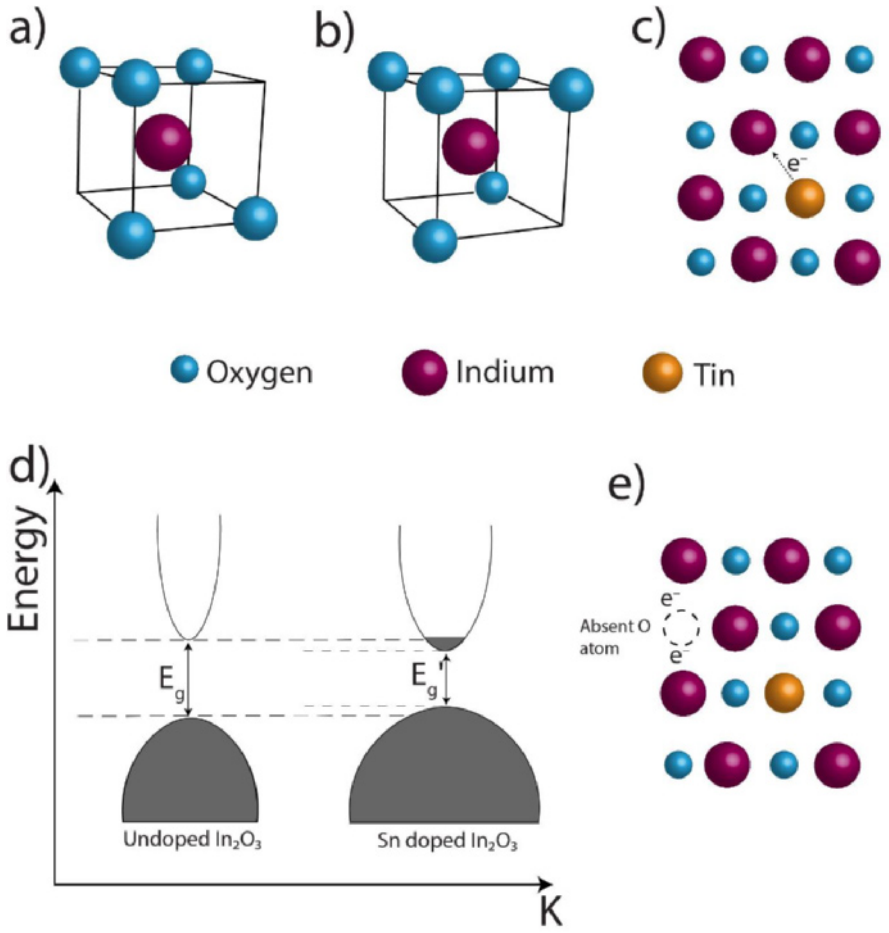

Figure 3.5. Indium oxide structure a) and b), c) Sn doping sites in In_2O_3 lattice. d) Band structure and effect of tin doping. e) Oxygen stoichiometry).

For the special case of ITO, impurity doping controls the conductivity of the material. Firstly, Sn^+ atoms are introduced and they replace In^+ atoms in the lattice (Figure 3.5c) and each replacement donates an electron to increase the carrier concentration and therefore the conductivity[113], [114]. The best performing ratio then becomes 10% SnO_2 to 90% In_2O_3 by weight. With the addition of Sn dopants, donor density increases, and the electronic states at conduction band are filled. This leads to widening of the optical bandgap (Moss-Burstein shift), [110], see Figure 3.5d.

Additional to the impurity doping, resistivity of ITO can be tuned by the stoichiometry. Lack of stoichiometry due to the oxygen vacancies is observed during the material deposition. An absent oxygen atom leaves two electrons which contributes to overall conductivity, see Figure 3.5e. For the most transparent oxides, the conductivity is primarily the result of oxygen vacancies. This provides an opportunity to precisely control the conductivity by varying the oxygen partial pressure during the deposition and manufacturing of amorphous structures. Using ITO as a transparent semiconducting oxide holds potential as a transistor channel

material. By controlling the oxygen partial pressure during deposition (higher oxygen content) oxygen vacancies are depleted and low electron density and high resistivity are provided, desired parameters to construct an accumulation mode semiconducting transistor channel [111]. This conductivity tunability allow to construct functional (capacitive sensing, transparency etc.) electronic devices. One device structure that can use ITO as a functional material is electrolyte gated field effect transistor (EGFET). ITO's properties such as transparency, high charge carrier mobility and low electrolytic capacitance make ITO an excellent candidate for transistors and electronic circuits.

To attain fully transparent EGFETs, ITO is used as the source and drain electrodes (conductive state) as well as for the channel material (semiconductor) in our device designs. During the sputter deposition by controlling the oxygen partial pressure we have achieved semiconducting (resistive) ITO and current collector (low sheet resistance) ITO in Paper **V**.

3.2.3. Other active materials

During the development of the thesis, several active materials are also investigated. To boost the areal capacitance, materials that possess high gravimetric capacitance can be introduced within the electrode structure. One of the most studied and commercially available materials are activated carbon and MnO_2, which allow for solution processing manufacturing. Activated carbon is mostly used in commercial devices due to the high electrical double layer capacitance, stability, and possibility of being produced from the biomass. It is water dispersible and can provide F/cm^2 capacitance[115]. Metal oxides, specifically Ruthenium oxide, is another promising material for high capacitance; however, the cost of ruthenium makes the cheaper manganese oxide one of the promising candidates. It has high theoretical capacitance (1000 F/g) and solution processability, where it can find itself within the symmetric supercapacitors and battery cathodes[116].

3.3. Electrolytes

Electrolytes are important components of the electrochemical devices, as they contain ions that can be mobilized with an electrical impulse. It can be an acid, base or salt dissolved in a solvent or solid network. These disassociated structures turn into ions, which can act as an ionic conductor under electric field. Electrolytes can be classified as aqueous, solid state and gel electrolytes[117]. Electrolytes have different operating voltage window or the cell voltage. Aqueous electrolytes can provide a safe window of 1 V, as the decomposition of water occurs at 1.23V. Organic solvents, nonaqueous electrolytes can provide operation voltage up to 2.7 V, however, they have lower ionic conductivity compared to aqueous ones. Ionic liquids, on the other hand are organic salts at low temperatures (≤100 °C) and can be operated up to 6V [118]. Ionic liquids are molten salts, possessing high ionic conductivity and have been used in energy storage systems in the last two decades. The liquid electrolytes that are water-based salt electrolytes, remain the ultimate choice for green technologies. Aqueous NaCl, KCl etc. between 0.01 M and 1 M concentrations have been used in Paper I. A gel electrolyte can be described as polymer (binder) mixed with salt. Poly (ethylene oxide) (PEO), Polyvinyl alcohol (PVA), Ethyl Cellulose, starch, polyvinylidene difluoride (PVDF) etc. mixed with different salts can provide good ionic conductivity with flexibility and stretchability. Depending on the

viscosity of the resulting gel electrolytes, they offer various coating possibilities including doctor blade, screen printing and spray coating [119]–[121]. Hydroxyethyl cellulose (HEC) is blended with imidazolium based ionic liquid, 1-Ethyl-3-methylimidazolium ethyl sulfate (EMIM-ES) to achieve printable gel electrolyte for paper **II, III, IV** and **VI**.

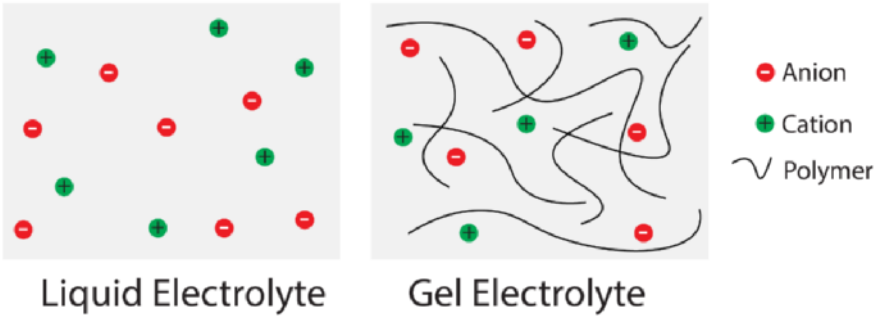

Figure 3.6. Types of electrolytes.

CHAPTER IV

4. Device Concepts Developed in the Thesis

This chapter summarizes the theoretical background regarding the devices that were designed and fabricated. Governing equations for material and device characterization and analysis, typical classification of electronic devices can be found in this chapter.

4.1. Ion Processes and Charge Transport

There are three processes in case of ion transport, originated from the movement of ions: migration, diffusion and convection[122]. Migration can be explained as ion movement driven by electric field. Ions diffuse from high concentration to low concentration in case of concentration gradient. Fick's first law, where the flux of particles if proportional to the concentration gradient[117].

$$J = -D\frac{\partial c}{\partial x} \tag{4.1}$$

where, J is the diffusion flux, D is the diffusion coefficient and c is the concentration.
In case of two or more dimensions,

$$J = -D\nabla c \tag{4.2}$$

Fick's second law states how diffusion affects the concentration change in time.

$$\frac{\partial c}{\partial t} = D\frac{\partial^2 c}{\partial x^2} \tag{4.3}$$

For the case of migration, the movement of charged species under an applied electric field[123], the total flux density can be expressed with Nernst-Planck equation (one dimensional case with absence of drift velocity)[124]:

$$J = -D\frac{\partial c}{\partial x} - \frac{zF}{RT}Dc\frac{\partial \varphi}{\partial x} \tag{4.4}$$

where J is the flux (mol s^{-1} cm^{-2}), D is the diffusion coefficient (cm^2/s), z is the charge, F is the Faraday constant, R is gas constant, T is the temperature, φ is the electric potential, c is the concentration (mol/cm^3).

In paper 2, the model system is described by the Nernst-Planck-Poisson (NPP) equations for charge carriers (ions and holes)[100]. Hole concentration ρ is located in the electrode material. Ions with concentrations c_i are located in both electrode and electrolyte fractions. The governing equations for ions expressed as:

$$\frac{dc_i}{dt} - \nabla\left(D_{c_i}\left(\nabla c_i + z_i f c_i \nabla V_{c_i}\right)\right) = 0 \tag{4.5}$$

$$-\frac{\varepsilon\nabla^2 V_c}{e} = \rho + c_{K^+} - c_{Cl^-} - c_{fix} \tag{4.6}$$

where V_c is an electrostatic potential in ionic phase, c_{fix} is the concentrations of fixed PSS-anions, $f = F/RT$, and i is anion and cation.

Equations for holes are modified to capture effects of a Gaussian-like density of states

$$\frac{d\rho}{dt} - \nabla\left(D_\rho\left(\nabla\rho + f\rho\nabla\left(V_\rho + \frac{\mu_\rho}{e}\right)\right)\right) = 0 \tag{4.7}$$

$$-\frac{\varepsilon\nabla^2 V_\rho}{e} = \rho - \left(V_\rho - V_c\right)C_{edl}^{sim} \tag{4.8}$$

where V_ρ is an electrostatic potential of holes, μ_ρ the chemical potential of holes, C_{edl}^{sim} is the intrinsic volumetric capacitance of PEDOT:PSS that originates from the double layer between charge carriers and counter-anions in PEDOT:PSS[98], [125].

The Nernst-Planck-Poisson model described above allows to calculate charge and discharge of the electrode using electrostatic interaction and calculate charge carrier concentrations (holes and ions), charging currents and potentials.

Convection can be defined as hydrodynamic transport, where ions can move because of the solvent motion such as laminar flow and gravity-induced flow.

4.2. Capacitor Principles

Capacitors for energy applications predate the invention of the battery. Alessandro Volta is the inventor of Voltaic pile in 1800, where he used Zn and Cu plates separated by paper soaked in vinegar[97]. However, before this invention, at the University of Leyden, the Leyden jar was developed in 1745 as a static energy source, which can be referred as a capacitor[117]. Today's capacitors are mostly used to store, and quick release of electrical energy and these components found applications in modern integrated circuit systems. One of the biggest technological advantages of capacitors is that they can provide high power density compared to batteries or fuel cells. However, the amount of stored charge is the limiting factor for high energy density[126].

A capacitor is a component that stores energy electrostatically. When two parallel plates are separated by a dielectric, a typical capacitor can be constructed. The capacitor is charged with an applied potential difference across the electrodes. The positive and negative charges migrate towards the electrodes of opposite polarity. For the case of a charged capacitor, this device can work as a voltage source for a relatively short time. The geometry of a capacitor is shown in Figure 4.1a. Inside of the dielectric material there are electrical dipoles, which can be aligned by an external electric field. After the charge distribution, the charge density ρ can be defined. The capacitance has the unit Farad (F) and is equal to ratio between stored charge, Q and the potential difference, V. Equation 4.9 defines the capacitance for the parallel plate capacitor, where A is the area, ε if the permittivity and d is the distance between the plate or the thickness of the dielectric.

$$C = \frac{Q}{V} = \varepsilon\frac{A}{d} \tag{4.9}$$

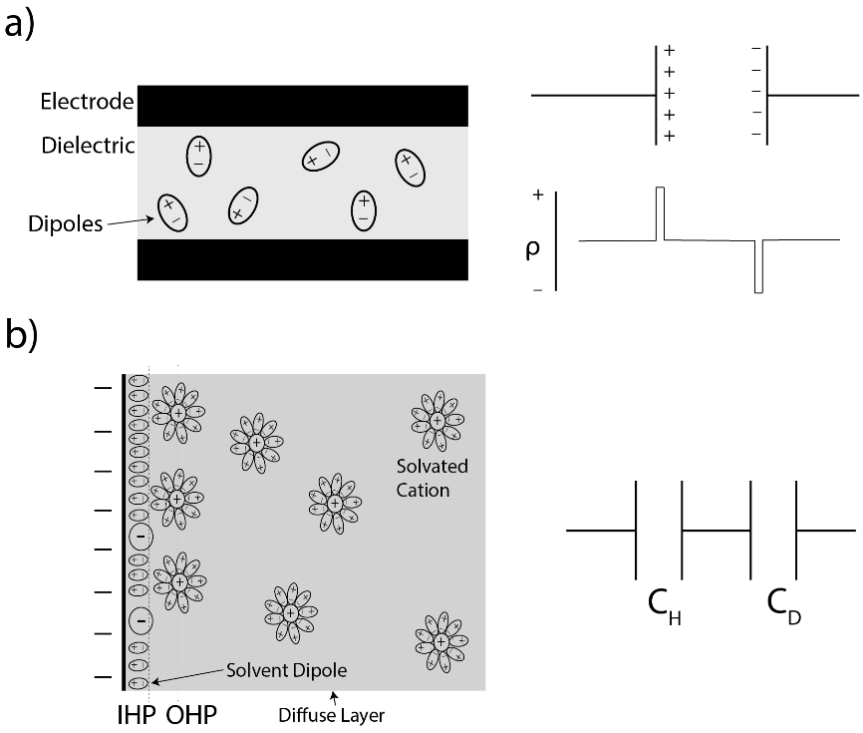

Figure 4.1. Capacitor Principles. a) Schematic of parallel plate capacitor. b) Schematics of electrical double layer.

The concept of double layer is an important principle, which has found many applications in our daily life electronics. It was first developed by Helmholtz in nineteenth century[117]. The non-Faradaic charge storage (electrostatics) concept is explained using an interface between the electrode and electrolyte (no electron transfer). The model states that two oppositely charged electrodes are separated by an Ångström level distance (typically 0.1 nm). The double layer is composed of Inner Helmholtz Plane (IHP), Outer Helmholtz plane (OHP), and the diffuse layer (Figure 4.1b). At the electrode electrolyte interface (Stern Layer), solvated ions are adsorbed by the electrode and at the diffuse layer, there is a gradient of ions. Therefore, two capacitances in series should be considered. The relation between capacitance of the interface, C_{EDL} the compact double layer capacitance (C_H) and diffuse layer capacitance (C_D) is given as equation 4.10.

$$\frac{1}{C_{EDL}} = \frac{1}{C_H} + \frac{1}{C_D} \tag{4.10}$$

There are many factors that determine the EDL capacitance such as conductivity of the electrode, area, porosity and electrolyte[97]. In EDL capacitors, the electrode material is highly porous, so the high surface area enables enhanced double layer capacitance, which brings attention to study this phenomenon in this thesis.

Commercial capacitors are highly used in our daily life. Ceramic chip capacitors and electrolytic capacitors are mostly used in integrated circuits, high power systems and AC applications (Figure 4.2). EDL supercapacitors are in use for high energy requiring applications and research towards their development is rapidly growing[117], [127].

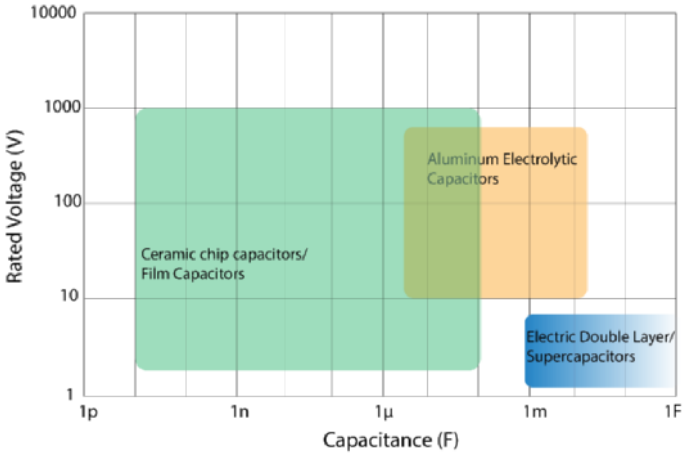

Figure 4.2. Capacitance and operation voltage for commercially available capacitors.

Several types of capacitors are available and can be classified by the mechanism or the material used (Figure 4.3). Each class has different application areas and provides different capacitance retention on cycle life and energy efficiency[117].

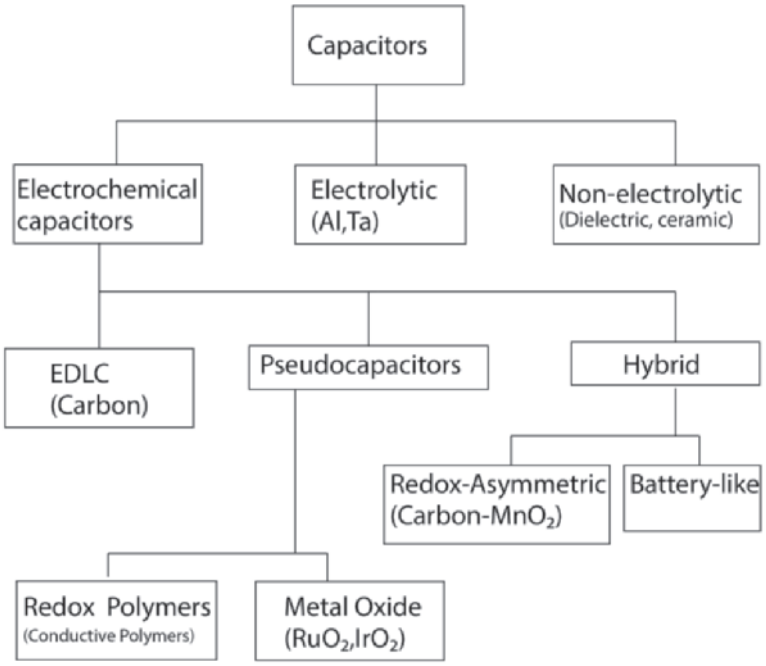

Figure 4.3. Classification of Capacitors.

Two parameters of a capacitor can define the performance, namely energy and power density, which can be expressed as per active material mass, unit area or unit volume[97]. The energy E (Joule) stored is dependent on the capacitance and square of the operation voltage:

$$Energy\ Density = E = \frac{1}{2}CV^2 \tag{4.11}$$

Power (Watts) can be defined as the rate of energy per time (discharge time).

$$Power\ Density = P = \frac{E}{\Delta t} \tag{4.12}$$

In case of a capacitor device, the resistance of each component (current collectors, electrode conductivity, electrolyte, and separator) should be included within the overall resistance. The sum of these, referred as equivalent series resistance (ESR). To calculate the maximum power density, ESR should be considered[126].

$$P_{max} = \frac{V^2}{4R_{ESR}} \tag{4.13}$$

C is the capacitance; V is the operating voltage, t is time. The m (active material mass) for gravimetric (kg), A (area), for areal (cm^2) and V (volume) for volumetric (cm^3) should be placed to the denominators of the equations 4.11, 4.12 and 4.13 to define the energy and power density. The overall performance can be represented by the power and energy density, and those numbers (energy storage device metrics) can be plotted in a graph called, Ragone plot[120]

(Figure 4.4). Supercapacitors are bridging the gap between high power density capacitors and high energy density batteries.

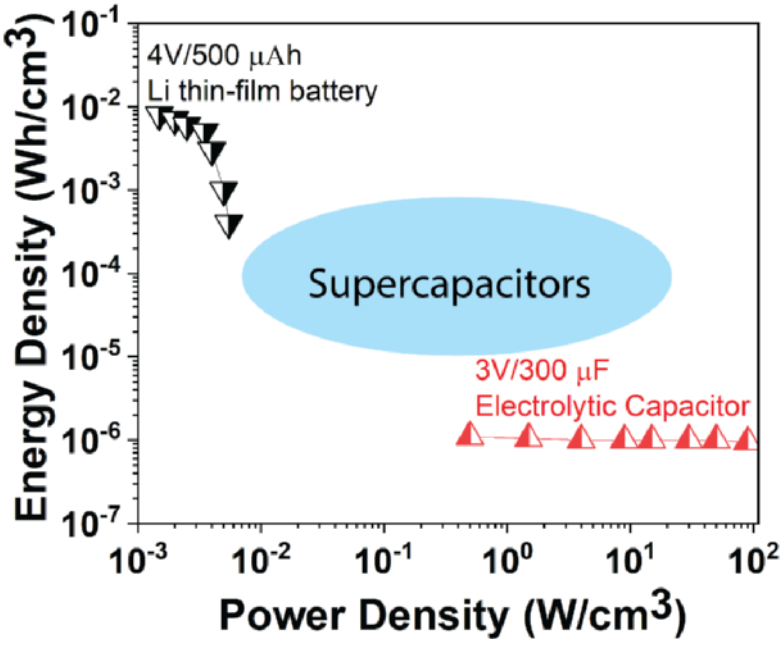

Figure 4.4. Energy and Power density comparison for energy storage devices (Ragone plot).

4.3. Supercapacitors and Batteries

In electrical energy storage systems, the energy can be stored in two different ways[97]. The first one is the chemical energy dependent Faradaic reactions as in the case of batteries. This indirect way is based on oxidation and reduction of the electrodes having opposite electrode potentials. The second one is the direct energy storage using electrostatic way, which is known as non-Faradaic process, i.e capacitors. To clarify the differences between electrochemical capacitor and batteries, the mechanisms should be explained[117]. For the double layer capacitor, the process is non-faradaic, meaning ideally no electron transfer takes place across the electrode interface and electrostatic charge storage is present. In batteries, the main Faradaic process is based on electron transfer, where change in the oxidation state of the electrodes occur. There is one intermediate process, where Faradaic charge transfer occurs due to the special thermodynamic conditions. This principle originated from the work called 'RuO_2: a new interesting electrode material', where upon an electrode potential there is a dependence on charge that pass Faradaically, typically the material changes its oxidation state due to a redox reaction [97]. This corresponds to the term called pseudocapacitance[128].

The huge capacitances (F/g) of carbon systems and metal oxides led to the term supercapacitor or ultracapacitor. This device can allow high capacitances in a small volume using porous materials. Several attractive application areas have been developed due to the high capacitance values and high-power density during the past decades.

The differences between a battery and a supercapacitor can be explained by studying the charging and discharging curves (Figure 4.5).

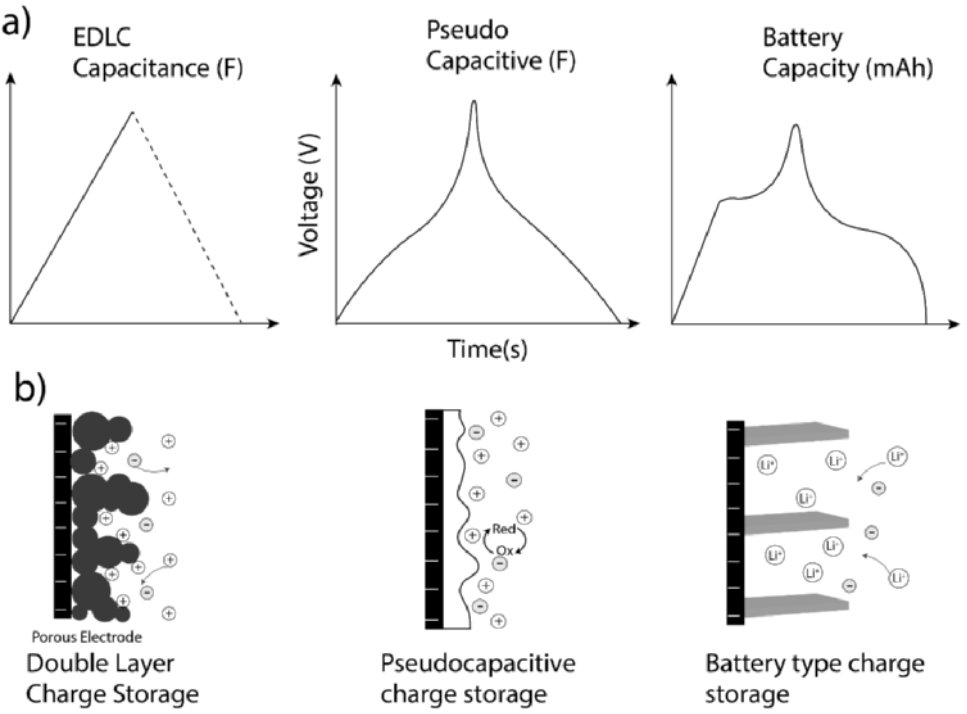

Figure 4.5. Galvanostatic charging and discharging (GCD) curves for different types of electrode systems. a) GCD curves of electrode materials, b) Electrode processes for charge storage mechanisms.

At the most fundamental level, because of the charge storage mechanism, there is a linear relationship between the charge and voltage, where the simple equation $C = i\,\frac{dV}{dt}$ can be used to calculate capacitance (F). Hence, EDLC resembles the same output curve as the typical electrolytic and dielectric capacitors. Pseudocapacitors can store charge through redox reactions, where these reactions can cause deviations from the ideal shape[126]. The equation for the capacitance can be derived as $C = i\int(\frac{1}{V(t)})dt$. Reporting GCD curves of batteries give information about insertion and extraction potentials about the electrode materials. Such GCD curves show clear redox peaks during charging and discharging. For the battery case, instead of capacitance, the capacity should be calculated (mAh g^{-1}). It should be noted that to understand the potential charge storage capability, a theoretical comparison of stored charges for supercapacitors and batteries should be given. For an EDLC, up to 2.0 electrons per atom, for pesudocapacitance 2.5 electrons per atom and for battery up to 3 electrons per atom or molecule of accessible surface can be accessible [97].

Supercapacitor	Battery
Charge discharge Curves are mirror output of one another	Not reversible
Behavior is capacitive	Not capacitive, redox dominant
High degree of reversibility	Irreversibility (materials and kinetics)
High power density	Poorer power density due to the kinetics
Low energy density	High energy density
High number of cycles	Less cycle numbers
Less temperature dependent	Temperature dependent activation

Table 4.1 Comparison of electrochemical capacitors and battery systems [97].

4.3.1. EDLC & Pseudocapacitors

The most well-known capacitor types for high energy density are EDLC and Pseudocapacitors. The double layer formation and electrostatics are the main charge storage mechanism for the EDL capacitors[129] and carbon is the most well-known and widely used material for the construction [117]. In EDLC, the active material is highly porous, and it creates high surface area. The double layer capacitance is enhanced due to the overlapped diffused layers in the very fine pores. The high surface area of the electrodes can supply more energy than a conventional capacitor due to the extended area for the ion penetration. The construction of EDLC is quite simple: two electrodes separated with an ion permeable separator to prevent any short circuit. Both electrode-electrolyte interfaces are considered as a capacitor, so that a complete cell is two capacitors in series. The specific capacitance generally is derived from the three-electrode measurement setup, where active material mass is considered. The cell capacitance is the overall measured capacitance from the two- electrode measurement. The specific (gravimetric) capacitance of an electrode, C is given by

$$C(F/g) = \frac{2\ x\ C_{cell}}{m} \tag{4.14}$$

Where m is the mass of active material.

High surface area carbons ($m^2\ g^{-1}$), carbon nanotubes, aerogels and graphene have been processed as EDL electrodes[130]. Specific capacitances up to 400 F/g have been reported[130], [131]. Commercial EDLC are in the real-life applications due to the low cost, chemical stability.

Pseudocapacitor working mechanism is based on fast and reversible redox reactions, where these reactions contribute to the double layer capacitance[36]. A charge transfer process takes place at the active material and the surface. The most common pseudocapacitive materials are transition metal oxides (RuO_2, MnO_2) and conductive polymers. As demonstrated in Figure 4.6, pseudocapacitive material undergo a reversible redox reaction, an electron transfer process occurs between oxidized and reduced species, thus pseudocapacitance arises with a dependence

on voltage. There are three types of pseudocapacitance: redox system, intercalation system and underpotential deposition[128].

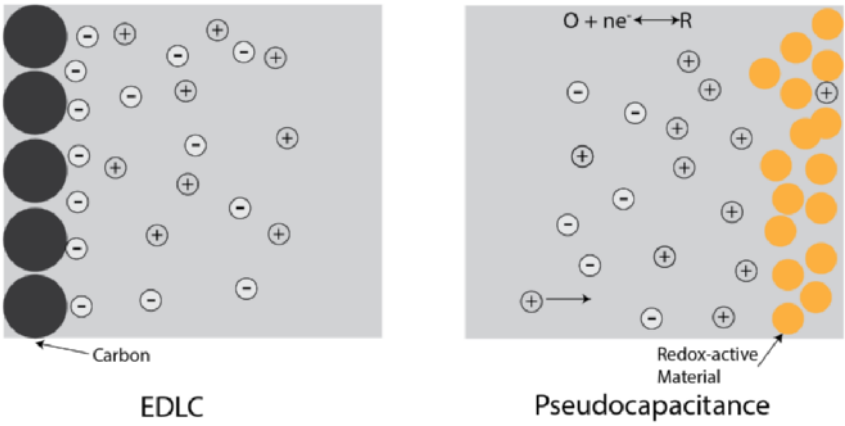

Figure 4.6. Charge storage mechanism in EDLC and Pseudocapacitors.

Conductive polymers (Polyaniline-PANI, Polypyrrole-PPy, PEDOT) are well known pseudocapacitive materials[96]. Using electrochemical oxidation and reduction reactions, introducing positive or negative charges into the conjugated polymer chains has given interest to these materials as supercapacitors[132]. Conducting polymers store electrochemical energy through their redox processes. Two main features of electrochemical property make these materials suitable for supercapacitor applications, first continuous range of oxidation with increasing electrode potential and secondly the reversibility of the redox reaction, i.e injection and reinjection of the charges[97]. The polymer electrode takes up ions in the process of p-doing and an ion inserted increases the electrical conductivity. Conductive polymers are p-doped with anions when oxidized and n-doped with cations when in the reduced state. Conductive polymers store charge within the entire volume and fast doping and de-doping of the ions. These materials are cheaper than the metal oxides and provide higher capacitances. However, the long-term stability and degradation are the main concern for this pseudocapacitive materials. The most common configuration is the symmetric; uses the same p-doped polymer for both electrodes, where the positive electrode is fully oxidized, and the negative is neutral. Because of its metal like signatures, in their conductive states of these polymers, it can be treated as if capacitance arises from the double layer. Paper **I** investigates the double layer capacitance of the PEDOT based composites using both experimental and theoretical methods.

Polyaniline (PANI) and Polypyrrole (PPy) are two of the most studied conductive polymers for supercapacitor applications. PANI shows high specific capacitance (1500 F/g), PPy has a capacity to deliver 500 F/g. These materials are based on electro-polymerization methods, where paper-based electrodes can be achieved for flexible conductive polymer-based supercapacitors[133], [134].

PEDOT (Poly(3,4-ethylenedioxythiophene)), due to its high conductivity, solution processability makes it an ideal candidate for engineering flexible supercapacitors. In particular,

one of the most studied conductive polymers, PEDOT exhibits efficient charge transport, low impedance, and high stability as cathode [50], [52], [135], [136]. In energy storage applications, PEDOT can be used as a capacitive coating material for Li-battery cathode and as an electrode material for supercapacitors, where the material can be produced with both physical deposition techniques and polymerization methods such as oCVD (oxidative chemical vapor deposition) and electro-polymerization[93], [137], [138]. The focus over the last decade has been dedicated to utilizing PEDOT-based materials, deposited through both electro-polymerization and vapor-phase (VP) methods or solution processed based methods[46]–[50]. It is reported that the Electro- and VP-polymerization methods can deliver high capacitance (up to 206 F/g) PEDOT electrodes[46], [47], [93]. In addition to that printing of water-dispersible PEDOT:PSS (PEDOT: polystyrene sulfonate) provide control over the thickness, large area coverage while maintaining sufficient energy density [51]–[53]. PEDOT:PSS has been incorporated into printing processes with paper-based materials to achieve fully printed paper energy storage systems, demonstrated in use cases and flexible electronics applications[51], [121].

4.3.2. Performance Parameters for Supercapacitors

The overall performance of a supercapacitor is influenced by several parameters, active material, which defines the capacitance (active material mass, porosity) and the operation voltage (electrolyte) and the internal resistance (ESR)[97], [126]. ESR is quite dependent on the intrinsic electronic resistance of the electrode, interfacial resistance between the electrode and the current collector, electrolyte's ionic resistance (in case of solid-state electrolyte, gel electrolyte and separator additional interface resistances should be included) and diffusion resistance. A high ESR is big issue and will limit the power density, where high power peaks can hardly achieve. One of the biggest advantages of using supercapacitors is delivering high power in short amount of time. In this thesis, it is aimed that the ESR can be lowered down by providing high conductivity electrodes and good adhesion between the supercapacitor components using printing methods.

The fabrication of energy storage devices is dependent on the processes, layer geometry and the architecture. Figure 4.7 shows the cell designs for the supercapacitors, micro-supercapacitors and batteries[139]. The good contact between high conductivity electrode and the current collectors will achieve the best performing device out of the selected materials and the manufacturing techniques.

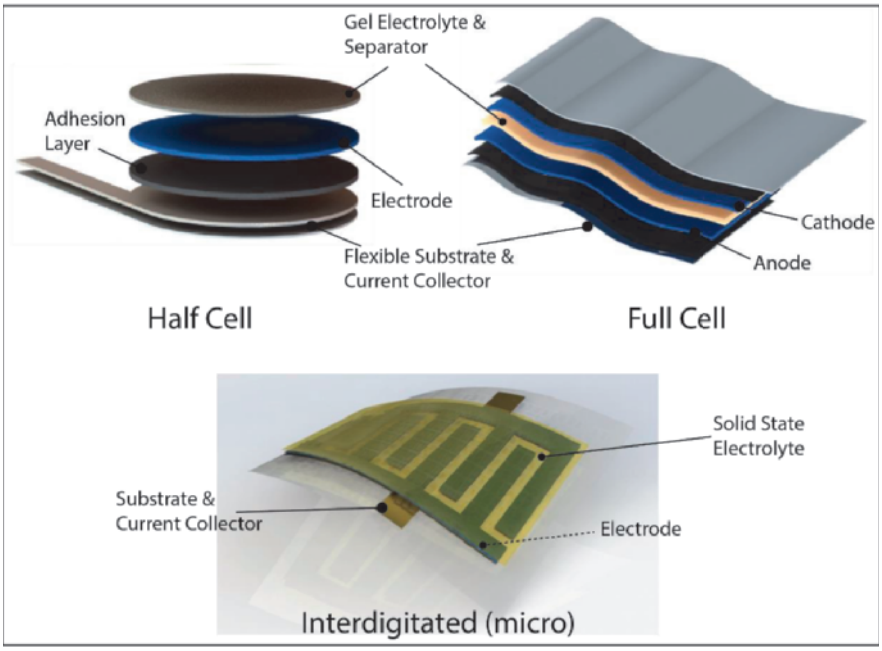

Figure 4.7. Device configurations for energy storage devices.

In general, the half-cell structure consists of electrode and the current collector. The full cell is the real device with anode and cathode for battery case and identical electrodes in a symmetric supercapacitor device structure. Micro-batteries or micro-supercapacitors can be constructed as interdigitated electrodes, where finger electrodes can be constructed as anode or cathode[140], [141]. This strategy allows to construct planar devices with less volume, therefore facilitates to save area for series and parallel connections to increase the operation voltage.

4.4. Electrolyte Gated Transistors (EGT)

Among all kinds of transistors, electrolyte gated transistors (EGT)s use an electrolyte between the channel and gate[142], whereas the traditional FET utilizes a solid state dielectric. Electrolyte gated field effect transistors (EGFET) and organic electrochemical transistors (OECT) are thin film transistors that fall under the category of EGT. In EGTs, the electrolyte is a liquid or a solid-state ionic conductor, where once an external electric field is applied, ions of opposite charge move toward the gate electrode and semiconductor electrolyte interface. In an EGT, the channel current can be modulated by the gate voltage via capacitive mechanism at the interface [143]. When it is compared to organic FETs, this electrolyte gating has a much larger capacitance, which allow operation at low voltages. An electrical double layer is formed at the impermeable semiconductor/electrolyte interface for the case of EGFETs, or a volumetric capacitance of the channel material plays a role in permeable semiconductors. In each case the electrolyte/semiconductor interaction play a part in the main switching mechanism for EGTs [144].

The two different mechanisms for the operation of EGTs are portrayed in Figure 4.8. For the case of an impermeable semiconductor channel, the applied voltage to the gate causes accumulation of ions at the semiconductor/electrolyte interface. An electrical double layers is formed, which cause gating, as in the FET working mechanism, that result in charge carrier accumulation or depletion [142]. Ultrathin electrical double layers formed at the interface result in high capacitance, which names these devices as electric double layer transistors (EDLT). In case of permeable semiconductor having EGTs, ions penetrate into the semiconducting film under the bias of V_G, changing the doping state of the semiconductor. The capacitance formed here is not EDL based but volumetric due to the redox activity.

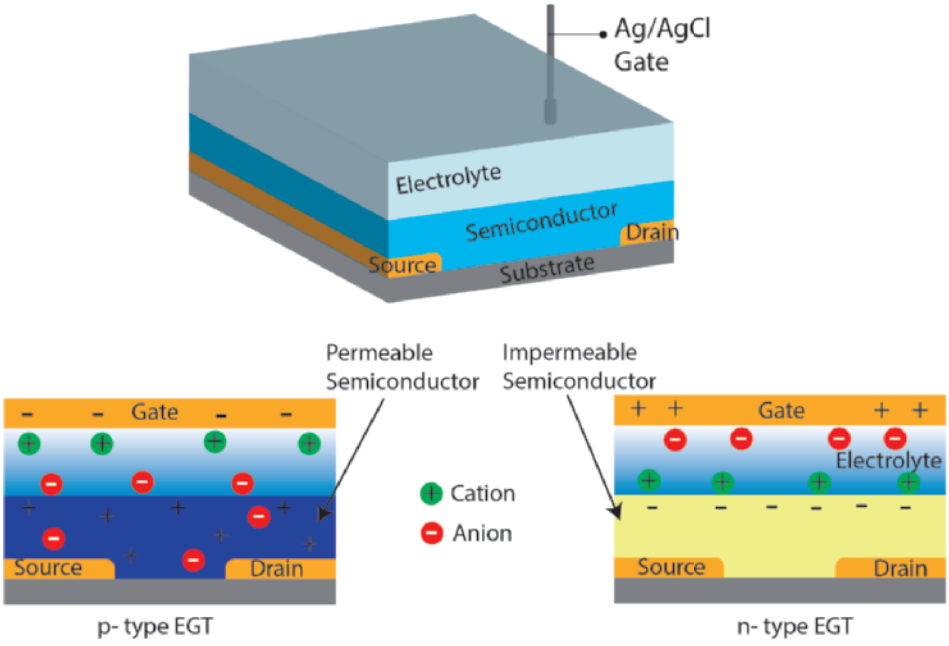

Figure 4.8. Schematics for EGT with an ion permeable (*left*) and an ion impermeable (right) semiconductor.

As a result of the EDL formed at the interface for the ion impermeable EGFET, this structure can be treated as a capacitor with Debye screening length (λ). These EDL capacitors can achieve up to 1-10 μF/cm², where the applied gate potential drops at the formed EDL interface[144]. For the linear regime, the channel current is given by the equation 4.15 when $V_D \leq (V_G - V_{th})$

$$I_{DS} = \frac{W}{L}\mu C\left[(V_G - V_{th})V_D - \frac{V_D^2}{2}\right] \tag{4.15}$$

When $V_D > (V_G - V_{th})$ in the saturation regime,

$$I_{DS} = \mu C \frac{W}{2L}(V_G - V_{th})^2 \tag{4.16}$$

where W and L are the channel width and length, respectively, μ is the charge carrier mobility, C is the capacitance of EDL formed at the interface, V_{Th} is the threshold voltage, V_D is the drain voltage, and V_G is the gate bias.
The typical transfer and output plots for n-type EGT are shown in Figure 4.9. It should be noted that for the case of an accumulation mode n-channel device, it is normally (at V_G=0) in the off-state, a positive gate bias is applied for the drain current flow [145].

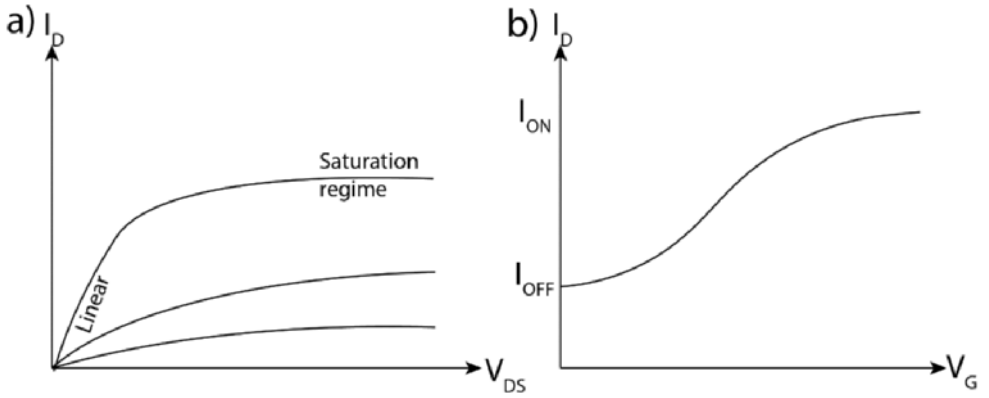

Figure 4.9. EGTs operating with n-type semiconductor. a) Output characteristics for an n-type EGT indicating the saturation and linear regimes, b) transfer characteristics.

Another key parameter for EGTs is the switching speed between OFF and ON states. The switching speed for FETs depends on the channel geometry, charge carrier mobility. For EGTs this relates to the polarization speed and EDL formation time, which define the switching speed and therefore the operation frequency[142].
The RC time constant describes the polarization time, where a small RC is desired for device operation,

$$RC = \frac{lC}{\sigma}, \tag{4.17}$$

where l is the electrolyte layer thickness, C is the double layer capacitance, and σ is the ionic conductivity.
Additionally, another reported parameter to evaluate the performance of an EGT is the transconductance (g_m), which defines the amplification by the equation,

$$g_m = \frac{\Delta I_D}{\Delta V_G} \tag{4.18}$$

OECTs (having permeable semiconductor) are well known for employing a conductive polymer that is ion permeable and can undergo redox reaction during operation. For a permeable semiconductor, for example PEDOT: PSS, the ions can penetrate through the semiconductor film, modulating its conductivity within an electrochemical process[144], [146]. A redox process occurs where PEDOT can undergo oxidation and reduction reactions. The ON and OFF mechanism can switch between oxidized PEDOT and neutral (insulating) PEDOT states. This

redox process occurs throughout the film volume and OECTs take advantage of high volumetric capacitance and therefore, in the case of an electrochemical transistor, the resulting steady state current equation is:

$$I_{DS} = \frac{W \cdot d}{L} \mu C^* \left[(V_G - V_{th}) V_D - \frac{V_D^2}{2} \right] \tag{4.19}$$

where W, L, and d are the channel width, length, and thickness, respectively, μ is the charge carrier mobility, C^* is the capacitance per unit volume, V_{Th} is the threshold voltage, V_D is the drain voltage, and V_G is the gate bias.

In summary, there are many types of EGTs such as OECTs, EGFETs, ion-sensitive field effect transistors (ISFETs), and electrical double layer transistors (EDLTs) that utilize different active materials. Conductive polymers, semiconductive oxides, and 2D materials are the main materials for the advancement of future sensing and low power electronic applications[5], [147]–[149].

CHAPTER V

5. Upscaling Energy Storage Devices with Printing Technologies

Printing methods are widely used in flexible electronics, and depending on the viscosity of the conducting ink, several methods can be selected for device fabrication. Roll to roll and sheet by sheet methods are preferred for mass production at low cost. By engineering the ink properties, devices including FETs, batteries and interconnects can be printed. For organic electronic device fabrication, printing methods such as inkjet printing, screen printing and spray coating were compatible with the inks developed in this thesis.

5.1. Ink Preparation and Theory

Inks are the mixtures of solute (powders or liquids) that are dispersed in a solvent to form dilute dispersions or pastes. Additives, binders, active materials and the nature of solvent define the properties of the ink[150]. For successful printing, the ink undergoes an optimization process with ink viscosity and surface tension being two important parameters to consider. Besides controlling ink properties, choosing a compatible substrate and choice of printing technique are equally important in process optimization. Understanding the ink-substrate interaction and finding the suitable printing method will increase the throughput of the manufacturing processes (Figure 5.1).

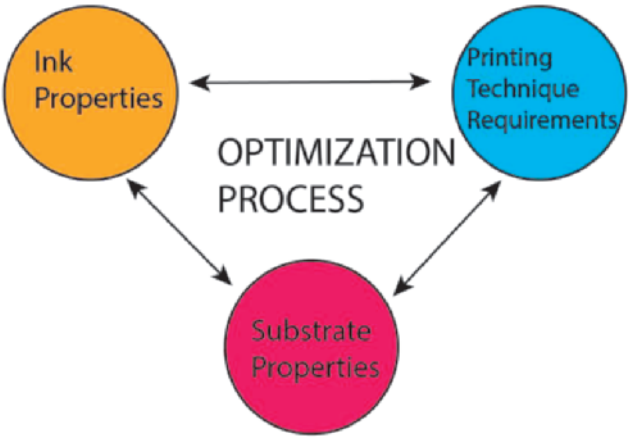

Figure 5.1. Methodology to optimize printing processes.

Rheology is the research field of understanding flow and deformation of matter. Rheology helps to understand ink or paste properties and defines their compatibility with a particular printing technology. Viscosity is a measure of the resistance of a liquid to flow [151], [152]. This concept can be studied by examining an ideal system, called parallel plate experiment (Figure 5.2).

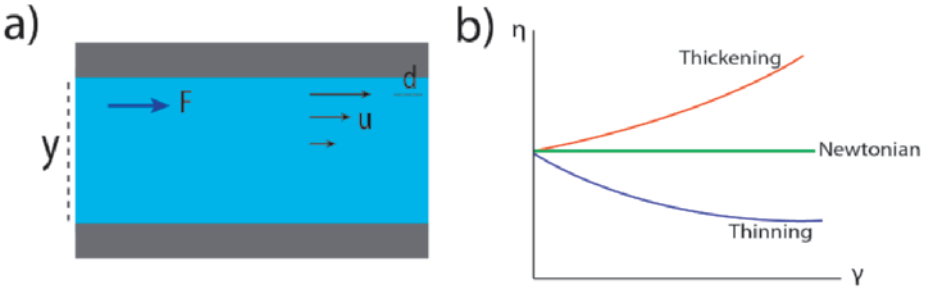

Figure 5.2. a) Geometry defined to understand the shear flow and governing equations, and b) viscosity vs shear rate graph to understand the behavior of fluids.

Shear stress is force (F) divided per unit area (A) can be given with:

$$\tau = \frac{F}{A} \tag{5.1}$$

For Newtonian liquid (ideal viscous behavior), shear strain is:

$$\gamma = \frac{d}{y} \tag{5.2}$$

In response to the force, the upper layer moves a distance of d and h is defined gap between plates.

Shear rate is given as velocity gradient:

$$\dot{\gamma} = \frac{u}{y} \quad (s^{-1}) \tag{5.3}$$

Shearing stress then becomes, newtons/m^2 or Pascal (Pa):

$$\tau = \eta\dot{\gamma} \tag{5.4}$$

Viscosity can be given as, $\eta = \frac{\tau}{\dot{\gamma}} = \frac{Pa}{s}$, where 1 Pa s = 10 poise and 1 m Pa s = 1 centipoise (cp).

Film formation during deposition depends on the ink; content of solute and solvent or the properties such as viscosity and surface tension. After describing fluid motion to characterize the systems, two parameters are introduced, Reynolds and Weber number. The Reynolds number (R_e) represents the ratio of inertial forces to viscous forces, and

$$R_e = \frac{\rho d v_0}{\eta} \tag{5.5}$$

Weber number (W_e) is ratio between inertia and surface tension:

$$W_e = \frac{\rho d v_0^2}{\gamma} \tag{5.6}$$

where v_0 is the impact velocity, ρ, d, η and γ are density, droplet diameter, viscosity, and surface tension, respectively.

These nondimensional numbers are Reynolds and Weber numbers can be described for the liquid phase and predict the behavior of the liquid systems.
Water can be used as an example, which has viscosity of 1.0 mPa.s, $R_e$of 50 and $W_e$of 69.16. These numbers can be used to understand mechanisms of jet breakup (droplet size and form)[153].
To optimize film formation in spray coating and screen printing, these parameters are important and together with the knowledge of wettability and surface roughness, optimum printing results can be achieved.

5.2. Spray Coating

Spraying or atomization is a technique, where a liquid is pushed (by gas or air) through a nozzle that produces droplets which are directed towards a surface[154]. Spray coating uses formation of small droplets from an ink solution with the air pressure and the droplets forming a thin layer that subsequently dries on a solid substrate. Briefly, with the gas pressure the liquid passes through a reservoir, a mixed liquid-gas flow is created. Due to the expansion a cone develops at the tip, where regions (dilute to very dilute) with a decreased density are developed[155]. Via the stream, the droplets (mist) are deposited to the sample surface. The shape and size of droplets can affect the deposited film morphology which, directly affect the film roughness and uniformity. Droplet size (defined by gas flow rate, viscosity), solvent evaporation speed (dictated by nozzle to sample distance), and nozzle types are the parameters to control homogeneous deposition. Figure 5.3a. shows the steps of a spray deposition. After the formation of small droplets (1-5 μm), they are transported to the substrate, where solvent evaporation occurs, and the dry particles form the film.
The deposition rate can be defined by the formula[155]:

$$\eta = \frac{\rho S}{cMv_s} v_{gr} \tag{5.6}$$

where, ρ is film density, S is the area, c is the concentration of the solution, M is the molecular mass of the solute, v_s is the spray rate, and v_{gr} is the film growth rate.
Liquid drop on the substrate is another sub-section of the deposition process (Splashing and deposition can occur during the deposition), that needs to be optimized[59]. The wetting plays an important role in the deposition, where surface tension is the parameter that defines the contact angle. As shown in Figure 5.3b, large contact angle (θ) represents hydrophobic surface, and small contact angle means hydrophilic surface. Choosing an appropriate substrate, control of the wettability (through additives), substrate morphology (with micro or nanostructured patterns) are the parameters to control the roughness and homogeneity of the deposited film[60].

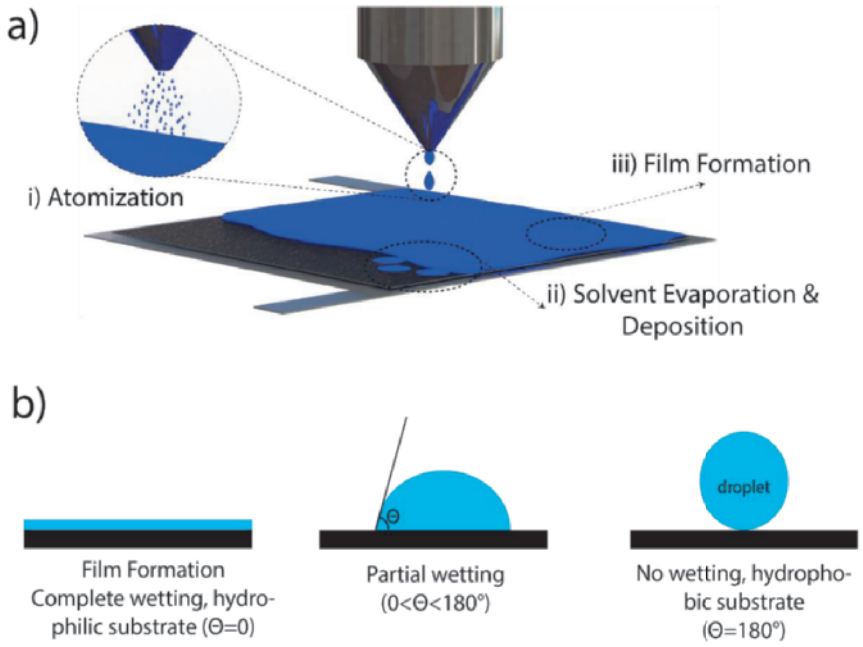

Figure 5.3. Film formation during the spray coating process. a) Film formation process with spray coating, (i) atomization process, mist of particles generated, at the process (ii) solvents evaporates and film islands are formed, (iii) with the cycles of spraying, small islands are interconnected, and thin- film starts to form. b) Liquid drop on a substrate.

Spray coating has been the method of choice for manufacturing thin coatings of nanomaterials or conformal deposition for the healthcare and food industry, as well as conductive composites [60], [153]. The handheld airbrush spray-coating allows for simple manufacturing, however the droplet volume is high, leading to bigger droplet size, with the drawbacks of less control over the thickness and clogging of nozzle[156]. Spray coating can generate small droplets by two different mechanism, namely ultrasonic spray coating and gas driven, pressurized systems. To achieve high quality yields in manufacturing, industrial air atomizing and ultrasonic spray technology can be used, where ultrafine droplets with narrow size distribution are formed, resulting in smooth films for large area applications, and offers roll to roll possibility as well due to the computerized, automatized systems[156]–[158]. In the case of ultrasonic systems, the spray head uses ultrasonic vibrations to form separated tiny droplets, causing quite low roughness and smoother films.

The well-known methods such as drop-casting and spin coating can deliver lab scale devices, however they are not compatible with roll-to-roll processes as area coverage is limited. Spray coating is an interesting method for organic electronics since several decades and promises to deliver unique properties to the fabrication. Spray coating is fast, low cost and compatible with large area, roll to roll system. During the development of the thesis, both the airbrush based, and automized spray coating systems were used. Figure 5.4 shows photos of the spray coating

setups that were used to manufacture paper electrode. These setups were used in Paper **II, II** and **IV**.

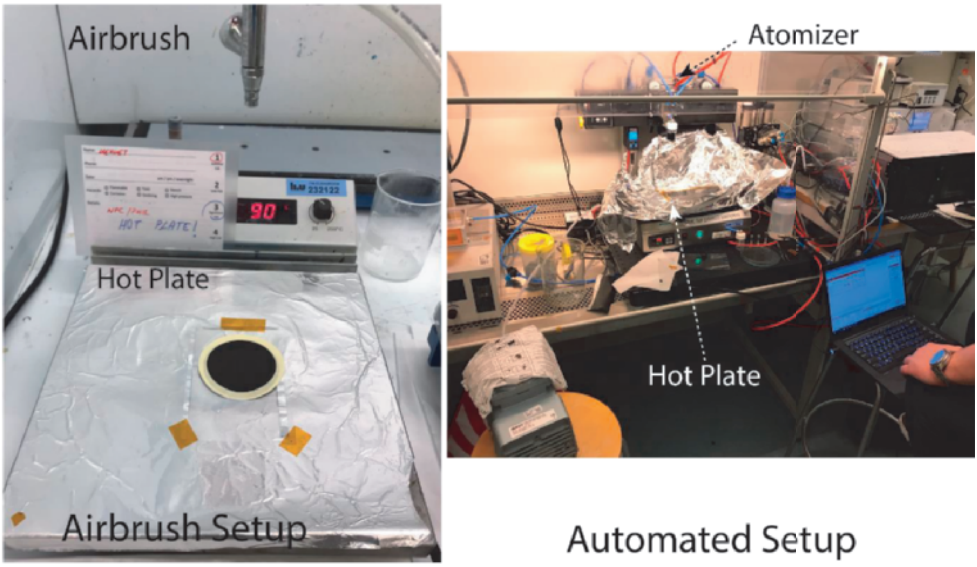

Figure 5.4. Typical setups for both airbrush and automated spray coating systems.

For the airbrush-based setup, the substrates were placed on a hot plate at 90 °C prior to spraying. The ink was spray-coated with an airbrush (CoCraft, 35 mm nozzle) using 2.0 to 3.0 bar on a substrate (having adhesion layer) through shadow mask (stainless steel, Kapton tape, paper). The airbrush was placed 7-15 cm above the substrate (nozzle to sample distance), and spraying protocol was followed (several seconds of spraying, several seconds of waiting). This spraying and waiting protocol was created to provide enough time for solvent evaporation and prevent accumulation of droplets at specific area onto the substrate.

For the automated setup, the experiments were performed using an industrial style atomizer-based spray setup. The nozzle was Compact JAU D555000 (Spray Systems Inc.), which was electronically controlled to open (spraying) and close (waiting) in every spray cycle. The sampling liquid was placed in a container at the spray nozzle and N_2 pressure was fixed at 1 bar with a flow of 30 l/min. The nozzle to substrate distance was set to be 20 cm. A vacuum hot plate (EMS 1000 series, Electronic Micro Systems) was used for quick evaporation of the solvent. To show large area electrode (18 cm by 20 cm), motorized linear stage (LTS300/M, Thorlabs Inc.) was used to move the spray nozzle across the sample surface. The range was selected 220 mm with a speed of 20 mm/s and an acceleration of 20 mm/s^2 for one pass. The spray deposition was performed while the head was crossing the sample surface with a pulsed operation mode. The ink was sprayed for 50 ms and the nozzle was closed for 950 ms for one cycle of operation. The automized setup was achieved to deposit up to 300 layers, which corresponds to 30 µm paper electrode.

To scale up energy devices, PEDOT:PSS based inks were developed to be used in spray deposition[159]. For the electrodes, spray coating allows for relatively thin semi-transparent PEDOT electrodes (<1 µm), which can provide moderate capacitances for the energy storage applications [135], [160], [161] In the thesis, spray coating is employed as the main electrode making technique to achieve thick yet flexible electrodes for wearable electronics.

5.3. Screen Printing

Screen printing uses stencil principle to push ink through the stencil (mask) on to a substrate using rubber squeegee. It has been used for decades for printing electronics and optoelectronic devices. During printing, the frame (reservoir) is filled with the ink, then a squeegee is drawn across the mesh. Forcing ink towards the opening of the screen results with a printed patterns on the substrate[152]. Typical schematics can be seen in Figure 5.5. Metal, stainless steel or nylon mesh can be for the printing of electronic materials, and through the dimensions of the threads of the mesh, the thickness of printed structure can be tuned. Additionally, the thickness can be controlled by the applied pressure, angle of the squeegee and the viscosity of the ink. Screen printing inks are designed as thick (paste-like), high viscosity inks, where binders (particles) with big dimensions are used and therefore minimum line with of 10-50 µm which results in high roughness of the printed structures with this technique[150], [162].

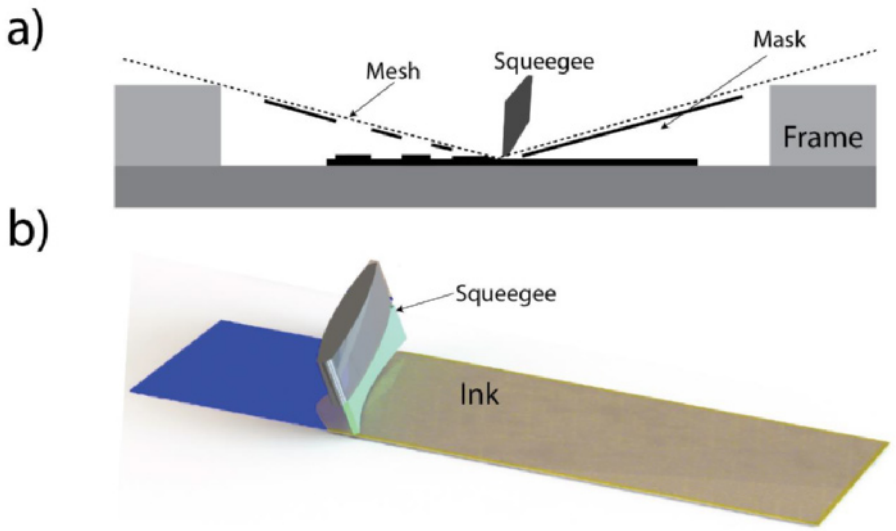

Figure 5.5. Schematics for screen printing. a) Side view of the process, showing the components of screen printing. b) 3D illustration of stencil printing.

There are several advantages of screen printing such as providing high aspect ratio and thick functional films (important for energy storage applications). It is cheap, versatile and provides roll to roll and sheet by sheet manufacturing compatibility. In the thesis, screen and stencil

printing are used for the printing of carbon adhesion layer and gel electrolyte for paper **II** and **III.** Dupont Carbon 7102 ink was printed on Al/PET current collector with two steps of printing, resulting in 20 μm thick adhesion layer (between the current collector Al and paper electrode). Silver paste for interconnects were also printed with stencil printing for series connection of supercapacitors. Gel electrolyte inks were developed to be printed by using screen mesh and paper stencil masks to pattern the gel electrolytes on top of the paper electrodes to fabricate all printed supercapacitors[163], [164].

5.4. Summary

During the development of the thesis work and the papers, several printing techniques are used and compared. Figure 5.6 summarizes the printing methods that have been employed to print device components. Screen printing and bar coating (Chapter 6) were the main techniques to print gel electrolytes, where high viscosity inks are required. Spray coating is well-known for depositing thin film organic materials (P3HT or hole transport layer) for transistors and photovoltaics for almost two decades [165]–[167]. Even though it has lost its popularity for years, recently it has gained lots of attention. Additionally, spray coating allows to prepare thin cellulose coatings, where it can open a way for new paper making methods[168]. In this thesis, it has been utilized as the main fabrication technique to achieve paper electrodes with wide range of thickness values from of 0.9 μm to 30 μm. The technique uses low viscosity inks with cellulose nanofibril binders and provides large area coverage. With the automated setup constructed, we have demonstrated large area, roll to roll manufacturing capability for energy storage devices. Spray coating provides solutions to the problems such as limited thickness, roughness control and delamination[163], [169]. It has been demonstrated as a competitive manufacturing method to achieve thick electrodes (high energy density) over large area to maintain up-scalable manufacturing. With these properties, it finds itself in a competition between screen printing and paper machine[170].

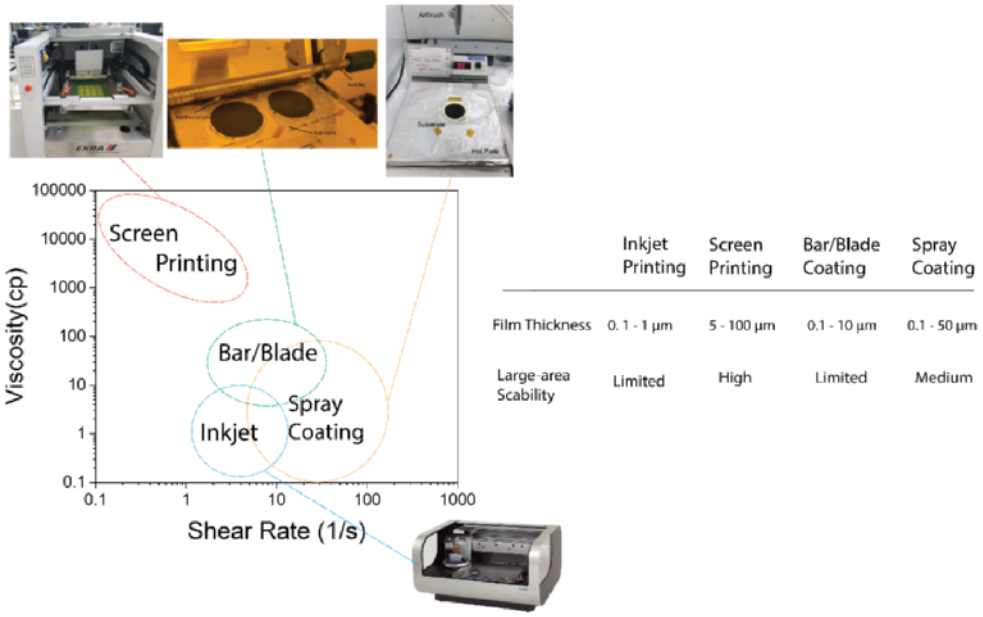

Figure 5.6. Comparison of printing methods, film thickness and scalability range.

Summary of electrode thickness of nanomaterials and conductive polymers vs. areal capacitance is given in Figure 5.7a. Screen printing provides electrode with thickness of more than 10 µm and up to now spray coating was used to fabricate nanometer thick functional coatings. With this work, we have bridged the gap between the capabilities of both techniques. Figure 5.7b, c shows the optical images of spray coated or screen-printed supercapacitor devices, which were all printed and ready to scale up for commercial use.

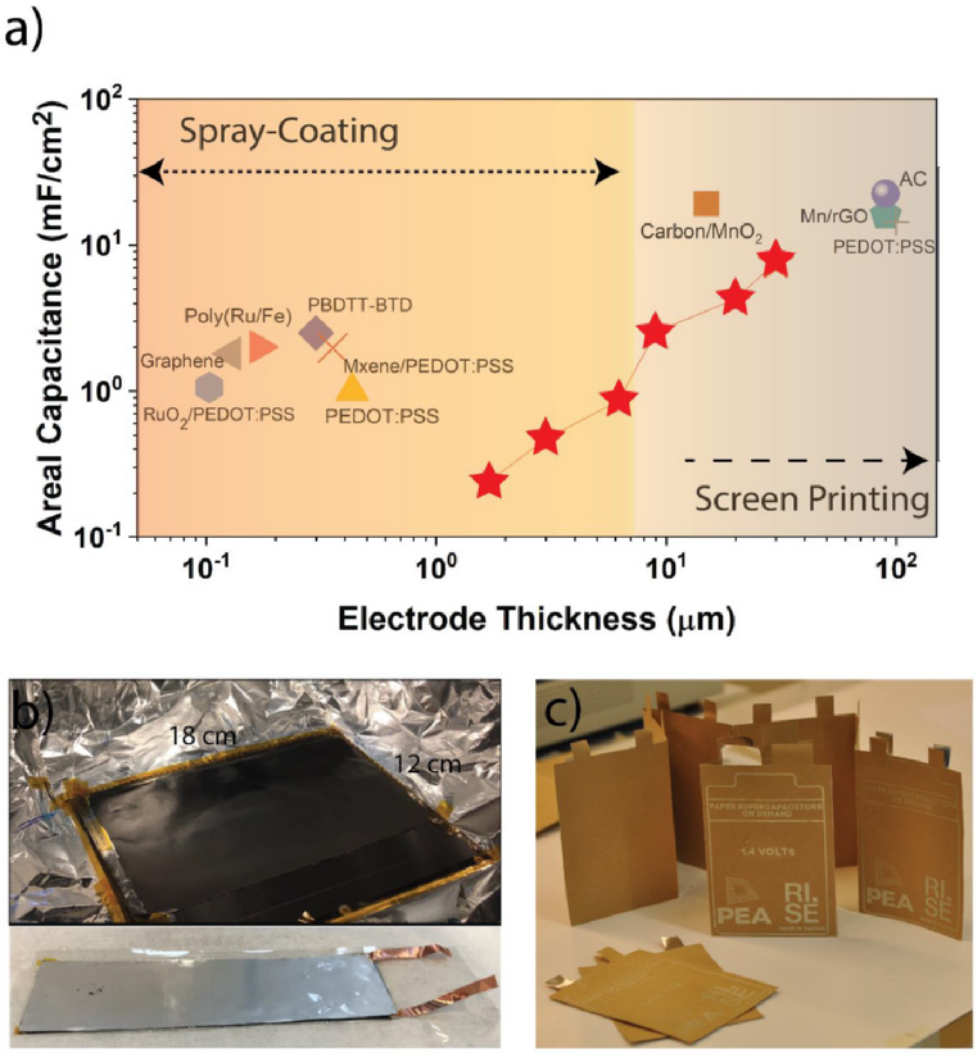

Figure 5.7. Comparison of spray coating and screen-printing for capacitive material. a) Plot for comparing areal capacitance with electrode thickness using different fabrication methods. Red stars show the thickness range of spray coated electrodes. Our work enables to cover a wide range of thicknesses, which can be achieved using both screen printing and spray coating. b) and c) Optical images for the large area devices developed with spray coating and screen printing.

CHAPTER VI

6. Methods and Characterizations

In addition to the printing methods that are presented in Chapter 5, several methods for material preparation, morphology characterization as well as electrochemical and electrical methods are described in this chapter.

6.1. Laboratory Scale Manufacturing

6.1.1. Drop casting

There are multiple ways of preparing polymer thin or thick film electrodes[171]. In this thesis, drop casting method is used for the paper electrode fabrication with different thicknesses in paper **I**. Figure 6.1a shows the typical polymer film preparation methods. In the drop-casting/solution-casting, the solution is casted in a petri dish with a certain volume and the solvent is evaporated in a controlled environment (i.e., in fume hood, on a hot plate). The thickness of the casted film is controlled with the volume of the ink or the dimensions of the host substrate. Solution casting is a useful method for simple fabrication of nanomaterials to achieve thick films of more than 10 µm (in case of drop-casting thin films are possible <100 nm). Usually, this method results in high roughness for the prepared films, however, there are other methods to prepare low roughness, high quality films such as spray coating and spin coating.

6.1.2. Spin coating and Bar coating

Spin coating is one of the most common methods to deposit uniform thin films that is either used in cleanroom processes i.e lithography, patterning of photoresist or to achieve lab scale fabrication of nanomaterials or polymeric materials. The material is dissolved in a solvent and casted on the substrate (glass or Si wafer), which is placed on to the rotating chuck. The centrifugal force distributes the solution with a defined rotation speed. The rotational speed (spread and spin) of the system is in between 100 – 5000 rpm, where it defines the thickness of the thin film after the solvent evaporates (Figure 6.1b). In addition to the spinning speed, the viscosity and material concentration also influence the film thickness. This technique provides quite low roughness when the recipe (spin speed and time) is well optimized, and the solution is homogenous. In this thesis, this method is integrated into the manufacturing process of thin paper electrodes and to deposit negative photoresist for photolithography process in paper **I** and **V**, respectively.

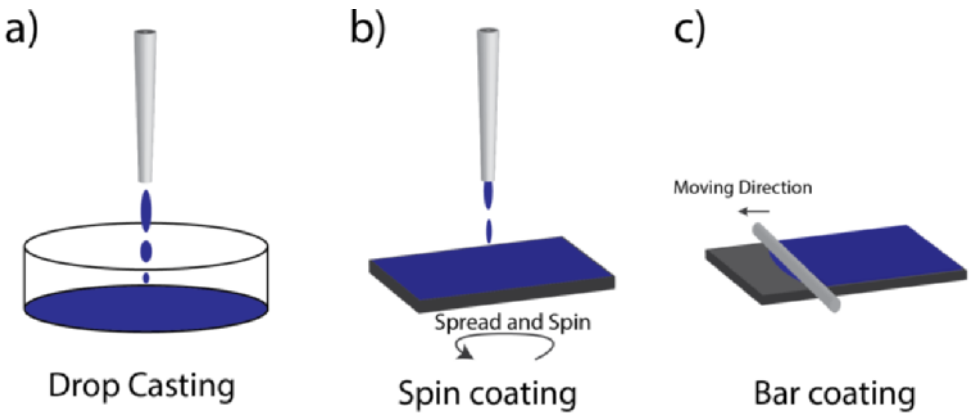

Figure 6.1. Schematic representation of solution processed, lab scale manufacturing methods. a) Drop casting, b) Spin coating, c) Bar coating.

Bar coating (Meyer Rod) is another useful method to achieve uniform coatings for the organic and nanoelectronics materials [50], [172]. The solution is placed on the substrate, and it spread across by a bar which has defined gaps, where the ink stays in between bar and substrate and the solvent evaporates after the coating. These gaps allow certain volume of the ink and therefore determines the thickness. This method is relatively low cost and easily scalable. The deposition of the film can be controlled by using additional heating mechanism and allows large area application. In this thesis, bar coating is used for gel electrolyte deposition in paper **II**.

6.1.3. Sputter Deposition

Physical vapor deposition (PVD) is a thin film deposition technique, where solid materials (metals) are transferred into vapor phase, then accumulates onto a substrate as a functional coating. This process is carried out in a vacuum chamber, where phase transition can be done using resistive heating, ion bombardment (sputtering) or electron-beam. The methods used in this thesis include thermal evaporation and sputtering.

The metal current collectors or contacts deposited onto flexible substrates are fabricated by thermal evaporation. In thermal evaporation, the energy to provide vapor phase transition, is delivered by heating. Metals including Cr, Ti, and Au were deposited during the development of the devices that are presented in the thesis.

Sputtering is a PVD method to deposit thin films by ejecting material from the target onto a substrate[173]. In a typical system, argon atoms are ionized by the plasma and accelerated towards the source material and eject atoms from the target. Figure 6.2 summarizes the sputtering process. Sputtering systems mostly involve magnetrons that use strong electric and magnetic fields to produce high density plasma. Conductive materials can be deposited by DC sputtering, however, to deposit conductive oxides or insulating material an RF power is needed[174]. Charge build-up can be avoided by using alternating potential, but it results in low deposition rates. Sputtering causes less radiative heating and therefore is a method of choice for temperature sensitive materials or substrates. The thin film properties can be defined by gas flow (Argon and oxygen rate), power, chamber pressure etc.

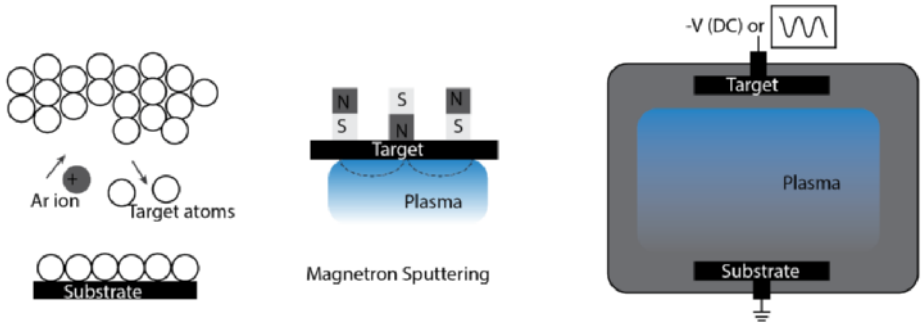

Figure 6.2. Schematic representation of magnetron sputtering for functional coatings.

This method is utilized to deposit both semiconducting and conducting ITO films for electrolyte gated FETs in paper **V**.

6.2. Photolithography

Other than the shadow masking (micromachined sheet that has openings and patterned features), which is the most common method to have patterned PVD deposition or organic materials on a substrate, photolithography has been used to define thin film structures with micron scale dimensions.

Photolithography is typically an ultraviolet (UV) light technique to transfer a geometric design onto a thin film or a substrate. This is the main patterning technique for integrated circuits and microelectromechanical systems. The method requires several steps to achieve desired structures (Figure 6.3). Typically, a photoresist is applied by spin coating or spray coating. Positive resists are solubilized by UV light therefore the pattern on the photomask is directly transferred on to the substrate. In negative one, photoresists are crosslinked by UV light and the negative image of the photomask is transferred to the substrate. After this step, the soluble (unwanted) part of the resist is removed by the developers. For the next step (after metal deposition or printing of polymers) either etching or lift off processes can be used to achieve the final structure, as demonstrated in Figure 6.3b.

To briefly explain the main micropatterning technique, Parylene peel off technique can be described as a fine shadow masking process using parylene as a sacrificial layer. In a typical process, the substrate is coated with an antiadhesion layer and a parylene C with a defined thickness (for thin film processes, around 1-2 µm thick)[82]. This coating becomes a mask for the patterning of active materials[175]. The openings and mask structure are designed by lithography and etching, thereby the shadow mask becomes in direct contact with the substrate. Afterwards, the deposition material (penetrated through the holes of Parylene C mask) is applied, and the parylene layer is peeled off using a tape or tweezer (dry peel off). Figure 6.3c shows the optical image of parylene peel-off, after the deposition of PEDOT:PSS to define interdigitated electrodes of symmetrical micro-supercapacitors. Photolithography has been used in the experiments of Paper **V** and Paper **VI**.

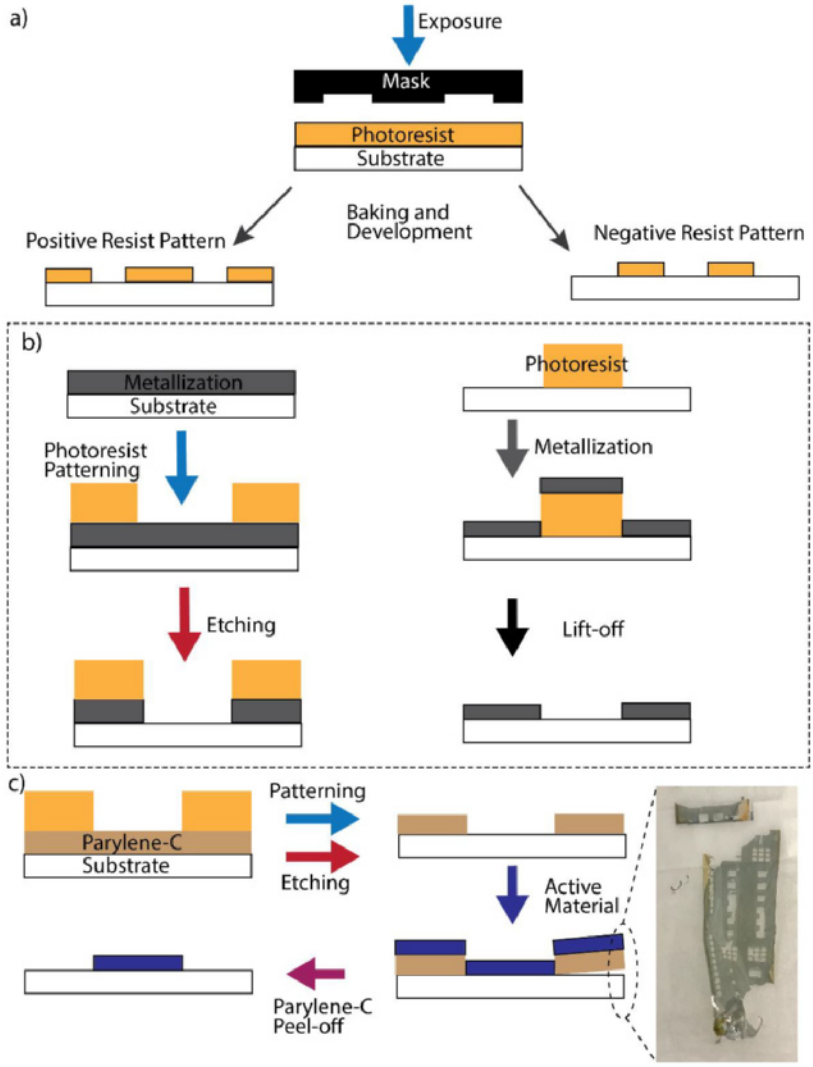

Figure 6.3. Photolithography steps. a) Mask design, Photoresist type selection and light exposure. b) Etching or lift off processes after metallization. c) Summary of parylene peel-off technique. After patterning of sacrificial parylene layer, which can be described as a shadow mask, the active material is deposited with coating or printing methods. Then, the sacrificial layer is peeled off from the substrate to achieve the desired, patterned active material.

6.3. Electrochemistry

Electrochemical characterization of the materials and devices are the main investigation method for the concepts presented in the thesis. Electrochemistry studies the relation between chemical reactions and the electrical current that passes through the system. It is a valuable method to investigate Faradaic and non-faradaic reactions, energy storage devices and to analyze the stability (corrosion) of the electronic devices[176]. Typical electrochemical setup consists of

electrochemical cell (three electrode setup) or a two terminal device connected to a potentiostat [177]. For a comprehensive introduction of the setups, the reader is referred to references [100], [176] and paper **I**. Several methods to study the electrode reactions and interfacial properties are presented in this chapter.

6.3.1. Cyclic Voltammetry

Cyclic voltammetry is the most widely used technique to gather information about electrochemical processes. CV is a voltage scanning method towards a time scale, where a triangular waveform between E_f (final potential) and E_i (initial potential) is used. The working electrode is swept at a constant scan rate and the potentiostat measures the current resulted from applied potential[176]. Figure 6.4a illustrates the typical CV voltage sweep. Typical CV curve for a basic redox process $O + ne^- \rightleftharpoons R$ can be extracted when the applied potential reaches the oxidation peak potential, and a cathodic current becomes prominent. After changing the polarity, a reduction current begins to increase. Cyclic voltammetry can be used for analyzing reversible processes, double layer formation, electron transfer reactions and extract the electroactive materials properties[178]. In the case of capacitive processes (non-faradaic, double layer, EDLC) a typical box shaped CV should be expected. However, in the case of pseudocapacitance, H_2O_2 formation and water splitting (faradaic processes), a duck shaped CV (anodic and cathodic peaks) is typically observed during the experimental processes as shown in Figure 6.4a [126], [177]. In summary, CV gives information about the capacitive or redox nature of the electroactive materials. Capacitance of a device can be calculated using the CV curve, however, in general these values are higher than the actual capacitance with electrode/electrolyte interface or overall volume of the electroactive film. Therefore, a constant current method is employed to extract the capacitance.

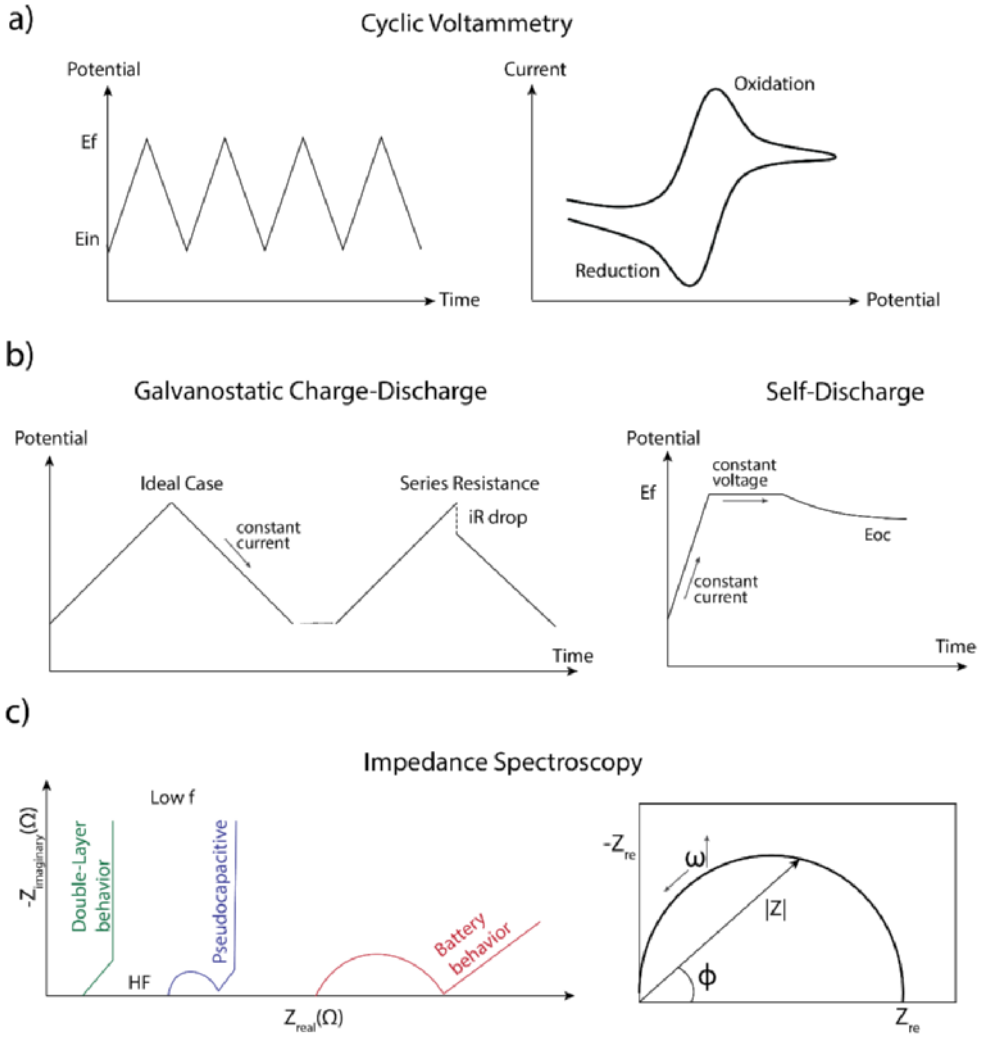

Figure 6.4. Most common electrochemical methods to understand electrode kinetics and device characteristics. a) Cyclic voltammetry, b) Galvanostatic test and self-discharge, c) Impedance spectroscopy.

6.3.2. Galvanostatic Charge-Discharge Test

Chronopotentiometry or Galvanostatic charge discharge technique (GCD) is an important electrochemical method to investigate charge capacity of energy storage devices[179]. This constant current method is useful to extract the capacitance, as it gives information about redox processes during charging and discharging. This method uses a constant current while measuring the potential. A GCD output for a capacitive system is shown in Figure 6.4b (left), where a constant current is applied to reach a defined final potential. The differences between the GCD curves for different types of capacitive and redox processes are given in Chapter 4.3.

Chronopotentiometry is mostly served to extract capacitance and equivalent series resistance of supercapacitors and batteries[126].

$$C = \frac{dQ}{dV} = \frac{\Delta t \times I}{V} \tag{6.1}$$

The equation 6.1 defines the capacitance in a certain potential range (V) and time, Δt.

Another useful information extracted from the GCD system is the resistance (DC) of entire system. Equivalent series resistance (ESR) evaluation by a voltage drop during the onset of discharging is the strongest aspects of this technique. It is calculated by dividing voltage drop (V_d) with the applied constant current (I) [126].

$$ESR\ (R) = \frac{V_d}{2I} \tag{6.2}$$

It is worth noting that the self-discharge (Figure 6.4b, right) is another method that includes Galvanostatic charging. It is typically used to evaluate the supercapacitors charge holding capacity under the condition of open-circuit potential for a certain amount of time. Self-discharge performance depends on electrochemical interface processes within the device layers, packaging (encapsulation) and device fabrication.

6.3.3. Impedance Spectroscopy

Understanding frequency dependent characteristics of an electrochemical system can be possible by electrochemical impedance spectroscopy (EIS) [97]. A small sinusoidal voltage (5-10 mV) is applied to measure the impedance of a cell as a function of frequency. Impedance data recording starts from high frequency region to low frequency region. Typical values for frequency are in between 100 kHz to 10 mHz. The resulting data is represented as Nyquist plot, where x-axis defines the real impedance and y-axis is the imaginary part of impedance ($Z = |Z|e^{j\emptyset}$). Figure 6.4c shows the Nyquist plot representations for EDLC, pseudocapacitive and battery behavior[179]. The point intersecting the x-axis at high frequency region gives the ESR. The signatures of pseudocapacitive or battery-like materials can be found as subsequent semicircles. In an EDLC, 45° line should start after the ESR point and be followed by a vertical line. For pseudocapacitive and battery materials, a semicircle can be identified, and the second intersection of the x-axis gives the charge transfer resistance (R_{CT}). R_{CT} is associated with the electrochemical reactions within the cell system[126].
In this thesis, EIS determines the ESR of the printed supercapacitors and is used to investigate the thickness dependent ESR change for the paper micro-supercapacitors for the papers **III** and **IV**.

6.4. Materials Characterizations

6.4.1. Scanning Electron Microscopy (SEM)

SEM is a strong method to investigate the morphology of a specimen. The specimen is scanned by an electron beam, where a high vacuum is necessary[180]. SEM offers resolution down to 1 nm with typical energy of electrons ranging from 0.5 to 20 keV. These electrons interact with

the atoms in the sample and produces various of signals. These signals come from the different parts of the specimen-electron interaction namely secondary electrons, Auger, back scattered electrons and X-Rays (Figure 6.5a). The most common SEM mode is the secondary electron imaging mode, where surface morphology imaging can be performed due to the limited escape space. For SEM imaging, the specimens should be electrically conductive to prevent charging. Thin film organic semiconductors, conductive fibrils and metal films morphology can be investigated with SEM.

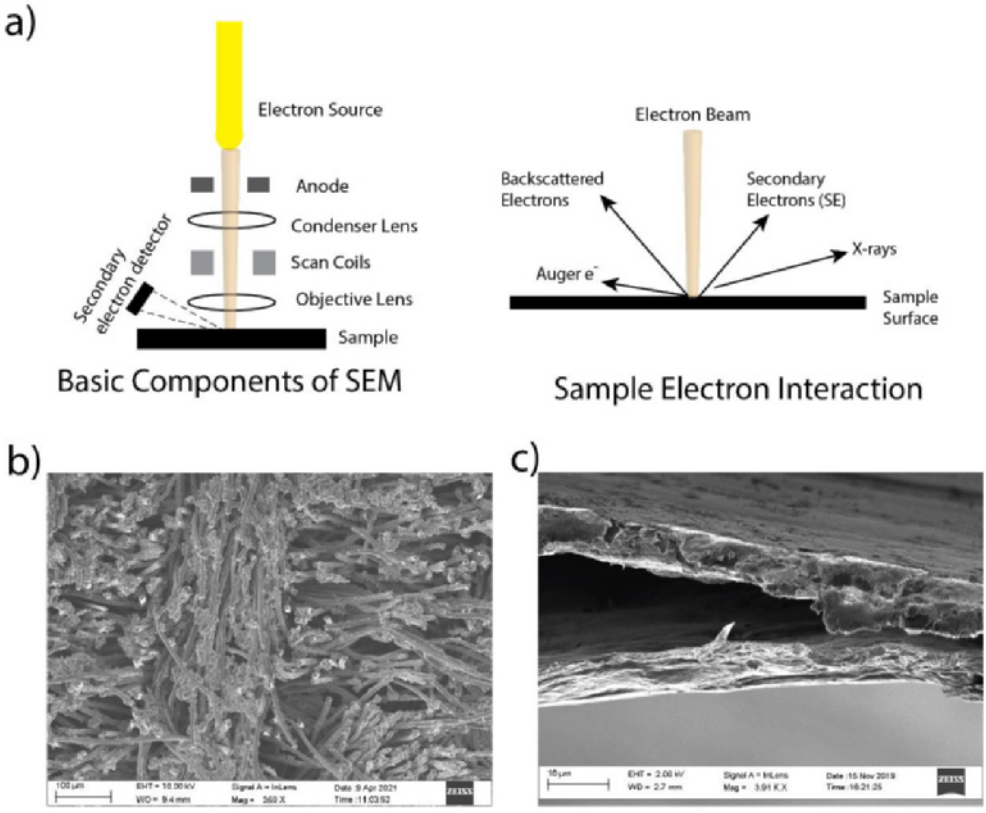

Figure 6.5. a) SEM system components and sample electron interaction, b) An SEM image showing activated carbon particles inside a rayon felt fiber matrix, c) Cross-section image of a paper electrode and carbon adhesion layer to measure the thickness of each layer.

In the thesis, the morphology of composites, and the cross-section of the organic energy storage devices is investigated with SEM. Figure 6.5b shows a carbon felt loaded with activated carbon particles, where 10 keV give enough energy to investigate the fibril and particle size. Thickness of the films is measured either by a surface profilometer (Dektak), or with fine cross-section image analysis with SEM. Figure 6.5c shows the printed layers of paper supercapacitors. By simply separating the carbon adhesion layer from the paper electrode, the thickness of each layer can be determined using SEM.

6.4.2. Advanced X-Ray Characterization

To understand material properties, small angle X-Ray and neutron scattering have been used to understand mesoscale structures, and wide angle X-Ray and neutron scattering for the understanding of the material down to molecular scale. X-ray diffraction and scattering methods provide wide range of information about the nano- or microstructure of both organic and inorganic materials.

For grazing incidents (GI) methods such as grazing incident small angle X-Ray scattering (GISAXS) and grazing incident wide angle X-Ray scattering (GIWAXS), a beam of x-rays travels to the substrate of interests at a grazing incidence angle (α_i). The scattered intensity is measured with 2D detectors with the angles of α_f and lateral angle 2θ (in plane), see Figure 6.6 [181]. For the grazing incidence geometry, the wave vector is defined as,

$$\vec{q} = \begin{pmatrix} q_x \\ q_y \\ q_z \end{pmatrix} = \overrightarrow{k_f} - \overrightarrow{k_i} = \frac{2\pi}{\lambda} = \begin{pmatrix} cos\alpha_f cos2\theta - cos\alpha_i \\ cos\alpha_f sin2\theta \\ sin\alpha_i + sin\alpha_f \end{pmatrix} \tag{6.2}$$

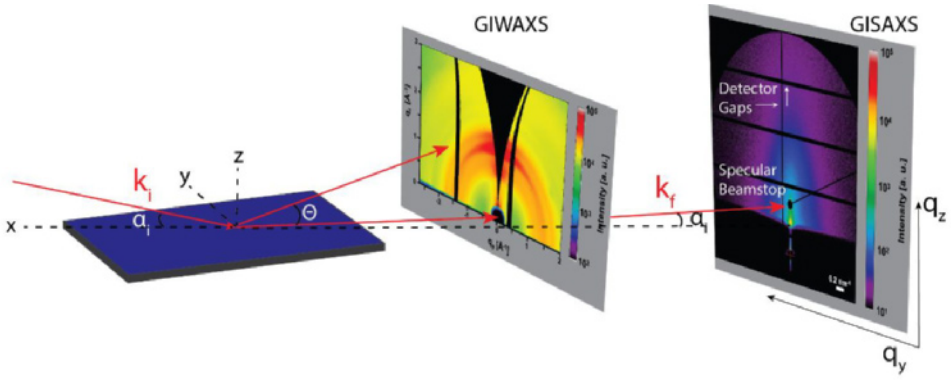

Figure 6.6. Schematic representation of x-ray grazing incident technique for GIWAXS and GISAXS measurements.

For practical applications, the interface morphology is often the limiting factor of the device performance[182]. The synchrotron-based characterization techniques with in situ and in operando capabilities are powerful tools to reveal nanoscale morphology at the interfaces and the surface analysis of the device layers/components for solar cells, supercapacitors and batteries [45], [183]–[185]. Another prominent example is to investigate changes in crystallinity of polymeric systems manufactured with different printing techniques. These investigations aim to achieve optimum performance by understanding morphology as well as kinetics, especially in conductive polymers[183], [186]. Considerable attention has been given to thin PEDOT films that have been investigated using GIWAXS to understand structural kinetics better during drying and film formation[187]. The morphology change and observing the changes of π- π stacking distance, as well as changes in the device performance metrics, i.e., conductivity and

mobility, have been reported by investigating the effect of additives (co-solvents, surfactants) and choice of printing [5], [186], [188]–[191].

For the interest of paper-based composites systems, several attempts have been made to characterize the effects of environmental changes on the crystallization of PEDOT during film formation and self-assembly around a cellulose nanofibrils [192],[54]. Here, we constructed an experimental setup to compare the morphology and structural changes when PEDOT/paper electrode is manufactured with spray coating and drop casting. It helped to understanding the morphology in relation to the manufacturing methods (lab-scale or printing/coating) to explain conductivity differences and π- π stacking distance of such organic composite system. Typical experimental configuration is demonstrated in Figure 6.7. The sample-to-detector distance SDD was maintained at SDD_{GISAXS} = (2644 ± 1) mm and SDD_{GIWAXS} = (128.5 ± 0.2) mm for GISAXS and GIWAXS, respectively. The scattered intensity was recorded using a Pilatus 1M ([172 × 172] μm^2, Dectris Ltd., Switzerland) for GISAXS and a Pilatus 300k ([172 × 172] μm^2) for GIWAXS experiments. The spray deposition was performed by spraying 60 times for 0.1 s and intermittence drying and the samples were measured for 100 ms at 10 positions to check for homogeneity. Paper **III** describes the use of X-Ray scattering characterization for the combination of an industrial scale, fast spray deposition process and compare drop-casted paper electrodes. The investigation of large-scale homogeneity is assisted with advanced surface mapping. In particular, the microstructure, morphology, and crystallinity of spray-coated paper electrodes were analyzed and the differences between the drop casted samples were presented.

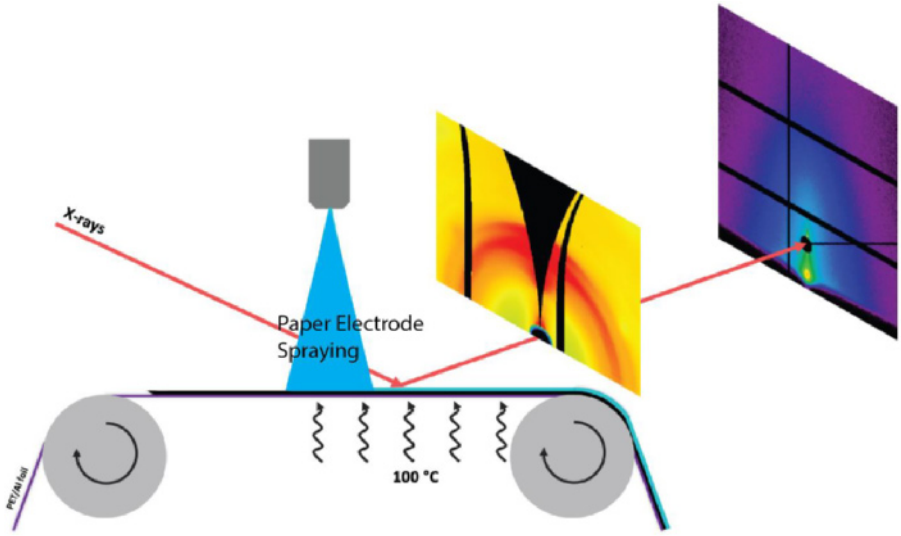

Figure 6.7. Spray coating setup constructed at the beamline to characterize paper electrode during spraying or after annealing.

6.4.3. Electrical Characterizations

In this thesis, several electrical and electrochemical methods were used to analyze the device properties. Figure 6.8 shows the images of the experimental setups during measurements and

the instrumentation for the development of the scientific articles. The electrical characterization of thin films, paper electrodes and composites were obtained by the four-point probe method. A schematic (Figure 6.8a) representation with two outer electrodes being responsible for current and two inner ones for the voltage measurements. Either *Ossila* four-point probe system is used to determine the conductivity and resistivity of the thin films directly or samples placed onto gold coated four-lines and a *Keithley* source meter is used to extract the resistivity. All electrochemical characterizations are performed by using *Biologic* potentiostat/galvanostat. Self-discharge performance was recorded by *Keithley* source meter with a custom made Labview software. As shown in the Figure 6.8b, while the solar cell is producing energy by the ambient light, the supercapacitor is getting charged, and the potentiostat records the open circuit voltage. Source measurement units (SMUs) are widely used to provide current and voltage to understanding the threshold voltage for electrochromic displays (Figure 6.8c). Additionally, the *Keithley* source meters were used to extract IV curves and transconductance of the electrolyte gated oxide transistors. Semiconductor parameter analyzer (*Keithley 4200 SCS*) was used to extract the output and transfer curves of EGFETs during bending test.

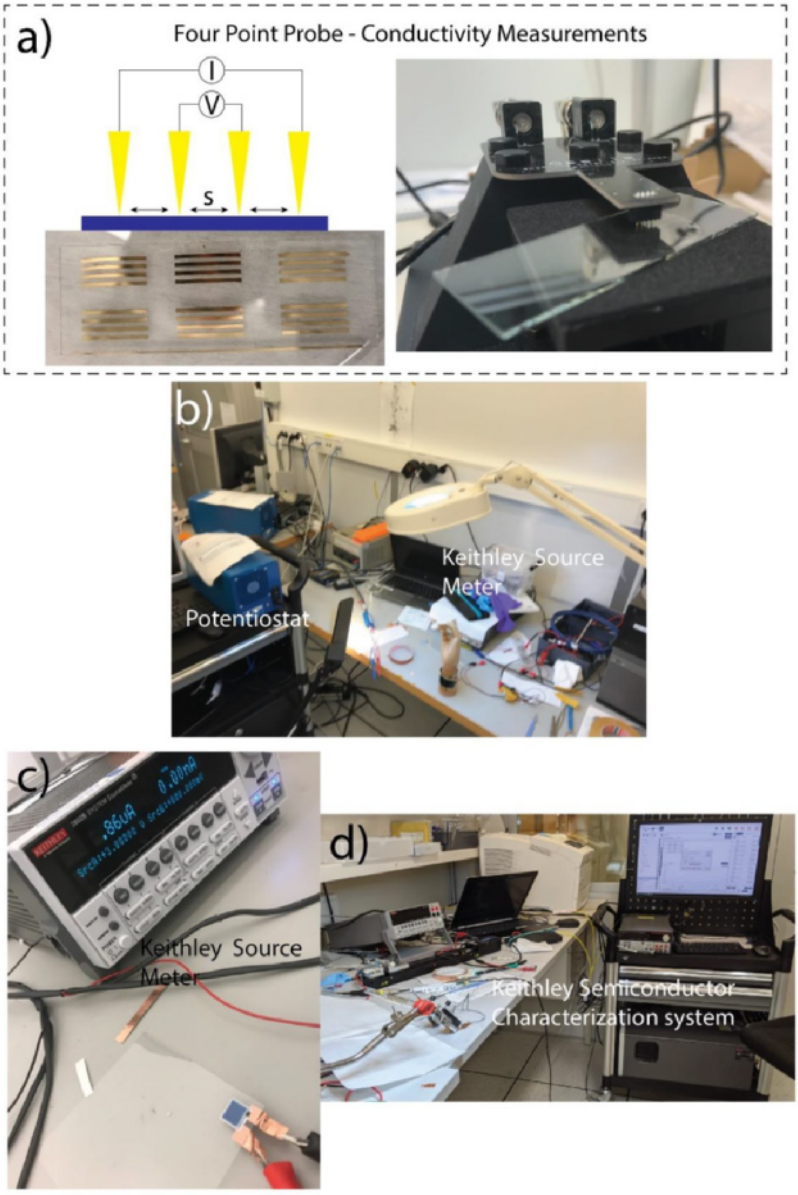

Figure 6.8. Summary of electrical and electrochemical setups. a) four-point probe method, optical image shows the Ossila conductivity measurement system. b) Experimental setup for electrochemical characterization of solarcell-supercapacitor integration with potentiostat and source measure unit. c) A Keithley source meter provides set current and voltage. d) Optical image shows the experimental setup to characterize EGFET output and transfer characteristics under bending conditions.

CHAPTER VII

7.1 Summary of the Papers

Paper I

Volumetric Double-Layer Charge Storage in Composites Based on Conducting Polymer PEDOT and Cellulose

In this paper, we have developed methods to describe PEDOT capacitance within a composite system, using both theoretical modelling and experimental techniques. The gravimetric capacitance of paper composites in a wide range of electrode thicknesses was calculated from GCD tests. The DFT method was used to extract intrinsic capacitance, which originates from the electrostatic interaction between PEDOT and negative counterion. Next, Nernst-Planck-Poisson equations were utilized to model the specific capacitance of the device system. To distinguish the effect of faradaic side reactions from the double layer capacitance, we have eliminated the current from H_2O_2 generation and confirmed electrical double layer (EDL) characteristics. Overall, the demonstrated methods have explained EDLs systems in PEDOT electroactive material embedded in a 1D host network cellulose nanofibrils (CNF) guide fundamental understanding of the capacitance, which is a step towards efficient sustainable electrodes for sustainable energy storage technology.

Paper II

Spray Coated Paper Supercapacitors

This work opens a new path for printing/coating of paper supercapacitor electrodes. Our first initiative in the spray coating of paper electrodes is successfully performed in this paper. Up to 7 µm thick paper electrodes were deposited on flexible plastic/aluminum current collectors using simple airbrush-assisted spray coating. In summary, we have implemented screen printing of adhesion layer for the current collector, spray coating of electrode and bar coating of gel electrolyte to achieve 140 µm thick flexible supercapacitors. This combination of printing methods enabled us to achieve low ESR values (0.22 Ω), which motivated us to further investigate these results in paper III. The optimum voltage range of such devices is investigated and a hybridization of two serially connected supercapacitors with flexible DC-DC converter is demonstrated. This paper demonstrates an example of flexible hybrid electronics to be used in smart packaging, which can target a wide range of applications such as internet of things and low power sensor networks.

Paper III

Upscaling Paper Supercapacitors for Printed Wearable Electronics

In this paper, we demonstrate a route to move from proof of concept to fast, scalable fabrication protocols using printing/coating methods. We improve the thickness control on the spray coating process of the paper electrodes, which steer towards 30 µm thick electrodes for organic symmetrical supercapacitors – a higher thickness rarely tested using spraying. The importance

of this work is in showing a facile route for the deposition of supercapacitor and battery electrodes using spray coating. We have implemented nanoscale surface investigation methods (GIWAXS/GISAXS) to understand the effect of the fabrication method on electrode morphology, device characteristics and especially ESR. We have achieved large area supercapacitors using coating and printing and demonstrated flexible wearable power packaging by combining a large area paper supercapacitor with a photovoltaic system that can harvest waste indoor light. Table 7.1 summarizes and compares the method of fabrication and achieved electrode thickness vs. capacitance values for other PEDOT based supercapacitors.

Electrode	Method of Fabrication	Electrode Thickness	Capacitance	ESR	Reference
PEDOT:PSS /Al	Casting	220 nm	51 µF	<1 Ω	[136]
PEDOT:PSS/Ag Grid	Inkjet	<1 µm	7.36 mF/cm^2	-	[193]
PEDOT:PSS Fiber	Wet spinning	d= 60 µm	119 mF/cm^2	100 Ω/cm	[194]
PEDOT:PSS/AgNF	Spin coating	90 nm	0.91 mF/cm^2	33.1 Ω	[195]
PEDOT coated Fabric	Polymerization	-	0.64 mF/cm^2	1<R<10	[196]
PEDOT:PSS	Spin coating	<1 µm	4.72 mF/cm^2	-	[197]
PEDOT:PSS/Aramid Fibers	Vacuum filtration	14.8 µm	111.5 F/g	7.3 Ω	[198]
PEDOT:PSS	Spin coating	300 nm	994 µF/cm^2	0.09 Ω/cm^2	[92]
PEDOT:PSS/H_2SO_4	Vacuum filtration	2.78 µm	50.1 F/cm^3	5.7 Ω	[199]
PEDOT:PSS coated textile	Drop casting	-	10 mF/cm^2	6.3 Ω	[200]
PEDOT Paper	Polymerization	8 µm	115 mF/cm^2	6.5 Ω	[201]
PEDOT Paper	Polymerization	200 µm	920 mF/cm^2	1.7 Ω	[202]
PEDOT:PSS/Pulp	Screen Printing	100 µm	9.2 mF/cm^2	0.61 Ω	[121]
PEDOT:PSS /CNF	Spray coating	30 µm	10 mF/cm^2	0.3 Ω	**This work**

Table 7.1. Comparison of for PEDOT based supercapacitors (for flexible devices with two-electrode configuration).

Paper IV

Ultrathin Paper Micro-supercapacitors for Electronic Skin Applications

In this paper, to expand the use of sequential spray coating and printing, we have designed skin compatible, ultrathin paper microsupercapacitors (P-µSc). Devices are fabricated on 2.0 µm parylene-C substrates, using a shadow mask current collector pattern followed by spray coated cellulose based electrode and gel electrolyte layers. Using this technique allows the control of total device thickness to around 10 µm. We have demonstrated three µSc connected in series as an on-chip demonstrator and designed an all printed, wearable energy storage package that

can power an ultrathin electrochromic display, for the first time. We have investigated mechanical stability of the 10 µm thick device system using finite element analysis to simulate strain and stress in the device layers. The P-µSc is operational at small bending radius (3 mm) and exhibits high capacitance retention (98%) after 10^3 bending cycles. The vision for next generation solar cell technology drives the motivation of having ultrathin energy storage, where our proposed route can assist the new device architectures for solution processed device technology. Table 7.2 summarizes and compares the method of fabrication and electrode thickness vs. capacitance values for microsupercapacitors.

Electrode	Electrode Thickness	Capacitance	Fab. Method	Reference
PEDOT	2 µm	6 mF/cm^2	Electropolymerization	[47]
ZnO/TiN	0.3 µm	1.24 mF/cm^2	Sputtering	[203]
MnO_2/CNT	2 µm	7.43 mF/cm^2	Spray coating	[204]
Nanocarbon	7 µm	1.7 mF/cm^2	Synthesis	[205]
CNT	10 µm	1.42 mF/cm^2	Synthesis	[206]
CNT	1 µm	0.51 mF/cm^2	Spray coating	[207]
PEDOT/MoO_3	0.56 µm	2.99 mF/cm^2	Spray/Laser	[208]
rGO	10 µm	3.4 mF/cm^2	Screen printing	[209]
PEDOT: PSS/Si NW	2.78 µm	3.4 mF/cm^2	ALD/drop-casting	[210]
Graphene	0.7 µm	0.7 mF/cm^2	Inkjet	[211]
Graphene/PANI	2.5 µm	3.31mF/cm^2	Synthesis/Spin coating	[212]
Graphene/PANI	0.5 µm	1.5 mF/cm^2	Synthesis/Polymerization	[213]
PEDOT: PSS/CNF	16 µm	6.8 mF/cm^2	Spray Coating	**This Work**

Table 7.2. A comparison table for microsupercapacitors fabricated with different methods. Adopted from [120].

Paper V

Ultrathin Indium tin oxide accumulation mode electrolyte-gated transistors for bioelectronics

With this paper, the trajectory of the thesis work moves to another active material, which is one of the most studied inorganic semiconductor materials, ITO. We have designed ultrathin, implantable n-type electrolyte gated transistors for electrophysiology applications. We also aimed to cancel out all faradaic reactions within the operation voltage using capping oxide layers i.e., tantalum oxide and aluminum nitride. The results are promising for implantable technology, which aims to operate more than 1000 cycles at the implanted area, without leaving any electrochemical footprint, especially peroxide and corrosion. The devices show mechanical robustness under bending tests and operate at small bending radius (6.5 mm), proving that it can be used to stimulate/amplify the Vagus nerve as well as other bioelectronics applications. Table 7.3 summarizes and compares the method of fabrication and On/Off ratio of our devices compared to other electrolyte gated transistors (EGT)s.

Active Material	Transparency	ON/OFF	Fabrication Method	Substrate	Reference
PEDOT:PSS	-	10^4	Inkjet Printing	PET	[214]
N1400	-	10^3	Inkjet Printing	PET	[214]
WO_3	-	10^3	Sputtering	PEN	[215]
SWCNT	83%	10^5	Aerosol Jet	Glass	[216]
GO	75%	3.8	Spin coating	PET	[217]
PEDOT:PSS	60%	10^2	Photolithography	Parylene-C	[77]
In_2O_3/ Al_2O_3	-	10^6	Precursor, DLP	Silicon	[71]
In_2O_3	-	10^3	Sputtering	PET	[70]
ITO		10^5	Sputtering	Glass	[72]
IGZO	-	10^5	Precursor/ Photolithography	PI	[218]
IGZO	-	10^7	Precursor/ Photolithography	Quartz	[219]
P3HT	-	10^4	Photolithography	PEN	[220]
ITO	75%	10^4	Sputtering/ Photolithography	Parylene-C	**This work**
ITO	-	10^5	Sputtering/ Photolithography	Parylene-C	**This work**

Table 7.3. A comparison table for EGFETs fabricated with different methods and materials.

Paper VI

Ultrathin polymer micro-capacitors for on-chip, flexible electronics

This work shows a route for fabrication of organic electroactive materials using interdigitated electrodes to be integrated with chips, bio-MEMS and implantable electronics. We have aimed to combine the best performing organic cathode materials to achieve fully encapsulated, thin, implantable battery cathodes and symmetric supercapacitors. PEDOT: PSS and polythiophene functionalized with tetraethylene glycol side chains P($g_4$2T-T) have been utilized to demonstrate ultra-flexible polymer supercapacitors using parylene peel-off technique. We have sandwiched polymer electrodes with printable gel electrolytes in between ultrathin substrates and encapsulation material to attain implantable organic supercapacitors with an overall thickness of 4 µm. With the help of micropatterning, interdigitated electrodes with 180 µm electrode width and 50 µm interspacing and up to 20 fingers were fabricated. Table 7.4 summarizes micro-energy storage device fabrication methods for different electroactive materials. The demonstrated devices show excellent electrochemical performance under extreme mechanical conditions, which holds a great promise for tissue or skin compliant implantable devices.

Micro Device Type (μ)	Electrode	Electrode Width, Spacing	Fabrication Method	Substrate	Total Thickness	Reference
Battery	NiSn/LMO	30 μm 10 μm	Electrodeposition	Glass	>100 μm	[221]
Supercapacitor	Graphene	500 μm 200 μm	Inkjet Printing	Kapton	>100 μm	[211]
Supercapacitor	PANI/PEDOT	500 μm 500 μm	Electropolymerization	PEN	>125 μm	[48]
Supercapacitor	Mxene	500 μm 450 μm	Laser Engraving	Paper	>100 μm	[222]
Battery	Zn/MnO_2	300 μm 150 μm	Laser Engraving	PET	74 μm	[223]
Battery	Co/Zn	1500 μm 500 μm	Laser Engraving	Textile	>1 mm	[224]
Battery	Graphite	30 μm 0.3 μm	Laser Engraving	PET	>125 μm	[225]
Battery	$Na_2VTi(PO_4)_3$	100 μm	Laser Engraving	Hydrogel	>100 μm	[226]
Battery	Zn/MnO_2	1000 μm 1000 μm	Screen Printing	PET	200 μm	[227]
Supercapacitor	$MoTe_2$	0.1 μm 0.1 μm	FIB	Silicon	>100 μm	[228]
Supercapacitor	Carbon	250 μm 100 μm	Photolithography	Silicon	>100 μm	[205]
Supercapacitor	CNT	300 μm 40 μm	Photolithography	Polyimide	>10 μm	[66]
Supercapacitor	Graphene	400 μm 100 μm	Laser Scribing	Kapton	7.6 μm	[229]
Supercapacitor	PEDOT:PSS P($g_4$2T-T)	100 μm 20 μm	Photolithography	Parylene-C	4 μm	**This Work**

Table 7.4. A comparison table for microbattery and microsupercapacitor devices fabricated with different methods to achieve minimum dimensions.

7.2. Conclusion

In this thesis, I have demonstrated various organic/inorganic electronic devices for wearable and implantable electronics. Understanding the double layer capacitance and using it in the real-life applications is one of the major steps in the developed technologies. Processing methods for both organic and inorganic materials are developed for applications, where the field demands a big step forward to achieve next generation flexible electronics devices. The thesis is built around applications of wearable electronics and electronic skin using various printing and microfabrication methods.

The devices and concepts presented in the thesis are the products of my passionate interest in flexible electronics and its applications. Since my master's degree on polymer electronics and personal initiatives in industry to implement printing technologies for life sciences, this interest has directed me to the collaborations and projects at LOE. The hybridization of organic/inorganic materials and the fabrication methods (printing and microfabrication) are the outcomes of five years of research at LOE. We have designed composite inks and experiments to fabricate functional devices as well as to understand capacitive behavior of the organic materials. The presented devices are not only planned as proof-of-concept demonstrators, but we have also inserted long-term operational and mechanical cycle tests to support their use in the proposed applications. Since the transition from academia to industry needs more profound concepts to realize commercial applications, collaborations with theoretical groups in both LOE, Sweden and with research facilities in Europe have been pursued. With these planning and collaborations, examples of new device concepts, nanoscale characterizations and fundamental electrochemical investigations were included.

Flexible electronics is a growing field with new materials, processing techniques and new application areas. Since decades, flexible materials such as PET, PEN, paper (thickness>100 μm) have been used as substrate, a great deal of printing techniques and manufacturing methods were investigated. There are lots of opportunities as the research field switches to ultrathin substrates (parylene-C, polyimide) because of advantages such as small bending radius operation, mechanical strength and sufficient volume for constructing thicker active layers. These properties provide not only an alternative but a route to fabricate next generation of wearables, electronic skin and biomedical devices. Skin compatibility and operation capability when it is wrapped or rolled provide the best device architectures for the future devices. Constructing functional electronics on such substrates and encapsulation layers will pave the way especially for developing batteries, sensors, hybrid CMOS circuits for implants, wearable health trackers, and robotics.

For the case of active materials, the field is full of functional organic and inorganic materials that can provide sufficient capacitance, high mobility and conductivity. Up to now inorganic semiconductors, functional oxides, polymer coatings and composites reveal functionalities to invent smart phones, watches and implants. I have no doubt that transferring these technologies on to flexible substrates will bring consumer-oriented applications. Providing roll to roll compatibility, supplying green methods, lowering down the cost and reaching more application areas will attract investment and attention from both industry and academia. I believe that small steps such as demonstrators, use cases and industry collaborations from research facilities will boost the flexible electronics field and enable a variety of commercial applications.

To sum up, with Paper I, II and III, we have investigated a green composite system as an electroactive material for energy storage. The printing methods, especially spray coating are utilized to deposit electrodes onto flexible commercial substrates to demonstrate scalability and the manufacturing of wearable energy storage devices. With these methods of fabrication, electrochemical approaches and demonstrators, the projects point to a sustainable route towards organic wearable concepts. Paper IV, V and VI expand the traditional flexible electronics by introducing ultrathin, encapsulated device architecture. Both energy storage devices and sensory systems were developed to achieve conformable electronics for skin-compliant and implantable electronics. Tools for mechanical analysis, long-term device testing and performance under harsh mechanical conditions were investigated for better understanding of dynamics during device operation. Addition of such studies played a role to figure out the needs of the field in order to shift from the scientific investigation and prototype development to commercial concepts with high-ranking technology readiness level and well-suited for clinical trials.

References

[1] T. R. Ray *et al.*, “Bio-integrated wearable systems: A comprehensive review,” *Chem. Rev.*, vol. 119, no. 8, pp. 5461–5533, 2019.

[2] M. Fahlman, S. Fabiano, V. Gueskine, D. Simon, M. Berggren, and X. Crispin, “Interfaces in organic electronics,” *Nat. Rev. Mater.*, vol. 4, no. 10, pp. 627–650, 2019.

[3] C. J. Bettinger, “Advances in Materials and Structures for Ingestible Electromechanical Medical Devices,” *Angew. Chemie - Int. Ed.*, vol. 57, no. 52, pp. 16946–16958, 2018.

[4] M. Irimia-Vladu, “‘Green’ electronics: Biodegradable and biocompatible materials and devices for sustainable future,” *Chem. Soc. Rev.*, vol. 43, no. 2, pp. 588–610, 2014.

[5] B. D. Paulsen, K. Tybrandt, E. Stavrinidou, and J. Rivnay, “Organic mixed ionic–electronic conductors,” *Nat. Mater.*, vol. 19, no. 1, pp. 13–26, 2020.

[6] Z. Wang, Y. H. Lee, S. W. Kim, J. Y. Seo, S. Y. Lee, and L. Nyholm, “Why Cellulose-Based Electrochemical Energy Storage Devices?,” *Adv. Mater.*, vol. 2000892, pp. 1–18, 2020.

[7] D. Zhao, Y. Zhu, W. Cheng, W. Chen, Y. Wu, and H. Yu, “Cellulose-Based Flexible Functional Materials for Emerging Intelligent Electronics,” *Adv. Mater.*, vol. 33, no. 28, 2021.

[8] J. Kim, R. Kumar, A. J. Bandodkar, and J. Wang, “Advanced Materials for Printed Wearable Electrochemical Devices: A Review,” *Adv. Electron. Mater.*, vol. 3, no. 1, pp. 1–15, 2017.

[9] X. Huang *et al.*, “Materials Strategies and Device Architectures of Emerging Power Supply Devices for Implantable Bioelectronics,” *Small*, vol. 16, no. 15, pp. 1–21, 2020.

[10] S. Gong and W. Cheng, “Toward soft skin-like wearable and implantable energy devices,” *Adv. Energy Mater.*, vol. 7, no. 23, pp. 1–33, 2017.

[11] S. Y. Yang *et al.*, “Powering Implantable and Ingestible Electronics,” *Adv. Funct. Mater.*, vol. 31, no. 44, 2021.

[12] J. Li, J. Zhao, and J. A. Rogers, “Materials and Designs for Power Supply Systems in Skin-Interfaced Electronics,” *Acc. Chem. Res.*, vol. 52, no. 1, pp. 53–62, 2019.

[13] F. Garnier, R. Hajlaoui, A. Yassar, and P. Srivastava, “All-Polymer Field-Effect Transistor Realized by Printing Techniques,” *Science (80-.).*, vol. 265, no. 5179, pp. 1684–1686, Sep. 1994.

[14] D. Hur, M. G. Say, S. E. Diltemiz, F. Duman, A. Ersöz, and R. Say, “3D Micropatterned All-Flexible Microfluidic Platform for Microwave-Assisted Flow Organic Synthesis,” *Chempluschem*, vol. 83, no. 1, pp. 42–46, 2018.

[15] M. M. Hamedi, A. Ainla, F. Güder, D. C. Christodouleas, M. T. Fernández-Abedul, and G. M. Whitesides, “Integrating Electronics and Microfluidics on Paper,” *Adv. Mater.*, vol. 28, no. 25, pp. 5054–5063, 2016.

[16] R. Su *et al.*, “3D printed self-supporting elastomeric structures for multifunctional microfluidics,” *Sci. Adv.*, vol. 6, no. 41, pp. 1–11, 2020.

[17] M. S. Mannoor *et al.*, “3D printed bionic ears,” *Nano Lett.*, vol. 13, no. 6, pp. 2634–2639, 2013.

[18] Ö. Biçen Ünlüer, S. Emir Diltemiz, M. G. Say, D. Hür, R. Say, and A. Ersöz, “A powerful combination in designing polymeric scaffolds: 3D bioprinting and cryogelation,” *Int. J. Polym. Mater. Polym. Biomater.*, 2020.

[19] Y. Sümbelli, S. Emir Diltemiz, M. G. Say, Ö. B. Ünlüer, A. Ersöz, and R. Say, “In situand non-cytotoxic cross-linking strategy for 3D printable biomaterials,” *Soft Matter*, vol. 17, no. 4, 2021.

[20] Ş. N. K. Elmas, R. Güzel, M. G. Say, A. Ersoz, and R. Say, “Ferritin based bionanocages as novel biomemory device concept,” *Biosens. Bioelectron.*, vol. 103, no. October 2017, pp. 19–25, 2018.

[21] M. G. Say, “High Performance Multimaterial Fibers and Devices ,” M.S Thesis, *Bilkent University*, 2016.

[22] Z. Wen *et al.*, “Self-powered textile for Wearable electronics by hybridizing fiber-shaped nanogenerators, solar cells, and supercapacitors,” *Sci. Adv.*, vol. 2, no. 10, 2016.

[23] S.-I. Park *et al.*, “Printed Assemblies of Inorganic Light-Emitting Diodes for Deformable and Semitransparent Displays,” *Science (80-.).*, vol. 325, no. 5943, pp. 977–981, Aug. 2009.

[24] X. Meng *et al.*, “A General Approach for Lab-to-Manufacturing Translation on Flexible Organic Solar Cells,” *Adv. Mater.*, vol. 31, no. 41, pp. 1–10, 2019.

[25] D. H. Kim *et al.*, “Epidermal electronics,” *Science (80-.).*, vol. 333, no. 6044, pp. 838–843, Aug. 2011.

[26] B. Lu *et al.*, “Pure PEDOT:PSS hydrogels,” *Nat. Commun.*, vol. 10, no. 1, 2019.

[27] J. Xu *et al.*, “Multi-scale ordering in highly stretchable polymer semiconducting films,” *Nat. Mater.*, vol. 18, no. 6, pp. 594–601, Jun. 2019.

[28] K. Fukuda, K. Yu, and T. Someya, “The Future of Flexible Organic Solar Cells,” *Adv. Energy Mater.*, vol. 10, no. 25, pp. 1–10, 2020.

[29] Y. R. Jeong, G. Lee, H. Park, and J. S. Ha, “Stretchable, Skin-Attachable Electronics with Integrated Energy Storage Devices for Biosignal Monitoring,” *Acc. Chem. Res.*, vol. 52, no. 1, pp. 91–99, 2019.

[30] K. D. Harris, A. L. Elias, and H. J. Chung, “Flexible electronics under strain: a review of mechanical characterization and durability enhancement strategies,” *J. Mater. Sci.*, vol. 51, no. 6, pp. 2771–2805, 2016.
[31] Muhammad M. Hussain and Nazek El-Atab, *Handbook of Flexible and Stretchable Electronics*. CRC Press, 2019.
[32] K. Yamagishi, S. Takeoka, and T. Fujie, “Printed nanofilms mechanically conforming to living bodies,” *Biomater. Sci.*, vol. 7, no. 2, pp. 520–531, 2019.
[33] L. Mao, Q. Meng, A. Ahmad, and Z. Wei, “Mechanical analyses and structural design requirements for flexible energy storage devices,” *Adv. Energy Mater.*, vol. 7, no. 23, 2017.
[34] K. Xu, Y. Lu, and K. Takei, “Multifunctional Skin-Inspired Flexible Sensor Systems for Wearable Electronics,” *Adv. Mater. Technol.*, vol. 4, no. 3, pp. 1–25, 2019.
[35] C. García Núñez, L. Manjakkal, and R. Dahiya, “Energy autonomous electronic skin,” *npj Flex. Electron.*, vol. 3, no. 1, 2019.
[36] D. P. Dubal, N. R. Chodankar, D. H. Kim, and P. Gomez-Romero, “Towards flexible solid-state supercapacitors for smart and wearable electronics,” *Chem. Soc. Rev.*, vol. 47, no. 6, pp. 2065–2129, 2018.
[37] L. Lu *et al.*, “Biodegradable Monocrystalline Silicon Photovoltaic Microcells as Power Supplies for Transient Biomedical Implants,” *Adv. Energy Mater.*, vol. 8, no. 16, pp. 1–8, 2018.
[38] R. Liu *et al.*, “An Efficient Ultra-Flexible Photo-Charging System Integrating Organic Photovoltaics and Supercapacitors,” *Adv. Energy Mater.*, vol. 10, no. 20, pp. 1–8, 2020.
[39] A. M. Zamarayeva *et al.*, “Flexible and stretchable power sources for wearable electronics,” *Sci. Adv.*, vol. 3, no. 6, p. e1602051, Jun. 2017.
[40] H. Yang *et al.*, “The effect of crosslinking on ion transport in nanocellulose-based membranes,” *Carbohydr. Polym.*, vol. 278, p. 118938, 2022.
[41] L. Wang, D. Chen, K. Jiang, and G. Shen, “New insights and perspectives into biological materials for flexible electronics,” *Chem. Soc. Rev.*, vol. 46, no. 22, pp. 6764–6815, 2017.
[42] D. Tobjörk and R. Österbacka, “Paper electronics,” *Adv. Mater.*, vol. 23, no. 17, pp. 1935–1961, 2011.
[43] F. Hoeng, A. Denneulin, and J. Bras, “Use of nanocellulose in printed electronics: a review,” *Nanoscale*, vol. 8, no. 27, pp. 13131–13154, 2016.
[44] F. Brunetti *et al.*, “Printed Solar Cells and Energy Storage Devices on Paper Substrates,” *Adv. Funct. Mater.*, vol. 29, no. 21, 2019.
[45] J. Chen and P. S. Lee, “Electrochemical Supercapacitors: From Mechanism Understanding to Multifunctional Applications,” *Adv. Energy Mater.*, vol. 11, no. 6, p. 2003311, Feb. 2021.
[46] Y. Diao, Y. Lu, H. Yang, H. Wang, H. Chen, and J. M. D’Arcy, “Direct Conversion of Fe2O3 to 3D Nanofibrillar PEDOT Microsupercapacitors,” *Adv. Funct. Mater.*, vol. 30, no. 32, pp. 1–8, 2020.
[47] N. Kurra, M. K. Hota, and H. N. Alshareef, “Conducting polymer micro-supercapacitors for flexible energy storage and Ac line-filtering,” *Nano Energy*, vol. 13, pp. 500–508, 2015.
[48] Q. Jiang, N. Kurra, and H. N. Alshareef, “Marker Pen Lithography for Flexible and Curvilinear On-Chip Energy Storage,” *Adv. Funct. Mater.*, vol. 25, no. 31, pp. 4976–4984, 2015.
[49] J. Li, W. Yan, G. Zhang, R. Sun, and D. Ho, “Natively stretchable micro-supercapacitors based on a PEDOT:PSS hydrogel,” *J. Mater. Chem. C*, vol. 9, no. 5, pp. 1685–1692, 2021.
[50] Y. Liu *et al.*, “Facile Fabrication of Flexible Microsupercapacitor with High Energy Density,” *Adv. Mater. Technol.*, vol. 1, no. 9, pp. 1–10, 2016.
[51] M. G. Say *et al.*, “Spray-coated paper supercapacitors,” *npj Flex. Electron.*, vol. 4, no. 1, pp. 1–7, 2020.
[52] A. Elschner, S. Kirchmeyer, W. Lovenich, U. Merker, and K. Reuter, *PEDOT: Principles and application of an Intrinsically Conducting Polymer*. 2010.
[53] Y. Wen and J. Xu, “Scientific Importance of Water-Processable PEDOT–PSS and Preparation, Challenge and New Application in Sensors of Its Film Electrode: A Review,” *J. Polym. Sci. Part A Polym. Chem.*, vol. 55, no. 7, pp. 1121–1150, 2017.
[54] C. J. Brett *et al.*, “Humidity-Induced Nanoscale Restructuring in PEDOT:PSS and Cellulose Nanofibrils Reinforced Biobased Organic Electronics,” *Adv. Electron. Mater.*, p. 2100137, May 2021.
[55] C. (John) Zhang *et al.*, “Highly flexible and transparent solid-state supercapacitors based on RuO2/PEDOT:PSS conductive ultrathin films,” *Nano Energy*, vol. 28, pp. 495–505, 2016.
[56] Z. S. Wu, Z. Liu, K. Parvez, X. Feng, and K. Müllen, “Ultrathin Printable Graphene Supercapacitors with AC Line-Filtering Performance,” *Adv. Mater.*, vol. 27, no. 24, pp. 3669–3675, 2015.
[57] S. Mondal, T. Yoshida, S. Maji, K. Ariga, and M. Higuchi, “Transparent Supercapacitor Display with Redox-Active Metallo-Supramolecular Polymer Films,” *ACS Appl. Mater. Interfaces*, vol. 12, no. 14, pp. 16342–16349, 2020.
[58] N. Singh *et al.*, “Paintable battery,” *Sci. Rep.*, vol. 2, no. 1, p. 481, Dec. 2012.
[59] A. L. Yarin, “Drop impact dynamics: Splashing, spreading, receding, bouncing..,” *Annu. Rev. Fluid*

Mech., vol. 38, pp. 159–192, 2006.
[60] A. Baldelli, A. Amirfazli, J. Ou, and W. Li, "Spray-on nanocomposite coatings: Wettability and conductivity," *Langmuir*, vol. 36, no. 39, pp. 11393–11410, 2020.
[61] H. Ma, H. L. Yip, F. Huang, and A. K. Y. Jen, "Interface engineering for organic electronics," *Adv. Funct. Mater.*, vol. 20, no. 9, pp. 1371–1388, 2010.
[62] J. Dodd, C. Kishiyama, H. Mukainakano, M. Nagata, and H. Tsukamoto, "Performance and management of implantable lithium battery systems for left ventricular assist devices and total artificial hearts," *J. Power Sources*, vol. 146, no. 1–2, pp. 784–787, 2005.
[63] A. T. Kutbee *et al.*, "Flexible and biocompatible high-performance solid-state micro-battery for implantable orthodontic system," *npj Flex. Electron.*, vol. 1, no. 1, pp. 1–7, 2017.
[64] M. Koo *et al.*, "Bendable inorganic thin-film battery for fully flexible electronic systems," *Nano Lett.*, vol. 12, no. 9, pp. 4810–4816, 2012.
[65] A. Vlad, N. Singh, C. Galande, and P. M. Ajayan, "Design Considerations for Unconventional Electrochemical Energy Storage Architectures," *Adv. Energy Mater.*, vol. 5, no. 19, pp. 1–53, 2015.
[66] J. Pu, X. Wang, R. Xu, S. Xu, and K. Komvopoulos, "Highly flexible, foldable, and rollable microsupercapacitors on an ultrathin polyimide substrate with high power density," *Microsystems Nanoeng.*, vol. 4, no. 1, 2018.
[67] Y. Yun, K. R. Nandanapalli, J. H. Choi, W. Son, C. Choi, and S. Lee, "Extremely flexible and mechanically durable planar supercapacitors: High energy density and low-cost power source for E-skin electronics," *Nano Energy*, vol. 78, p. 105356, 2020.
[68] Z. Liu, Z. S. Wu, S. Yang, R. Dong, X. Feng, and K. Müllen, "Ultraflexible In-Plane Micro-Supercapacitors by Direct Printing of Solution-Processable Electrochemically Exfoliated Graphene," *Adv. Mater.*, vol. 28, no. 11, pp. 2217–2222, 2016.
[69] P. Barquinha, R. Martins, L. Pereira, and E. Fortunato, *Transparent Oxide Electronics: From Materials to Devices*. 2012.
[70] F. T. Biosensing *et al.*, "Flexible Multiplexed In 2 O 3 Nanoribbon Aptamer- Transistors for Biosensing," *iScience*, no. 23, p. 101469, 2020.
[71] H. Ren *et al.*, "Interface Engineering of Metal-Oxide Field-Effect Transistors for Low-Drift pH Sensing," *Adv. Mater. Interfaces*, vol. 8, no. 20, pp. 1–10, 2021.
[72] T. Sakata, S. Nishitani, A. Saito, and Y. Fukasawa, "Solution-Gated Ultrathin Channel Indium Tin Oxide-Based Field-Effect Transistor Fabricated by a One-Step Procedure that Enables High-Performance Ion Sensing and Biosensing," *ACS Appl. Mater. Interfaces*, vol. 13, no. 32, pp. 38569–38578, 2021.
[73] L. Q. Guo *et al.*, "Oxide Neuromorphic Transistors Gated by Polyvinyl Alcohol Solid Electrolytes with Ultralow Power Consumption," *ACS Appl. Mater. Interfaces*, vol. 11, no. 31, pp. 28352–28358, 2019.
[74] S. Oh *et al.*, "Flexible artificial Si-In-Zn-O/ion gel synapse and its application to sensory-neuromorphic system for sign language translation," *Sci. Adv.*, vol. 7, no. 44, pp. 1–11, 2021.
[75] M. Lee *et al.*, "Brain-Inspired Photonic Neuromorphic Devices using Photodynamic Amorphous Oxide Semiconductors and their Persistent Photoconductivity," *Adv. Mater.*, vol. 29, no. 28, 2017.
[76] D. W. Park *et al.*, "Graphene-based carbon-layered electrode array technology for neural imaging and optogenetic applications," *Nat. Commun.*, vol. 5, 2014.
[77] W. Lee *et al.*, "Transparent, conformable, active multielectrode array using organic electrochemical transistors," *Proc. Natl. Acad. Sci. U. S. A.*, vol. 114, no. 40, pp. 10554–10559, 2017.
[78] Y. Jimbo *et al.*, "Ultraflexible Transparent Oxide/Metal/Oxide Stack Electrode with Low Sheet Resistance for Electrophysiological Measurements," *ACS Appl. Mater. Interfaces*, vol. 9, no. 40, pp. 34744–34750, 2017.
[79] W. Yang *et al.*, "A fully transparent, flexible PEDOT:PSS-ITO-Ag-ITO based microelectrode array for ECoG recording," *Lab Chip*, vol. 21, no. 6, pp. 1096–1108, 2021.
[80] V. Zardetto, T. M. Brown, A. Reale, and A. Di Carlo, "Substrates for flexible electronics: A practical investigation on the electrical, film flexibility, optical, temperature, and solvent resistance properties," *J. Polym. Sci. Part B Polym. Phys.*, vol. 49, no. 9, pp. 638–648, 2011.
[81] J. J. Kim, Y. Wang, H. Wang, S. Lee, T. Yokota, and T. Someya, "Skin Electronics: Next-Generation Device Platform for Virtual and Augmented Reality," *Adv. Funct. Mater.*, vol. 31, no. 39, pp. 1–34, 2021.
[82] J. Ortigoza-Diaz *et al.*, "Techniques and considerations in the microfabrication of parylene c microelectromechanical systems," *Micromachines*, vol. 9, no. 9, 2018.
[83] S. Rongpipi, D. Ye, E. D. Gomez, and E. W. Gomez, "Progress and opportunities in the characterization of cellulose – an important regulator of cell wall growth and mechanics," *Front. Plant Sci.*, vol. 9, no. March, pp. 1–28, 2019.
[84] A. Isogai, T. Saito, and H. Fukuzumi, "TEMPO-oxidized cellulose nanofibers," *Nanoscale*, vol. 3, no. 1,

pp. 71–85, 2011.
[85] L. Wågberg, G. Decher, M. Norgren, T. Lindström, M. Ankerfors, and K. Axnäs, “The build-up of polyelectrolyte multilayers of microfibrillated cellulose and cationic polyelectrolytes,” *Langmuir*, vol. 24, no. 3, pp. 784–795, 2008.
[86] J. Dong and G. Portale, “Role of the Processing Solvent on the Electrical Conductivity of PEDOT:PSS,” *Adv. Mater. Interfaces*, vol. 7, no. 18, 2020.
[87] M. J. Donahue *et al.*, “Tailoring PEDOT properties for applications in bioelectronics,” *Mater. Sci. Eng. R Reports*, vol. 140, no. August 2019, p. 100546, 2020.
[88] X. Crispin *et al.*, “The origin of the high conductivity of poly(3,4-ethylenedioxythiophene)-poly(styrenesulfonate) (PEDOT-PSS) plastic electrodes,” *Chem. Mater.*, vol. 18, no. 18, pp. 4354–4360, 2006.
[89] S. Kee *et al.*, “Controlling Molecular Ordering in Aqueous Conducting Polymers Using Ionic Liquids,” *Adv. Mater.*, vol. 28, no. 39, pp. 8625–8631, 2016.
[90] J. Rivnay *et al.*, “High-performance transistors for bioelectronics through tuning of channel thickness,” *Sci. Adv.*, vol. 1, no. 4, pp. 1–6, 2015.
[91] A. Inoue, H. Yuk, B. Lu, and X. Zhao, “Strong adhesion of wet conducting polymers on diverse substrates,” *Sci. Adv.*, vol. 6, no. 12, pp. 1–11, 2020.
[92] M. Zhang *et al.*, “An ultrahigh-rate electrochemical capacitor based on solution-processed highly conductive PEDOT:PSS films for AC line-filtering,” *Energy Environ. Sci.*, vol. 9, no. 6, pp. 2005–2010, 2016.
[93] H. Wang, H. Yang, Y. Diao, Y. Lu, K. Chrulski, and J. M. D’Arcy, “Solid-State Precursor Impregnation for Enhanced Capacitance in Hierarchical Flexible Poly(3,4-Ethylenedioxythiophene) Supercapacitors,” *ACS Nano*, vol. 15, no. 4, pp. 7799–7810, Apr. 2021.
[94] M. Bianchi *et al.*, “Scaling of capacitance of PEDOT:PSS: Volume: Vs. area,” *J. Mater. Chem. C*, vol. 8, no. 32, pp. 11252–11262, 2020.
[95] I. Sahalianov, S. K. Singh, K. Tybrandt, M. Berggren, and I. Zozoulenko, “The intrinsic volumetric capacitance of conducting polymers: Pseudo-capacitors or double-layer supercapacitors?,” *RSC Adv.*, vol. 9, no. 72, pp. 42498–42508, 2019.
[96] A. M. Bryan, L. M. Santino, Y. Lu, S. Acharya, and J. M. D’Arcy, “Conducting Polymers for Pseudocapacitive Energy Storage,” *Chem. Mater.*, vol. 28, no. 17, pp. 5989–5998, 2016.
[97] B. E. Conway, *Electrochemical supercapacitors: scientific fundamentals and technological applications*. Springer Science, Business Media, 2013.
[98] K. Tybrandt, I. V Zozoulenko, and M. Berggren, “Chemical potential-electric double layer coupling in conjugated polymer-polyelectrolyte blends,” *Sci. Adv.*, vol. 3, no. 12, pp. 1–7, 2017.
[99] C. M. Proctor, J. Rivnay, and G. G. Malliaras, “Understanding volumetric capacitance in conducting polymers,” *J. Polym. Sci. Part B Polym. Phys.*, vol. 54, no. 15, pp. 1433–1436, 2016.
[100] I. Sahalianov *et al.*, “Volumetric Double-Layer Charge Storage in Composites Based on Conducting Polymer PEDOT and Cellulose,” *ACS Appl. Energy Mater.*, vol. 4, no. 8, pp. 8629–8640, 2021.
[101] A. Malti *et al.*, “An organic mixed ion-electron conductor for power electronics,” *Adv. Sci.*, vol. 3, no. 2, pp. 1–9, 2015.
[102] S. K. Singh, X. Crispin, and I. V. Zozoulenko, “Oxygen Reduction Reaction in Conducting Polymer PEDOT: Density Functional Theory Study,” *J. Phys. Chem. C*, vol. 121, no. 22, pp. 12270–12277, 2017.
[103] R. Kerr, C. Pozo-Gonzalo, M. Forsyth, and B. Winther-Jensen, “Influence of the polymerization method on the oxygen reduction reaction pathway on PEDOT,” *ECS Electrochem. Lett.*, vol. 2, no. 3, pp. 29–32, 2013.
[104] V. Gueskine, A. Singh, M. Vagin, X. Crispin, and I. Zozoulenko, “Molecular Oxygen Activation at a Conducting Polymer: Electrochemical Oxygen Reduction Reaction at PEDOT Revisited, a Theoretical Study,” *J. Phys. Chem. C*, vol. 124, no. 24, pp. 13263–13272, 2020.
[105] E. Miglbauer, P. J. Wójcik, and E. D. Głowacki, “Single-compartment hydrogen peroxide fuel cells with poly(3,4-ethylenedioxythiophene) cathodes,” *Chem. Commun.*, vol. 54, no. 84, pp. 11873–11876, 2018.
[106] E. Mitraka *et al.*, “Electrocatalytic Production of Hydrogen Peroxide with Poly(3,4-ethylenedioxythiophene) Electrodes,” *Adv. Sustain. Syst.*, vol. 3, no. 2, p. 1800110, 2019.
[107] S. Li *et al.*, “Nanometre-thin indium tin oxide for advanced high-performance electronics,” *Nat. Mater.*, vol. 18, no. 10, pp. 1091–1097, 2019.
[108] K. Nomura, H. Ohta, A. Takagi, T. Kamiya, M. Hirano, and H. Hosono, “Room-temperature fabrication of transparent flexible thin-film transistors using amorphous oxide semiconductors,” *Nature*, vol. 432, no. November, p. 488, 2004.
[109] E. Fortunato, P. Barquinha, and R. Martins, “Oxide semiconductor thin-film transistors: A review of recent advances,” *Adv. Mater.*, vol. 24, no. 22, pp. 2945–2986, 2012.
[110] S. C. Dixon, D. O. Scanlon, C. J. Carmalt, and I. P. Parkin, “N-Type doped transparent conducting

binary oxides: An overview," *J. Mater. Chem. C*, vol. 4, no. 29, pp. 6946–6961, 2016.
[111] C. I. Bright, *Deposition and Performance Challenges of Transparent Conductive Oxides on Plastic Substrates*. 2010.
[112] M. Vosgueritchian, D. J. Lipomi, and Z. Bao, "Highly conductive and transparent PEDOT:PSS films with a fluorosurfactant for stretchable and flexible transparent electrodes," *Adv. Funct. Mater.*, vol. 22, no. 2, pp. 421–428, 2012.
[113] J. C. C. Fan and J. B. Goodenough, "X-ray photoemission spectroscopy studies of Sn-doped indium-oxide films," *J. Appl. Phys.*, vol. 48, no. 8, pp. 3524–3531, 1977.
[114] Z. Ma, Z. Li, K. Liu, C. Ye, and V. J. Sorger, "Indium-Tin-Oxide for High-performance Electro-optic Modulation," *Nanophotonics*, vol. 4, no. 1, pp. 198–213, 2015.
[115] D. Belaineh *et al.*, "Printable carbon-based supercapacitors reinforced with cellulose and conductive polymers," *J. Energy Storage*, vol. 50, no. November 2021, p. 104224, 2022.
[116] J. Kang *et al.*, "Electroplated Thick Manganese Oxide Films with Ultrahigh Capacitance," *Adv. Energy Mater.*, vol. 3, no. 7, pp. 857–863, 2013.
[117] B. Francois, *Supercapacitors*. Weinheim, Germany: Wiley-VCH Verlag GmbH & Co. KGaA, 2013.
[118] F. Béguin, V. Presser, A. Balducci, and E. Frackowiak, "Carbons and electrolytes for advanced supercapacitors," *Adv. Mater.*, vol. 26, no. 14, pp. 2219–2251, 2014.
[119] S. Thiemann *et al.*, "Cellulose-based ionogels for paper electronics," *Adv. Funct. Mater.*, vol. 24, no. 5, pp. 625–634, 2014.
[120] M. G. Say *et al.*, "Ultrathin Paper Microsupercapacitors for Electronic Skin Applications," *Adv. Mater. Technol.*, vol. 2101420, p. 2101420, Jan. 2022.
[121] R. Brooke *et al.*, "Supercapacitors on demand: All-printed energy storage devices with adaptable design," *Flex. Print. Electron.*, vol. 4, no. 1, 2019.
[122] N. John and K. Thomas-Alyea, *Electrochemical Systems*, 3rd Editio. Wiley-Interscience, 2004.
[123] H. L. Lord, W. Zhan, and J. Pawliszyn, "Fundamentals and applications of needle trap devices: a critical review.," *Anal. Chim. Acta*, vol. 677, no. 1, pp. 3–18, Sep. 2010.
[124] J. J. Jasielec, "Electrodiffusion Phenomena in Neuroscience and the Nernst–Planck–Poisson Equations," *Electrochem*, vol. 2, no. 2, pp. 197–215, 2021.
[125] M. O. Bamgbopa, J. Edberg, I. Engquist, M. Berggren, and K. Tybrandt, "Understanding the characteristics of conducting polymer-redox biopolymer supercapacitors," *J. Mater. Chem. A*, vol. 7, no. 41, pp. 23973–23980, 2019.
[126] T. S. Mathis, N. Kurra, X. Wang, D. Pinto, P. Simon, and Y. Gogotsi, "Energy Storage Data Reporting in Perspective—Guidelines for Interpreting the Performance of Electrochemical Energy Storage Systems," *Adv. Energy Mater.*, vol. 9, no. 39, p. 1902007, Oct. 2019.
[127] P. Sharma and T. S. Bhatti, "A review on electrochemical double-layer capacitors," *Energy Convers. Manag.*, vol. 51, no. 12, pp. 2901–2912, 2010.
[128] D. Tie, S. Huang, J. Wang, J. Ma, J. Zhang, and Y. Zhao, "Hybrid energy storage devices: Advanced electrode materials and matching principles," *Energy Storage Mater.*, vol. 21, no. September 2018, pp. 22–40, 2019.
[129] D. C. Grahame, "Electrode Processes and the Electrical Double Layer," *Annu. Rev. Phys. Chem.*, vol. 6, no. 1, pp. 337–358, 1955.
[130] M. Hamedi, E. Karabulut, A. Marais, A. Herland, and G. Nyström, "Nanocellulose aerogels functionalized by rapid layer-by-layer assembly for high charge storage and beyond," *Angew. Chemie - Int. Ed.*, vol. 52, no. 46, pp. 12038–12042, 2013.
[131] A. Alonso *et al.*, "Activated carbon produced from Sasol-Lurgi gasifier pitch and its application as electrodes in supercapacitors," *Carbon N. Y.*, vol. 44, no. 3, pp. 441–446, 2006.
[132] G. Wang, L. Zhang, and J. Zhang, "A review of electrode materials for electrochemical supercapacitors," *Chem. Soc. Rev.*, vol. 41, no. 2, pp. 797–828, 2012.
[133] S. Li *et al.*, "Flexible Supercapacitors based on bacterial cellulose paper electrodes," *Adv. Energy Mater.*, vol. 4, no. 10, pp. 1–7, 2014.
[134] N. Kurra, J. Park, and H. N. Alshareef, "A conducting polymer nucleation scheme for efficient solid-state supercapacitors on paper," *J. Mater. Chem. A*, vol. 2, no. 40, pp. 17058–17065, 2014.
[135] G. S. Gund *et al.*, "MXene/Polymer Hybrid Materials for Flexible AC-Filtering Electrochemical Capacitors," *Joule*, vol. 3, no. 1, pp. 164–176, 2019.
[136] T. Wakabayashi, M. Katsunuma, K. Kudo, and H. Okuzaki, "PH-Tunable High-Performance PEDOT:PSS Aluminum Solid Electrolytic Capacitors," *ACS Appl. Energy Mater.*, vol. 1, no. 5, pp. 2157–2163, 2018.
[137] J. Kim, J. K. Yoo, Y. S. Jung, and K. Kang, "Li3V2(PO4)3/Conducting polymer as a high power 4 V-class lithium battery electrode," *Adv. Energy Mater.*, vol. 3, no. 8, pp. 1004–1007, 2013.
[138] G. L. Xu *et al.*, "Building ultraconformal protective layers on both secondary and primary particles of

layered lithium transition metal oxide cathodes," *Nat. Energy*, vol. 4, no. 6, pp. 484–494, 2019.
[139] X. Wang, X. Lu, B. Liu, D. Chen, Y. Tong, and G. Shen, "Flexible energy-storage devices: Design consideration and recent progress," *Adv. Mater.*, vol. 26, no. 28, pp. 4763–4782, 2014.
[140] Z. Zhu *et al.*, "Recent Advances in High-Performance Microbatteries: Construction, Application, and Perspective," *Small*, vol. 16, no. 39, pp. 1–28, 2020.
[141] J. Wang, F. Li, F. Zhu, and O. G. Schmidt, "Recent Progress in Micro-Supercapacitor Design, Integration, and Functionalization," *Small Methods*, vol. 3, no. 8, pp. 1–27, 2019.
[142] S. H. Kim *et al.*, "Electrolyte-gated transistors for organic and printed electronics," *Adv. Mater.*, vol. 25, no. 13, pp. 1822–1846, 2013.
[143] W. Huang *et al.*, "Dielectric materials for electrolyte gated transistor applications," *J. Mater. Chem. C*, vol. 9, no. 30, pp. 9348–9376, 2021.
[144] H. Ling, D. A. Koutsouras, S. Kazemzadeh, Y. Van De Burgt, F. Yan, and P. Gkoupidenis, "Electrolyte-gated transistors for synaptic electronics, neuromorphic computing, and adaptable biointerfacing," *Appl. Phys. Rev.*, vol. 7, no. 1, 2020.
[145] S. M. Sze and K. K. Ng, *Physics of Semiconductor Devices: Third Edition*. 2006.
[146] J. T. Friedlein, R. R. McLeod, and J. Rivnay, "Device physics of organic electrochemical transistors," *Org. Electron.*, vol. 63, no. September, pp. 398–414, 2018.
[147] T. M. Higgins *et al.*, "Electrolyte-Gated n-Type Transistors Produced from Aqueous Inks of WS2 Nanosheets," *Adv. Funct. Mater.*, vol. 29, no. 4, 2019.
[148] H. Yuan, H. Shimotani, A. Tsukazaki, A. Ohtomo, M. Kawasaki, and Y. Iwasa, "High-density carrier accumulation in ZnO field-effect transistors gated by electric double layers of ionic liquids," *Adv. Funct. Mater.*, vol. 19, no. 7, pp. 1046–1053, 2009.
[149] K. Hong, S. H. Kim, A. Mahajan, and C. D. Frisbie, "Aerosol jet printed p- and n-type electrolyte-gated transistors with a variety of electrode materials: Exploring practical routes to printed electronics," *ACS Appl. Mater. Interfaces*, vol. 6, no. 21, pp. 18704–18711, 2014.
[150] Y. Z. Zhang *et al.*, "Printed supercapacitors: Materials, printing and applications," *Chem. Soc. Rev.*, vol. 48, no. 12, pp. 3229–3264, 2019.
[151] S. K. Aggarwal, *Review of "Handbook of Atomization and Spray: Theory and Applications,"* vol. 50, no. 3. 2012.
[152] Leach R.H, *The Printing Ink Manual*. Springer, 2007.
[153] R. D. Andrade, O. Skurtys, and F. A. Osorio, "Atomizing Spray Systems for Application of Edible Coatings," *Compr. Rev. Food Sci. Food Saf.*, vol. 11, no. 3, pp. 323–337, May 2012.
[154] A. H. Lefebvre and V. G. Mcdonell, *Atomization and Sprays, Second Edition.* 1989.
[155] S. V. Roth, "A deep look into the spray coating process in real-time - The crucial role of x-rays," *J. Phys. Condens. Matter*, vol. 28, no. 40, 2016.
[156] A. Reale *et al.*, "Spray Coating for Polymer Solar Cells: An Up-to-Date Overview," *Energy Technol.*, vol. 3, no. 4, pp. 385–406, 2015.
[157] A. Abdellah, B. Fabel, P. Lugli, and G. Scarpa, "Spray deposition of organic semiconducting thin-films: Towards the fabrication of arbitrary shaped organic electronic devices," *Org. Electron.*, vol. 11, no. 6, pp. 1031–1038, 2010.
[158] F. Ely *et al.*, "Handheld and automated ultrasonic spray deposition of conductive PEDOT:PSS films and their application in AC EL devices," *Org. Electron.*, vol. 15, no. 5, pp. 1062–1070, 2014.
[159] C. Girotto, D. Moia, B. P. Rand, and P. Heremans, "High-performance organic solar cells with spray-coated hole-transport and active layers," *Adv. Funct. Mater.*, vol. 21, no. 1, pp. 64–72, 2011.
[160] T. M. Higgins and J. N. Coleman, "Avoiding Resistance Limitations in High-Performance Transparent Supercapacitor Electrodes Based on Large-Area, High-Conductivity PEDOT:PSS Films," *ACS Appl. Mater. Interfaces*, vol. 7, no. 30, pp. 16495–16506, 2015.
[161] Y. Guo, W. Li, H. Yu, D. F. Perepichka, and H. Meng, "Flexible Asymmetric Supercapacitors via Spray Coating of a New Electrochromic Donor–Acceptor Polymer," *Adv. Energy Mater.*, vol. 7, no. 2, pp. 1–7, 2017.
[162] L. Liu, Y. Feng, and W. Wu, "Recent progress in printed flexible solid-state supercapacitors for portable and wearable energy storage," *J. Power Sources*, vol. 410–411, no. April 2018, pp. 69–77, 2019.
[163] M. G. Say *et al.*, "Spray-coated paper supercapacitors," *npj Flex. Electron.*, vol. 4, no. 1, 2020.
[164] R. Brooke *et al.*, "Supercapacitors on demand: All-printed energy storage devices with adaptable design," *Flex. Print. Electron.*, vol. 4, no. 1, p. 15006, 2019.
[165] C. K. Chan *et al.*, "High performance airbrushed organic thin film transistors," *Appl. Phys. Lett.*, vol. 96, no. 13, pp. 8–11, 2010.
[166] D. Khim *et al.*, "Spray-printed organic field-effect transistors and complementary inverters," *J. Mater. Chem. C*, vol. 1, no. 7, pp. 1500–1506, 2013.
[167] C. Girotto, D. Moia, B. P. Rand, and P. Heremans, "High-performance organic solar cells with spray-

coated hole-transport and active layers," *Adv. Funct. Mater.*, vol. 21, no. 1, pp. 64–72, 2011.
[168] W. Ohm *et al.*, "Morphological properties of airbrush spray-deposited enzymatic cellulose thin films," *J. Coatings Technol. Res.*, vol. 15, no. 4, pp. 759–769, 2018.
[169] X. Wang *et al.*, "A Consecutive Spray Printing Strategy to Construct and Integrate Diverse Supercapacitors on Various Substrates," *ACS Appl. Mater. Interfaces*, vol. 9, no. 34, pp. 28612–28619, 2017.
[170] Y. Khan, A. Thielens, S. Muin, J. Ting, C. Baumbauer, and A. C. Arias, "A New Frontier of Printed Electronics: Flexible Hybrid Electronics," *Adv. Mater.*, vol. 32, no. 15, 2020.
[171] Q. Li *et al.*, "Review of printed electrodes for flexible devices," *Front. Mater.*, vol. 5, no. January, pp. 1–14, 2019.
[172] D. Khim *et al.*, "Simple bar-coating process for large-area, high-performance organic field-effect transistors and ambipolar complementary integrated circuits," *Adv. Mater.*, vol. 25, no. 31, pp. 4302–4308, 2013.
[173] P. J. Kelly and R. D. Arnell, "Magnetron sputtering: A review of recent developments and applications," *Vacuum*, vol. 56, no. 3, pp. 159–172, 2000.
[174] K. Ellmer and T. Welzel, "Reactive magnetron sputtering of transparent conductive oxide thin films: Role of energetic particle (ion) bombardment," *J. Mater. Res.*, vol. 27, no. 5, pp. 765–779, 2012.
[175] M. J. Donahue *et al.*, "High-Performance Vertical Organic Electrochemical Transistors," *Adv. Mater.*, vol. 30, no. 5, 2018.
[176] J. Wang, *Analytical Electrochemistry, Third Edition*. 2006.
[177] N. Elgrishi, K. J. Rountree, B. D. McCarthy, E. S. Rountree, T. T. Eisenhart, and J. L. Dempsey, "A Practical Beginner's Guide to Cyclic Voltammetry," *J. Chem. Educ.*, vol. 95, no. 2, pp. 197–206, 2018.
[178] X. Pu *et al.*, "Understanding and Calibration of Charge Storage Mechanism in Cyclic Voltammetry Curves," *Angew. Chemie*, vol. 133, no. 39, pp. 21480–21488, 2021.
[179] S. Zhang and N. Pan, "Supercapacitors performance evaluation," *Adv. Energy Mater.*, vol. 5, no. 6, pp. 1–19, 2015.
[180] B. J. Inkson, *Scanning Electron Microscopy (SEM) and Transmission Electron Microscopy (TEM) for Materials Characterization*. Elsevier Ltd, 2016.
[181] A. Hexemer and P. Müller-Buschbaum, "Advanced grazing-incidence techniques for modern soft-matter materials analysis," *IUCrJ*, vol. 2, pp. 106–125, 2015.
[182] C. J. Schaffer *et al.*, "Morphological Degradation in Low Bandgap Polymer Solar Cells – An In Operando Study," *Adv. Energy Mater.*, vol. 6, no. 19, 2016.
[183] X. Gu *et al.*, "Comparison of the Morphology Development of Polymer–Fullerene and Polymer–Polymer Solar Cells during Solution-Shearing Blade Coating," *Adv. Energy Mater.*, vol. 6, no. 22, pp. 1–12, 2016.
[184] O. Ghodbane, F. Ataherian, N. L. Wu, and F. Favier, "In situ crystallographic investigations of charge storage mechanisms in MnO 2-based electrochemical capacitors," *J. Power Sources*, vol. 206, no. 2012, pp. 454–462, 2012.
[185] J. Park *et al.*, "Organic Semiconductor Cocrystal for Highly Conductive Lithium Host Electrode," *Adv. Funct. Mater.*, vol. 29, no. 32, pp. 1–9, 2019.
[186] C. M. Palumbiny, F. Liu, T. P. Russell, A. Hexemer, C. Wang, and P. Müller-Buschbaum, "The crystallization of PEDOT:PSS polymeric electrodes probed in situ during printing," *Adv. Mater.*, vol. 27, no. 22, pp. 3391–3397, 2015.
[187] B. D. Paulsen *et al.*, "Time-Resolved Structural Kinetics of an Organic Mixed Ionic–Electronic Conductor," *Adv. Mater.*, vol. 32, no. 40, 2020.
[188] G. Wang *et al.*, "Aggregation control in natural brush-printed conjugated polymer films and implications for enhancing charge transport," *Proc. Natl. Acad. Sci. U. S. A.*, vol. 114, no. 47, pp. E10066–E10073, 2017.
[189] C. M. Palumbiny, J. Schlipf, A. Hexemer, C. Wang, and P. Müller-Buschbaum, "The Morphological Power of Soap: How Surfactants Lower the Sheet Resistance of PEDOT:PSS by Strong Impact on Inner Film Structure and Molecular Interface Orientation," *Adv. Electron. Mater.*, vol. 2, no. 4, pp. 1–9, 2016.
[190] K. Wang *et al.*, "Wide Potential Window Supercapacitors Using Open-Shell Donor–Acceptor Conjugated Polymers with Stable N-Doped States," *Adv. Energy Mater.*, vol. 9, no. 47, pp. 1–8, 2019.
[191] Q. Wei, M. Mukaida, Y. Naitoh, and T. Ishida, "Morphological change and mobility enhancement in PEDOT:PSS by adding co-solvents," *Adv. Mater.*, vol. 25, no. 20, pp. 2831–2836, 2013.
[192] D. Belaineh *et al.*, "Controlling the Organization of PEDOT:PSS on Cellulose Structures," *ACS Appl. Polym. Mater.*, vol. 1, no. 9, pp. 2342–2351, 2019.
[193] T. Cheng *et al.*, "Inkjet-printed flexible, transparent and aesthetic energy storage devices based on PEDOT:PSS/Ag grid electrodes," *J. Mater. Chem. A*, vol. 4, no. 36, pp. 13754–13763, 2016.
[194] D. Yuan *et al.*, "Twisted yarns for fiber-shaped supercapacitors based on wetspun PEDOT:PSS fibers

from aqueous coagulation," *J. Mater. Chem. A*, vol. 4, no. 30, pp. 11616–11624, 2016.
[195] S. B. Singh, T. Kshetri, T. I. Singh, N. H. Kim, and J. H. Lee, "Embedded PEDOT:PSS/AgNFs network flexible transparent electrode for solid-state supercapacitor," *Chem. Eng. J.*, vol. 359, no. November 2018, pp. 197–207, 2019.
[196] X. Yu *et al.*, "Stretchable, Conductive, and Stable PEDOT-Modified Textiles through a Novel In Situ Polymerization Process for Stretchable Supercapacitors," *Adv. Mater. Technol.*, vol. 1, no. 2, pp. 1–8, 2016.
[197] T. Cheng, Y. Z. Zhang, J. D. Zhang, W. Y. Lai, and W. Huang, "High-performance free-standing PEDOT:PSS electrodes for flexible and transparent all-solid-state supercapacitors," *J. Mater. Chem. A*, vol. 4, no. 27, pp. 10493–10499, 2016.
[198] Y. Li *et al.*, "A strong and highly flexible aramid nanofibers/PEDOT:PSS film for all-solid-state supercapacitors with superior cycling stability," *J. Mater. Chem. A*, vol. 4, no. 44, pp. 17324–17332, 2016.
[199] Z. Li *et al.*, "Free-standing conducting polymer films for high-performance energy devices," *Angew. Chemie - Int. Ed.*, vol. 55, no. 3, pp. 979–982, 2016.
[200] L. Manjakkal, A. Pullanchiyodan, N. Yogeswaran, E. S. Hosseini, and R. Dahiya, "A Wearable Supercapacitor Based on Conductive PEDOT:PSS-Coated Cloth and a Sweat Electrolyte," *Adv. Mater.*, vol. 1907254, 2020.
[201] B. Anothumakkool, R. Soni, S. N. Bhange, and S. Kurungot, "Novel scalable synthesis of highly conducting and robust PEDOT paper for a high performance flexible solid supercapacitor," *Energy Environ. Sci.*, vol. 8, no. 4, pp. 1339–1347, 2015.
[202] Z. Wang, P. Tammela, J. Huo, P. Zhang, M. Strømme, and L. Nyholm, "Solution-processed poly(3,4-ethylenedioxythiophene) nanocomposite paper electrodes for high-capacitance flexible supercapacitors," *J. Mater. Chem. A*, vol. 4, no. 5, pp. 1714–1722, 2016.
[203] Y. Wang *et al.*, "A low-temperature-operated direct fabrication method for all-solid-state flexible micro-supercapacitors," *J. Power Sources*, vol. 448, no. November 2019, p. 227415, 2020.
[204] B. D. Boruah, A. Maji, and A. Misra, "Flexible Array of Microsupercapacitor for Additive Energy Storage Performance over a Large Area," *ACS Appl. Mater. Interfaces*, vol. 10, no. 18, pp. 15864–15872, 2018.
[205] D. Pech *et al.*, "Ultrahigh-power micrometre-sized supercapacitors based on onion-like carbon," *Nat. Nanotechnol.*, vol. 5, no. 9, pp. 651–654, 2010.
[206] J. Lin *et al.*, "3-Dimensional Graphene Carbon Nanotube Carpet-Based Microsupercapacitors With High Electrochemical Performance," *Nano Lett.*, vol. 13, no. 1, pp. 72–78, 2013.
[207] H. Kim *et al.*, "Encapsulated, High-Performance, Stretchable Array of Stacked Planar Micro-Supercapacitors as Waterproof Wearable Energy Storage Devices," *ACS Appl. Mater. Interfaces*, vol. 8, no. 25, pp. 16016–16025, 2016.
[208] M. Yoonessi *et al.*, "Hybrid Transparent PEDOT:PSS Molybdenum Oxide Battery-like Supercapacitors," *ACS Appl. Energy Mater.*, vol. 2, no. 7, pp. 4629–4639, 2019.
[209] S. Liu *et al.*, "Nitrogen-doped reduced graphene oxide for high-performance flexible all-solid-state micro-supercapacitors," *J. Mater. Chem. A*, vol. 2, no. 42, pp. 18125–18131, 2014.
[210] A. Valero, A. Mery, D. Gaboriau, P. Gentile, and S. Sadki, "One step deposition of PEDOT-PSS on ALD protected silicon nanowires: Toward ultrarobust aqueous microsupercapacitors," *ACS Applied Energy Materials*, vol. 2, no. 1. pp. 436–447, 2019.
[211] J. Li *et al.*, "Scalable Fabrication and Integration of Graphene Microsupercapacitors through Full Inkjet Printing," *ACS Nano*, vol. 11, no. 8, pp. 8249–8256, Aug. 2017.
[212] B. Song, L. Li, Z. Lin, Z. K. Wu, K. sik Moon, and C. P. Wong, "Water-dispersible graphene/polyaniline composites for flexible micro-supercapacitors with high energy densities," *Nano Energy*, vol. 16, pp. 470–478, 2015.
[213] Z. Liu *et al.*, "High Power In-Plane Micro-Supercapacitors Based on Mesoporous Polyaniline Patterned Graphene," *Small*, vol. 13, no. 14, pp. 1–5, 2017.
[214] L. Basiricò, P. Cosseddu, B. Fraboni, and A. Bonfiglio, "Inkjet printing of transparent, flexible, organic transistors," *Thin Solid Films*, vol. 520, no. 4, pp. 1291–1294, 2011.
[215] P. Barquinha *et al.*, "Flexible and Transparent WO3 Transistor with Electrical and Optical Modulation," *Adv. Electron. Mater.*, vol. 1, no. 5, pp. 1–7, 2015.
[216] M. Held *et al.*, "Dense Carbon Nanotube Films as Transparent Electrodes in Low-Voltage Polymer and All-Carbon Transistors," *Adv. Electron. Mater.*, vol. 4, no. 10, pp. 1–7, 2018.
[217] Q. He *et al.*, "Transparent, flexible, all-reduced graphene oxide thin film transistors," *ACS Nano*, vol. 5, no. 6, pp. 5038–5044, 2011.
[218] Y. Yao *et al.*, "Flexible complementary circuits operating at sub-0.5 V via hybrid organic-inorganic electrolyte-gated transistors," *Proc. Natl. Acad. Sci. U. S. A.*, vol. 118, no. 44, pp. 1–8, 2021.

[219] S. Park *et al.*, “Sub-0.5 v Highly Stable Aqueous Salt Gated Metal Oxide Electronics,” *Sci. Rep.*, vol. 5, pp. 1–9, 2015.
[220] B. Nketia-Yawson *et al.*, “Ultrahigh Mobility in Solution-Processed Solid-State Electrolyte-Gated Transistors,” *Adv. Mater.*, vol. 29, no. 16, 2017.
[221] J. H. Pikul, H. Gang Zhang, J. Cho, P. V. Braun, and W. P. King, “High-power lithium ion microbatteries from interdigitated three-dimensional bicontinuous nanoporous electrodes,” *Nat. Commun.*, vol. 4, pp. 1–5, 2013.
[222] N. Kurra, B. Ahmed, Y. Gogotsi, and H. N. Alshareef, “MXene-on-Paper Coplanar Microsupercapacitors,” *Adv. Energy Mater.*, vol. 6, no. 24, pp. 1–8, 2016.
[223] W. Lai *et al.*, “High performance, environmentally benign and integratable Zn//MnO2 microbatteries,” *J. Mater. Chem. A*, vol. 6, no. 9, pp. 3933–3940, 2018.
[224] Y. Wang *et al.*, “Wearable Textile-Based Co−Zn Alkaline Microbattery with High Energy Density and Excellent Reliability,” *Small*, vol. 16, no. 16, pp. 1–9, 2020.
[225] Q. Liu *et al.*, “The First Flexible Dual-Ion Microbattery Demonstrates Superior Capacity and Ultrahigh Energy Density: Small and Powerful,” *Adv. Funct. Mater.*, vol. 30, no. 38, pp. 1–10, 2020.
[226] G. Zhang *et al.*, “Biocompatible Symmetric Na-Ion Microbatteries with Sphere-in-Network Heteronanomat Electrodes Realizing High Reliability and High Energy Density for Implantable Bioelectronics,” *ACS Appl. Mater. Interfaces*, vol. 10, no. 49, pp. 42268–42278, 2018.
[227] X. Wang *et al.*, “Scalable fabrication of printed Zn//MnO2 planar micro-batteries with high volumetric energy density and exceptional safety,” *Natl. Sci. Rev.*, vol. 7, no. 1, pp. 64–72, 2020.
[228] P. Zhuang *et al.*, “FIB-Patterned Nano-Supercapacitors: Minimized Size with Ultrahigh Performances,” *Adv. Mater.*, vol. 32, no. 14, p. 1908072, Apr. 2020.
[229] M. F. El-Kady and R. B. Kaner, “Scalable fabrication of high-power graphene micro-supercapacitors for flexible and on-chip energy storage,” *Nat. Commun.*, vol. 4, 2013.

PART 2
INCLUDED PUBLICATIONS

Papers

The papers associated with this thesis have been removed for copyright reasons. For more details about these see:

https://doi.org/10.3384/9789179293543

FACULTY OF SCIENCE AND ENGINEERING

Linköping Studies in Science and Technology, Dissertation No. 2234, 2022
Department of Science and Technology

Linköping University
SE-581 83 Linköping, Sweden

www.liu.se